REPORT NO. DOT-TSC-OST-75-26.II

LEAN MIXTURE ENGINES TESTING AND EVALUATION PROGRAM

Volume II: Comprehensive Discussion

Mack W. Dowdy
Frank W. Hoehn
Tom G. Vanderbrug

NOVEMBER 1975

FINAL REPORT

DOCUMENT IS AVAILABLE TO THE PUBLIC
THROUGH THE NATIONAL TECHNICAL
INFORMATION SERVICE, SPRINGFIELD,
VIRGINIA 22161

Prepared for

U.S. DEPARTMENT OF TRANSPORTATION

Office of the Secretary
Office of the Assistant Secretary for
Systems Development and Technology
Office of Systems Engineering
Washington DC 20590

Technical Report Documentation Page

1. Report No.	2. Government Accession No.	3. Recipient's Catalog No.
DOT-TSC-OST-75-26. II		

4. Title and Subtitle	5. Report Date
LEAN MIXTURE ENGINES TESTING AND EVALUATION PROGRAM Volume II: Comprehensive Discussion	November 1975
	6. Performing Organization Code
7. Author(s) Mack W. Dowdy, Frank W. Hoehn and Tom G. Vanderbrug	8. Performing Organization Report No. JPL 5040-12, Vol. II DOT-TSC-OST-75-26. II
9. Performing Organization Name and Address Jet Propulsion Laboratory* 4800 Oak Grove Drive Pasadena, CA 91103	10. Work Unit No. (TRAIS) OS 614/R6506
	11. Contract or Grant No. RA 74-38 TMP-0223
12. Sponsoring Agency Name and Address U.S. Dept. of Transportation, Office of the Secretary, Office of the Assistant Secretary for Systems Development and Technology, Office of Systems Engineering, Washington, D.C. 20590	13. Type of Report and Period Covered Final Report May-Dec. 1974
	14. Sponsoring Agency Code

15. Supplementary Notes

*Under Contract to: U.S. Department of Transportation
Transportation Systems Center, Kendall Square
Cambridge, MA 02142

16. Abstract

This report is aimed at defining analytically and demonstrating experimentally the potential of the "lean-burn concept." Fuel consumption and emissions data are obtained on the engine dynamometer for the baseline engine, and two lean-burn configurations of the same engine and data comparisons are made. Individual cylinder equivalence ratios are measured to evaluate the cyclinder-to-cylinder distribution. Pressure-time traces from individual cylinders are used to get information about ignition delay, combustion duration and cycle-to-cycle pressure variations. Fuel consumption and emissions data for one lean-burn configuration are obtained over the Federal Driving Cycle using a chassis dynamometer and the results are compared with the stock baseline results. Using experimental results and information from the existing literature, the potential of the "lean-burn concept" is assessed using the Blumberg-Kummer cycle analysis program.

17. Key Words	18. Distribution Statement
Automobiles Fuel Consumption Exhaust Emissions	Document is available to the public through the National Technical Information Service, Springfield, Virginia 22161.

19. Security Classif. (of this report)	20. Security Classif. (of this page)	21. No. of Pages	22. Price
UNCLASSIFIED	UNCLASSIFIED	120	

Form DOT F 1700.7 (8-72) Reproduction of completed page authorized

PREFACE

This report covers work done by the Jet Propulsion Laboratory (JPL) for the Department of Transportation, Transportation System Center (DOT/TSC) from 28 May 1974 to 31 December 1974, and is considered a final report covering work done under this contract.

This report addresses itself to a restricted set of near-term objectives, the achievement of which will represent, nonetheless, significant progress toward the overall DOT/TSC objective of defining analytically and demonstrating experimentally the potential of "the lean burn concept".

Specifically, this report first presents the results of a literature search which documents the concept that improved fuel economy and reduced exhaust emissions are inherent advantages of lean-mixture operation. The limits of lean operation and the idealized lean-mixture concept are developed, followed by a treatment of the importance of and the roles played by mixture distribution and homogeneity, spark, control of combustion chamber flame propagation, and the effects of compression ratio on lean-limit operation. The reduced power output attendant upon lean-mixture operation is discussed as are emissions control techniques in the lean region.

Second, the stock baseline description of the engine and vehicle is presented. Both engine dynamometer and chassis dynamometer fuel consumption and emissions data are presented. These data are used to describe the baseline from which departures were made in order to configure a lean-burn engine.

Third, a lean-burn engine configuration is described and engine dynamometer fuel consumption data and chassis dynamometer fuel consumption and emissions data are presented.

Fourth, an analysis of the lean-burn engine is presented. The analysis describes the Blumberg-Kummer cycle program; discusses the stock engine and the lean-burn engine and compares the two engines. In addition, the effects of combustion duration, compression ratio, and cylinder-to-cylinder maldistribution are discussed.

Fifth, a second lean-burn engine configuration is described and engine dynamometer fuel consumption and emissions data are presented. The cylinder-to-cylinder distribution of equivalence ratios is evaluated from exhaust gas composition measurements from individual cylinders. Information about ignition delay, combustion duration, and cycle-to-cycle pressure variations is presented based on pressure-time traces from individual cylinders.

Finally, the potential of the lean-burn concept is discussed with respect to fuel consumption and emissions.

CONTENTS

CONTENTS (Contd)

TABLES

FIGURES

FIGURES (Contd)

FIGURES (Contd)

1. LITERATURE SEARCH

1.1 Introduction

The inherent advantages of lean-mixture engine operation that have stimulated continuing research and development for the past two decades are improved fuel economy and reduced exhaust emissions. The factors that have apparently prevented incorporation of the lean-mixture engine concept on a mass production basis are manufacturing production risks, poor driveability, and reduced power output for any given engine size. The objective of this literature search is to identify significant achievements and the most promising methods for obtaining acceptable lean-engine operation while minimizing equipment complexity and development risks.

Normal air-to-fuel ratios (A/F) for production automobile engines range from 12 to 19.[1] Increasing the A/F ratio above 19 generally increases fuel consumption, causes poor driveability, and increases hydrocarbon emissions due to lean-limit misfire. Engine tests performed by various experimentors (Table 1) have demonstrated significant extensions of the equipment lean limit by relatively simple improvements to the ignition and induction systems.

The present effort considers only those modifications to conventional engines which lead to improved lean-burn operation for near-term (1977 to 1980) applications. Other lean-burn concepts currently being pursued are stratified charge, fuel injection, and prechamber mechanisms.

1.2 Lean Mixture Operation Limits

The maximum obtainable lean limit, or the spark-ignited flammability limit for air/gasoline mixtures, has recently been experimentally bracketed by Shell Research investigators[2] to occur at an A/F of 33 ± 3. This maximum limit, however, was obtained under controlled laboratory conditions utilizing an adiabatic "rapid compression machine". This device is reported to simulate engine combustion chamber conditions, but is not completely representative of actual multicylinder engine operation.

TABLE 1. SUMMARY OF SIGNIFICANT LEAN MIXTURE ENGINE TESTING

Reference	Engine	Displacement	Combustion chamber	Baseline max. A/F	Engine modifications	Modified max. A/F	Equipment lean limit extension, percent
21	CFR	-	Disk	19.5	Manifold fuel injection, dual spark plugs, spark plug location	25.0	28.2
3	CFR	-	Hemi	19.5	Atomized/vaporized fuel, vaned intake valve spark plug gap and projection, spark energy and duration (Texaco ignition system)	24.0	23.1
31	CFR	-	Bowl	19.5	Vaporized fuel, spark plug location, combustion chamber shape	24.0	23.1
1	4-cyl.	96.7 CID	-	15.1	Fuel injection, spark plug, variable F/A and spark advance (optimizer)	23.5	55.6
9	4-cyl.	1982 CC	Heron	18.4	Spark plug gap and projection, spark energy, vaned intake valve, combustion chamber shape, intake air temperature	21.0	14.1
16	4-cyl.	1800 CC	-	18.0	Heat pipe vaporization	21.0	16.7
14	4-cyl.	91 CID	-	20.2	Vaporized fuel	22.5	11.4
34	6-cyl.	-	-	17.8	Vaporized fuel	22.5	26.4
4	V-8	318 CID	-	18.0	Induction system, spark energy	23.6	31.1

The standard test procedure[3,4] used to detect maximum obtainable lean limit is to observe from pressure traces the cycle-to-cycle combustion variations or cyclic dispersion. Cyclic dispersion is caused by variations in combustion chamber flame development and propagation, resulting with nominal deviations in peak cylinder pressures ranging from 50 to 100 psi. As the lean limit is approached, misfire occurs and the cylinder pressure trace is similar to the motored pressure trace. Lean limit misfire is usually defined as occurring when 5% of the cycles are completed without ignition of the mixture.

Extension of the lean mixture operational limit is dependent upon mixture homogeneity, mixture distribution, turbulence, and spark, i.e., the primary factors controlling flame growth and propagation. Although the relative importance of these factors may vary from engine to engine (Table 1), it has generally been established[1,4] that mixture, turbulence, and spark contribute equally towards extension of the lean limit.

1.3 Idealized Lean Mixture Concept

An idealized lean mixture theory can be formed by combining information collected from a broad overview of available literature on lean mixture engine operation. Optimum air/fuel distribution, turbulence distribution, and spark location are presented in Figure 1, which is an idealized schematic of the lean mixture combustion chamber environment. Figure 1 shows a uniform, homogeneous air/fuel mixture throughout most of the combustion chamber, with a rich mixture zone at the plug location and a lean mixture zone near the chamber surfaces. Plug quenching is offset in the rich mixture zone, thereby promoting transition from the flame kernel to the flame front. Hydrocarbon (HC) emissions, preignition, and knock are inhibited in the lean mixture zones. Turbulent intensity is similarly uniform through the combustion chamber, except for decreased levels at the spark plug and chamber walls. A relatively lower level of turbulent intensity in these regions is required to allow establishment of the flame front at the plug and to reduce wall quenching at combustion chamber surfaces. The centrally located spark plug has a large gap, long extension, and a small electrode diameter, with long spark duration and high energy. This plug configuration will ideally minimize quenching effects while exposing a large surface area, long duration spark to the mixture.

1.4 Mixture Distribution and Homogeneity

A prerequisite for providing a homogeneous mixture to the combustion chamber of each engine cylinder is uniform cylinder-to-cylinder mixture distribution and uniform cycle-to-cycle mixture distribution. Mixture maldistribution causes power loss, increased fuel consumption, surge, and misfire. The effects of mixture maldistribution are more important in lean mixture engines which operate at equivalence ratios near the lean flammability limit of the fuel.

Normally carburetted induction system modifications that have been demonstrated to improve mixture distribution are: finely tuned, dribble-free carburetor[5, 6]; manifold partitions; and various lips, extensions, deflectors, orifices or nozzles, risers[7, 8]; increased mixing volume[7, 8]; and heat manifolds[5, 6, 9]. Special induction system devices that have been developed are

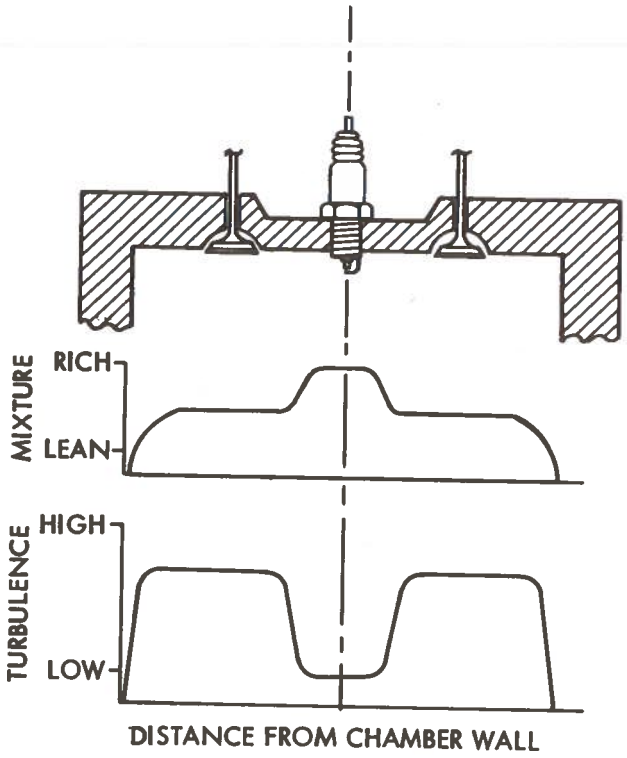

FIGURE 1. LEAN MIXTURE ENGINE IDEALIZED COMBUSTION CHAMBER ENVIRONMENT

fuel atomizers and mixers[10, 11, 12, 13]. Unfortunately, most devices utilized to improve mixture distribution and homogeneity (as well as mixture turbulence) have an associated penalty in volumetric efficiency. This penalty, however, is partially compensated[14] by an increase in power output or thermal efficiency.

Although many of the above devices appear promising, selection of the best method for improving mixture distribution and homogeneity is constrained by hardware availability and lack of adequate baseline comparative data. Reported percentage improvements in operational lean limits (Table 1) or fuel economy[15] are seldom referenced to the same baseline engine configuration or engine operating/loading conditions. The Ethyl Corporation (page 29R of Ref.

15), for example, presents emissions and fuel economy improvement data for the "Lean Thermal Reactor System" by comparing a 1971 modified car with a 1973 unmodified baseline car.

The availability of hardware for improving mixture distribution and homogeneity is minimal. Most devices are in the initial prototype phase of development and have been experimentally tuned or specifically designed for one engine/manifold combination. (Table 4-16, page 92 of Ref. 15.) The "Vapipe" system[16], for example, has been in the initial development phase since May 1973, and is specifically matched to an 1800 cc European 4-cylinder engine. As estimated 6-month development effort[17] would be required to provide a prototype Vapipe system for a full sized V-8 engine. The Ethyl Corporation lean reactor system[15] is also not readily available for test on any V-8 engine except the 360 CID Plymouth. A long development time would be required to produce prototype test hardware for any other type of engine, owing to the need for extensive redesign of intake and exhaust manifolds.

Dresser Industries has developed a system that reportedly provides excellent mixture homogeneity and distribution. Unpublished data obtained from the manufacturer[18] indicates maximum A/F from 22 to 23 without misfire and all cylinders within ±0.2 A/F. Although the "Dresserator" system has been demonstrated on both Ford and Chevrolet vehicles, this device is not generally available for outside testing owing to the proprietary nature of the device.

The Autotronics System[15] is one of the few mixture devices that is available as off-the-shelf hardware. Good performance has been demonstrated using the Autotronics System in conjunction with ultra-lean, hydrogen enriched, low emissions engine experimental work reported in Ref. 19.

Table 1 indicates that fuel vaporization or a combination of fuel atomization and vaporization has been found to provide superior mixture distribution as well as charge homogeneity. Vaporization alone may not completely eliminate cylinder-to-cylinder maldistribution[7,20] unless adequate manifold swirl or other means of mixing are used. Variations in cycle-to-cycle combustion chamber residual gases have also been found to be a source of charge inhomogeneity[4,7] which ultimately results in cyclic dispersion.

1.5 Spark

The spark configuration required to extend lean limit operation has been established with adequate certainty[3, 9, 12, 21, 22]:

GAP WIDTH	- Equal to or greater than 0.060 inch
GAP EXTENSION	- Equal to or greater than 0.300 inch
ELECTRODE DIAMETER	- Equal to or less than 0.050 inch
SPARK DURATION	- 20 to 25° of crank angle
SPARK CURRENT	- Equal to or greater tha 30 mA
SPARK TIMING	- 30 to 50° advance

Improvements in lean limit operation produced by a modified ignition system that provides good spark conditions varies from 0.5%[23] to 28%[21]. The large differences in reported improvements can be attributed to a failure to determine if the test engine was spark limited, mixture limited, or turbulence limited. Some of the discrepancies can be resolved, for example, with the observation[24] that the leanest ignitable mixture is a quiescent mixture. As mixture turbulence or velocity is increased, either enrichment or greater spark energy (theoretically, infinite energy at the lean limit) is required to ignite the mixture.

The preceding arguments should be acknowledged when considering the relatively small improvements in lean limit obtained with dual spark plug or extended spark duration systems. Only 6% improvement was reported[21] with a dual spark plug system, and similarly[9] only 3% improvement with a capacitance discharge system that could provide multiple spark for over 45° of crank angle. Also, tests performed in Ref. 3 indicated that with correct spark energy, gap, and projection, the A/F limit could be increased from 21 to 23.8 by increasing spark duration to 25° of crank angle. Spark duration had no effect on lean limit extension, however, after installation of an intake charge turbulator (vaned intake valve). Thus it can be seen that improved ignition systems are necessary to successfully extend operation to leaner conditions; however, because of the interaction of flame initiation with turbulence level and mixture homogeneity, the size of the resulting improvement cannot be

predicted. It is clear, however, that the maximum extension of the lean operating limit would not be realized without an improved ignition system.

1.6 Combustion Chamber Flame Propagation Control

Combustion chamber flame propagation velocity is primarily controlled by heat and mass transfer at the flame front[24]. Turbulence, therefore, has the largest effect on flame propagation since turbulence controls flame front area, heat loss to chamber surfaces, and the physical movement of burning particles to unburned regions. Secondary factors affecting flame propagation are the temperature gradient across the flame front, gas thermal properties (emissivity, conductivity, specific heat), gas concentration (A/F), and active radial diffusion due to concentration gradients.

Turbulent intensity near the spark plug at the time of ignition has the largest effect on cyclic dispersion[4,25,26,27,28,29]. During this initial state of combustion, the spark kernel interacts with the local flow field and develops into a fully developed, turbulent flame front. Excessively high or irregular turbulence will inhibit development, completely quench, or produce a distorted flame front that affects total burn time and peak chamber pressure. Small scale, uniform turbulence is therefore desirable at the spark plug. Ideally, turbulent eddy size should be much smaller than the initial flame kernel[26].

Turbulent intensity in the remainder of the combustion chamber should be relatively high and uniform. Excessive turbulence, however, will increase heat loss to the unburned mixture, thereby prematurely quenching the flame front.

Certain types of turbulence, such as large scale swirl, are not desirable for lean mixtures owing to flame front distortion. In addition, small vortices usually accompany the main swirl[29], producing nonuniform turbulence.

Combustion chamber turbulence is difficult to control since it consists of constantly changing, superimposed flow fields produced by intake charge flow, piston velocity, and combustion chamber shape. The vaned collar intake valve

[3,9,30] and either the "heron"[9] or the "bowl"[31] combustion chamber shapes have demonstrated the most promise towards obtaining turbulence control for the lean mixture application.

1.7 Effect of Compression Ratio on Lean Limit

Increasing the compression ratio above 10 or 11 does not significantly extend the lean limit[32]. In fact, all experimental work reviewed shows initial combustion pressure has no detectable influence on lower flammability limits[2,24].

Very little experimental work has been performed on knock limitations for lean mixture, spark-ignited, gasoline engines as affected by compression ratio. Theoretically, the lean mixture engine will allow operation at a higher compression ratio (thus at higher thermal efficiency) since "end gas" conditions that tend to reduce knock are present. According to Ref. 33, these conditions are lower end gas temperature, density, reactivity, and energy release.

1.8 Power Output Influenced by Lean Mixture Operation

Although good fuel economy and reduced emissions can be realized with lean mixture operation, the maximum power output of the engine is reduced. Power output is proportional to air flow rate, thermal efficiency and equivalence ratio. Thus, for a given air flow rate, power decreases as the equivalence ratio is reduced; however, some of this reduced power is offset by increases in thermal efficiency achieved with lean operation. For example, operation at an A/F of 22.5 has shown power output to be reduced by as much as 33%[14] to 39%[34]. Full power performance can be obtained in lean mixture engines by using fuel enrichment for peak power demands.

1.9 Emissions Controls for Lean Mixture Concept

Evaluation of emissions control methods is augmented by utilizing acceptable analytical prediction methods. The available literature reveals many analytical spark-ignited engine "models" have been developed specifically for prediction of emissions. A summary of material pertient to analysis of engine performance and exhaust emissions is presented in Appendix A.

Leaning the A/F mixture beyond 16 consistently reduces NO_x and CO emissions, but HC emissions decrease to a minimum and then begin to increase at A/F greater than 20 or 22[14]. Since NO_x and CO emissions are inherently decreased with leaning, the bulk of lean mixture emissions experimental work has focused on control of HC.

The increase in HC emissions, as the lean limit is approached, is generally attributed to operation at the engine or "equipment" lean limit[35]. At this point incomplete combustion, borderline misfire, or high cyclic dispersion causes unreacted fuel or HC to be present in the exhaust. Reduction of HC emissions due to the "equipment lean limit" is dependent upon improving combustion chamber mixture, turbulence, and spark, as previously discussed.

Excluding misfire, the majority of HC emissions are formed at combustion chamber surfaces and crevices, owing to wall quenching[6,35]. Wall quenching occurs when the heat release in the flame front is balanced by adjacent wall-surface heat transfer. Wall-surface heat transfer mechanisms are the local turbulence, temperature gradient, and gas thermal properties. Controlling any of these mechanisms to decrease wall-surface heat transfer will decrease HC emissions, owing to a reduction in the effective quench distance or volume.

An effective method of reducing HC emissions[36,37,38] is to increase wall surface temperature (from 150° to 300°F). High wall temperatures have also been found to reduce HC[39] because of decreased adsorption of unburned fuel into the oil film coating the combustion chamber walls. Undesirable effects of high wall temperatures are, however, increased engine octane requirements, reduced volumetric efficiency, accelerated oil oxidation, and increased NO_x and CO emissions[36]. Low wall temperatures (less than 150°F to 200°F) are also undesirable because of a high probability of gasoline wall condensation[40].

More than 50% of all quench-layer-formed HC emissions have been shown to originate in the top-land crevice volume between the piston and cylinder wall[35,36,41]. Two-wall quenching prevents flame propagation into the crevice. Increasing the piston/wall clearance to greater than 0.006-inch precludes this problem, but large crevice areas are susceptible to build-up of deposits which would gradually reduce the clearances to again prevent flame propagation[35].

Unburned HC can be purged from the crevice volume by using or allowing increased blowby[36]. Recirculation of blowby is undesirable in the lean engine where a homogeneous, diluent free mixture is required. Hot blowby gases also cause deterioration and contamination of engine oil.

Elimination of the crevice by moving the compression ring to the top of the piston has been demonstrated to be the best method of controlling HC emissions produced in the top-land crevice volume[36,41]. The most promising development is the "top-land piston"[34] that employs a plasma-applied-molybdenum, graphite-impregnated piston ring face coating. Uncomplicated in design, the top-land piston also reportedly contributes to decreased CO emissions, 50% reduction in blowby, decreased friction horsepower, and increased power output.

Other sources of HC emissions are combustion chamber rough surfaces and engine oil consumption. Smoothing the as-cast combustion chamber from a surface roughness of 540 μin. to 16 μin. reduced HC emissions by 14%[39]. Sporadic and variable increases in HC emissions have been shown to originate with cyclic variations in oil droplets entering the combustion chamber[36]. In addition to directly affecting exhaust HC, combustion chamber oil also produces surface deposits and plug fouling, both of which have demonstrated increased HC emissions[39].

Excluding piston/cylinder/ring wear, oil consumption is basically a production problem and can vary from engine to engine and cylinder to cylinder due to differences in bore profile as affected by thermal and mechanical stresses. Methods of oil control are the tapered bore[35], improved scuff resistant oil rings[41], and smooth (7-15 RMS) cylinder bore[41]. A reduction in oil consumption to essentially zero has been demonstrated with the "sealed ring-orifice" design[39].

1.10 Conclusions

The current status of lean mixture engine technology has been reviewed and presented. The most promising methods for obtaining lean mixture engine operation are summarized as follows:

- Vaporized fuel[16].
- Improved induction system mixing[7].
- High energy, extended duration ignition[3].
- Correct spark plug and location[21].
- Increased combustion chamber turbulence[30].
- Bowl combustion chamber shape[31].
- Increased compression ratio[2].
- Top land piston ring and improved oil control piston ring[41].
- Smooth combustion chamber surfaces[39].

2. STOCK BASELINE

2.1 Description

The baseline engine was a 1973 Chevrolet V-8 with 350 cubic inches displacement (CID) which was selected as being representative of a high production engine in general public use for passenger vehicles. Factory specifications for this engine are given in Table 2.

TABLE 2. ENGINE MANUFACTURERS SPECIFICATIONS

Engine: 1973 Chevrolet V-8
Bore: 4.00 in.
Stroke: 3.48 in.
Displacement: 349.7 cu in.
Compression Ratio: 8.5
Advertised HP: 175 @ 4000 RPM
Advertised Torque: 260 lb-ft @ 2800 RPM
Induction System:
Carburetor: Rochester 4 bbl 7043202
Fuel Pump: Diaphragm type
Intake Manifold: Dual plane type
Ignition System:
Distributor: Delco Remy 1112094 @ 12° BTC basic
Spark Plugs: AC R44 @ 0.035-in. gap
Firing Order: 1-8-4-3-6-5-7-2
Exhaust System: Dual exhaust
Emission Devices:
Air injection reactor (AIR)
Exhaust gas recirculation (EGR)
Positive crankcase ventilation (PCV)
Modified spark advance

The stock ignition system is the standard breaker point type consisting of a coil, condenser, distributor, wiring, and spark plugs. The spark advance characteristic is determined by the 12° BTDC basic advance and the contributions of the centrifugal and vacuum advance mechanisms. The centrifugal and vacuum advance characteristics for this engine are given in Figure 2.

Factory-installed devices for emission control include an air injection reactor (AIR) pump, an exhaust gas recirculation (EGR) system, and a positive crankcase ventilation (PCV) system. The AIR system is designed to reduce hydrocarbon and carbon monoxide emissions by introducing air into the exhaust manifold.

The EGR system recirculates a portion of the exhaust gases to a region directly below the carburetor throttle plates. These exhaust gases dilute the incoming charge, resulting in lower peak combustion temperatures which produce less NO_x emissions. EGR flow rate is controlled by balancing the intake manifold vacuum against the spring tension in the EGR value. Maximum EGR rates are 8-12% for the Chevrolet V-8.

The PCV system maintains a positive flow of crankcase blow-by gases into the engine air intake system.

2.2 Engine Dynamometer Results

All engine tests were accomplished using Indolene-Leaded Motor Fuel No. 30 which has a stoichiometric A/F of 14.45 and a lower heating value of 19,030 Btu/lbm.

Several engine modifications were made for the engine dynamometer test configuration to improve the experimental setup and to permit the taking of additional diagnostic data. The stock diaphragm fuel pump was replaced with a pressurized fuel tank to permit a more accurate measurement of gasoline flowrate. The standard carbon-core spark plug wires were replaced with metallic conductor, silicone-insulated ignition wire. The stock dual exhaust manifolds were replaced with special Heddman headers to permit exhaust gas

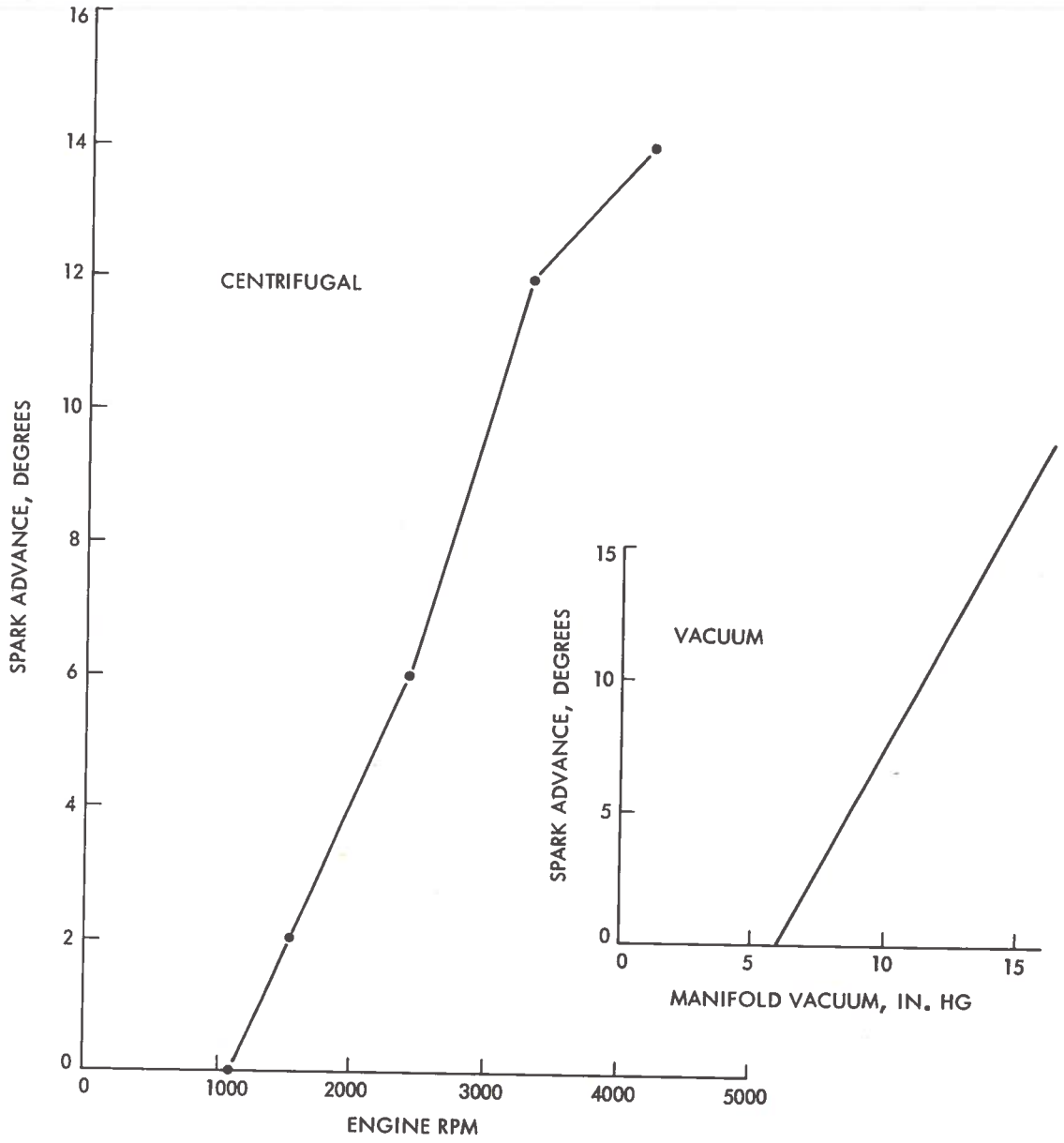

FIGURE 2. SPARK ADVANCE CURVES FOR 1112094 DISTRIBUTOR

sampling of the individual cylinders. The AIR pump was disconnected for the baseline tests since the air injection tube manifolds were not compatible with the special exhaust headers. The engine-driven cooling fan was not in operation during the engine dynamometer tests.

The exhaust gas was continuously analyzed to determine the concentration of carbon monoxide (CO), carbon dioxide (CO_2), nitrogen oxides (NO_x), and unburned hydrocarbons. The CO_2 and CO analyzers operate on the principle of infrared absorption. Nitric oxide (NO) and nitrogen dioxide (NO_2) were measured with a chemiluminescent instrument. Oxides of nitrogen are reported as the sum of NO and NO_2 contained in a gas sample as if the NO were in the form of NO_2. Hydrocarbons were measured with a flame ionization detector.

The stock carburetor is designed to meter gasoline into the airstream in such quantities as are required to maintain the proper fuel-to-air ratio (F/A) for all speeds and loads. Under idling and low load conditions, a richer mixture is used to offset the effects of exhaust gas dilution resulting from a closed or almost-closed throttle. With medium load conditions, the mixture can be made leaner to give improved economy. To achieve maximum power, a rich mixture is again necessary. The variation in F/A with load at 2000 RPM is given in Figure 3 for the Chevrolet V-8 tuned to factory specifications. The data is presented in terms of the equivalence ratio (ϕ) which is defined as the F/A of the mixture divided by the stoichiometric F/A for the fuel.

In its final form the baseline data is presented in terms of contour plots of BSFC, equivalence ratio and brake specific emissions on the BMEP-RPM plane which are shown in Figures 4, 5, 6, 7, and 8. Several-data-smoothing operations are used in processing the data for contour plots. All data is corrected to the nominal RPM by assuming that the indicated specific fuel consumption and equivalence ratio are constant for the correction. The corrected data is then curve-fitted by a 3rd-order polynominal. Typical curve-fit plots of BSFC and brake specific emissions are shown in Figures 9, 10, 11 and 12 for 2000 RPM. Additional curve-fit plots are included in Appendix B. The contour plots are made by interpolating only within the bounds of the test data.

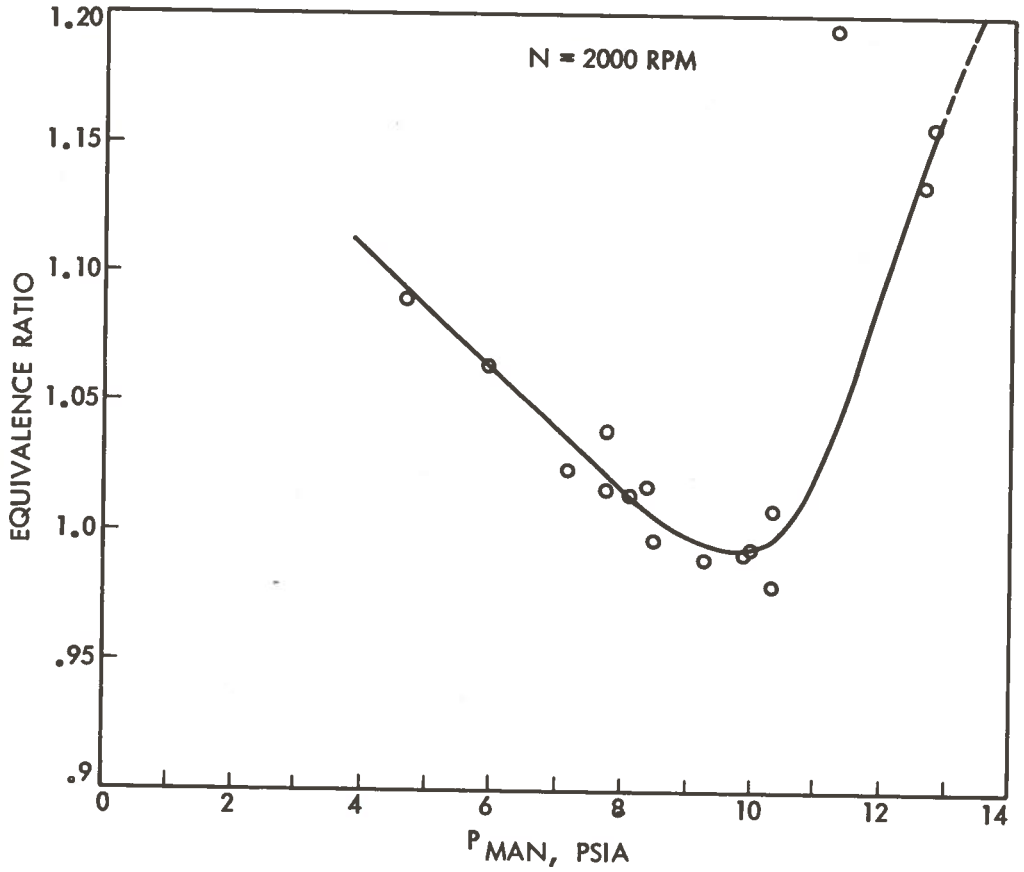

FIGURE 3. EQUIVALENCE RATIO VS. LOAD FOR STOCK ENGINE

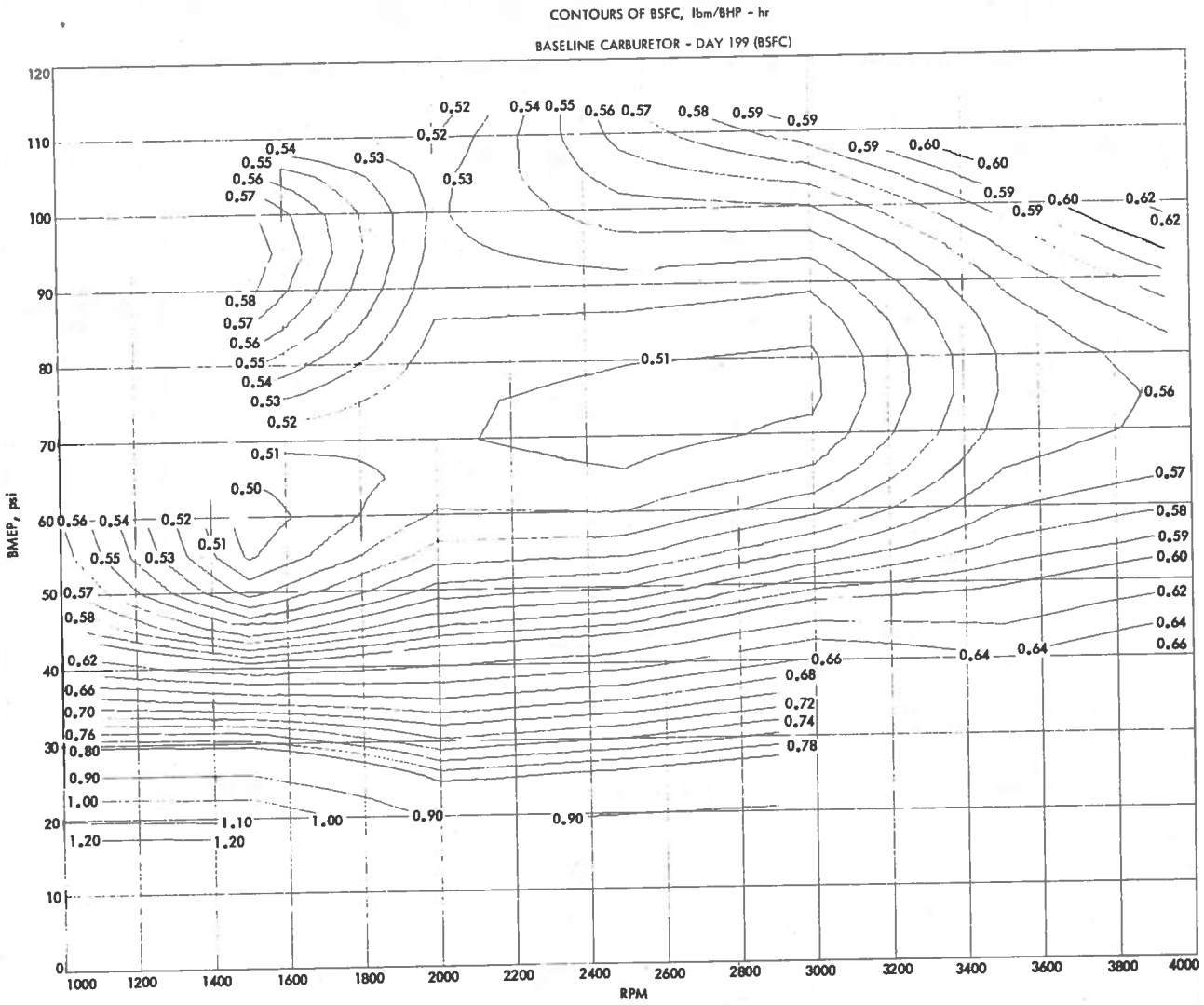

FIGURE 4. BSFC CONTOUR MAP FOR BASELINE ENGINE

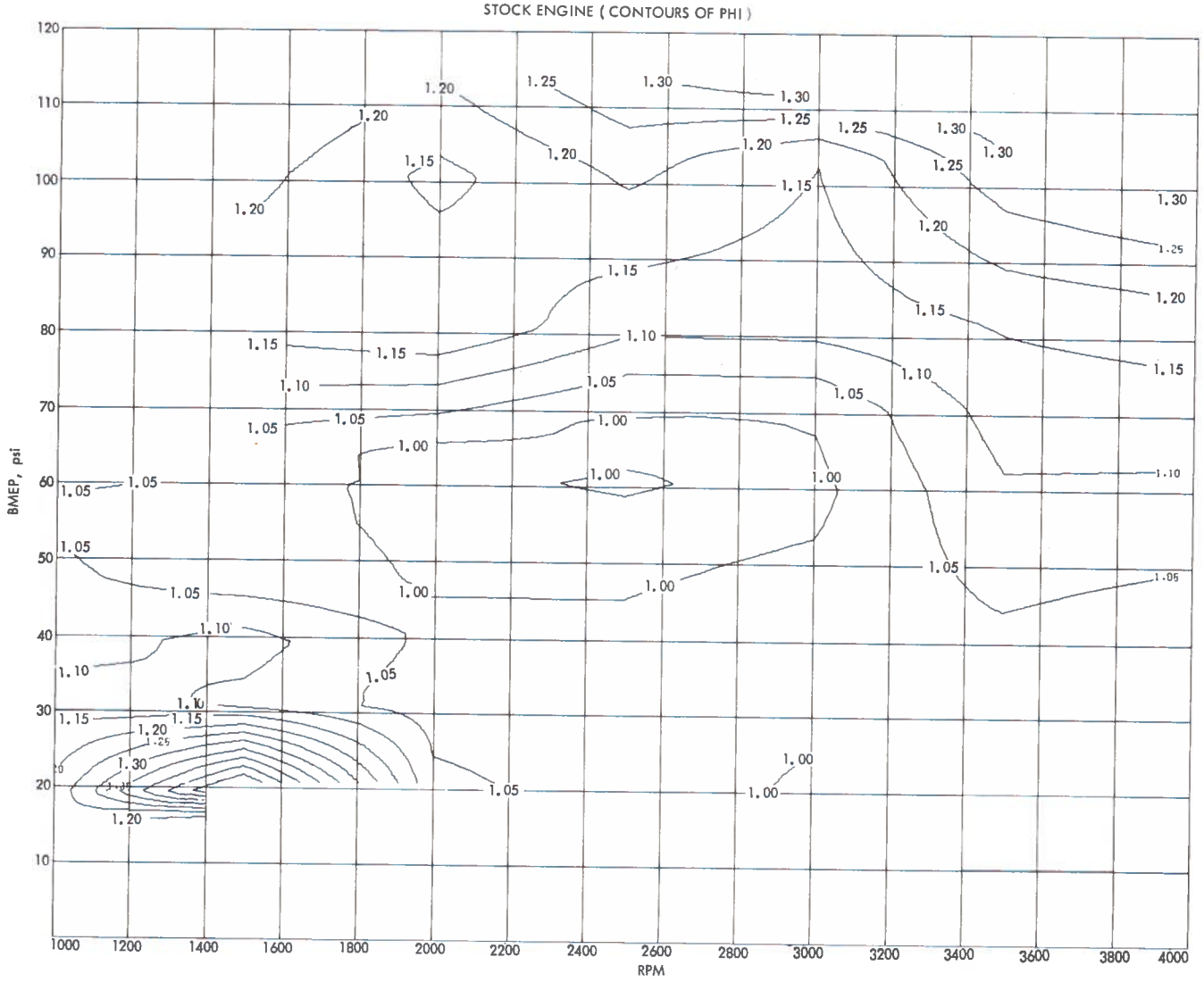

FIGURE 5. EQUIVALENCE RATIO CONTOUR MAP FOR BASELINE ENGINE

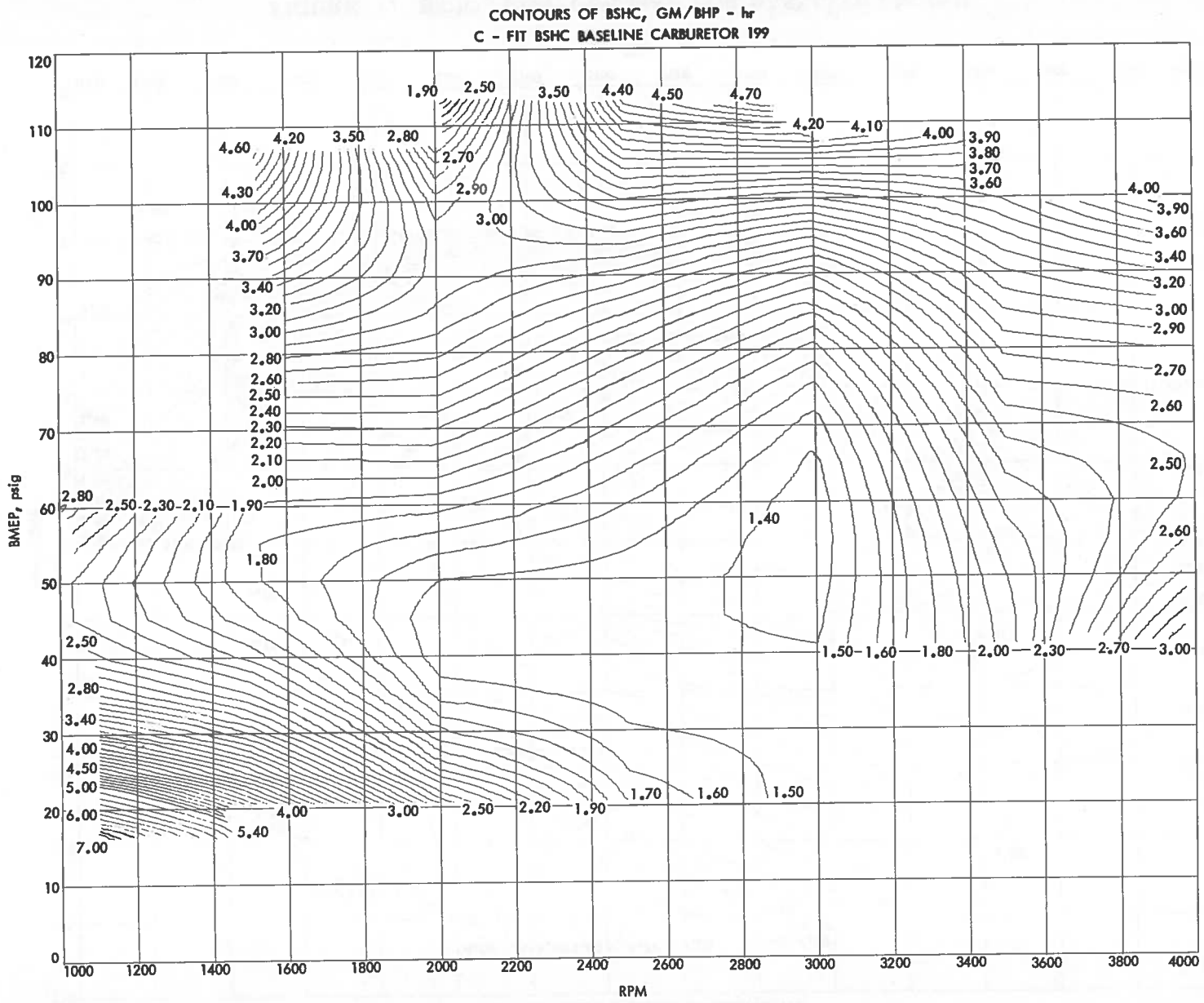

FIGURE 6. BSHC CONTOUR MAP FOR BASELINE ENGINE

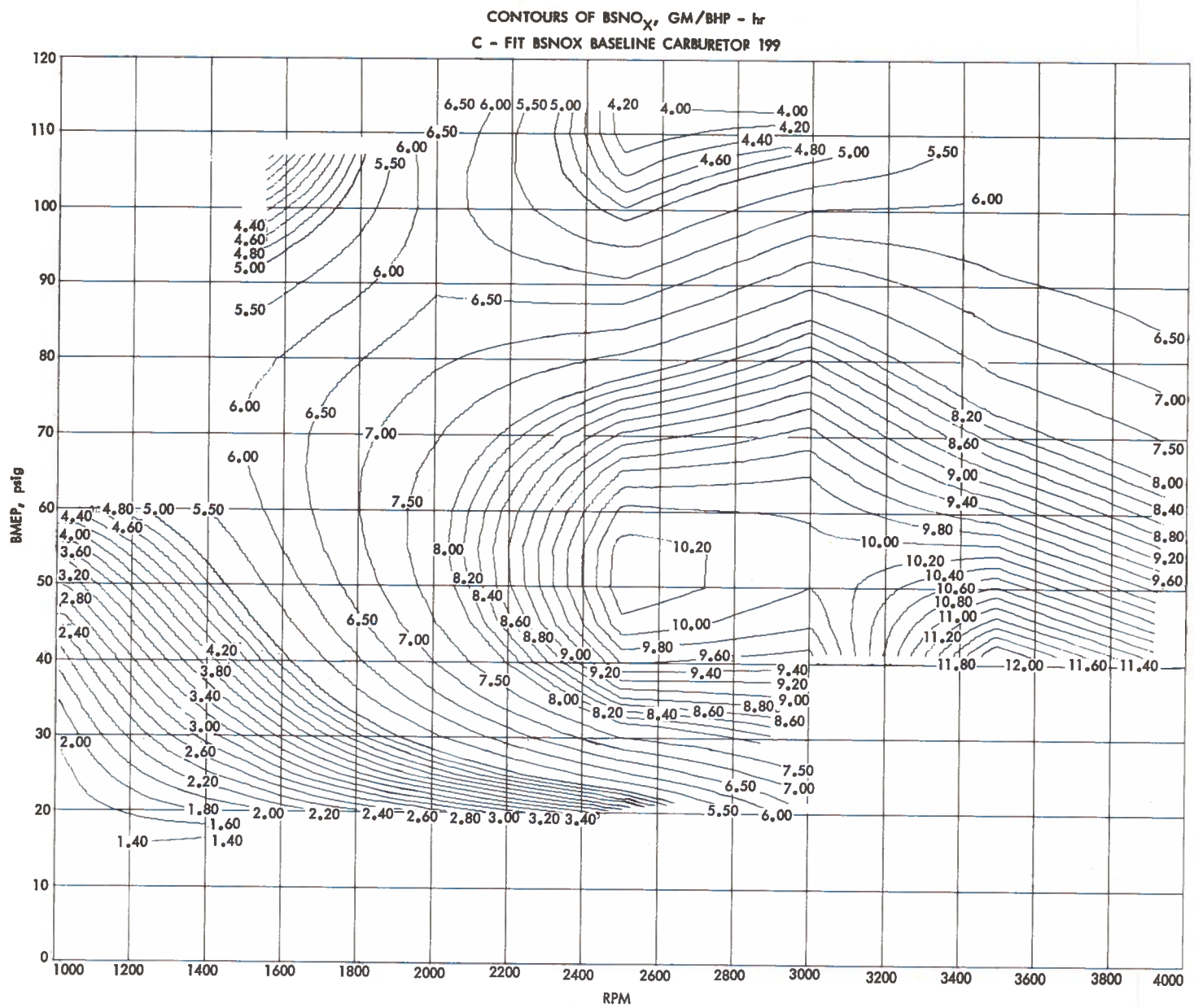

FIGURE 7. BSNO$_X$ CONTOUR MAP FOR BASELINE ENGINE

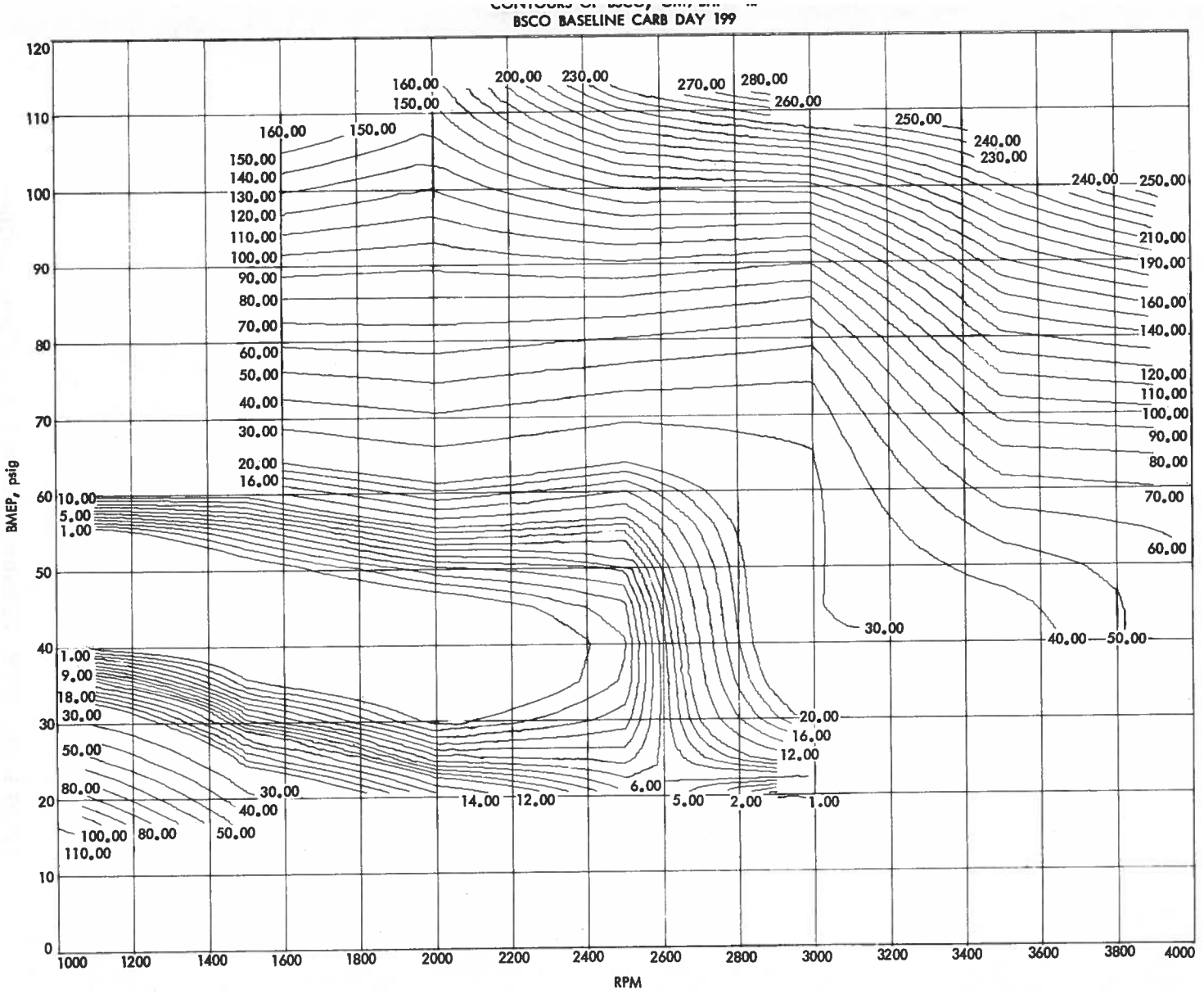

FIGURE 8. BSCO CONTOUR MAP FOR BASELINE ENGINE

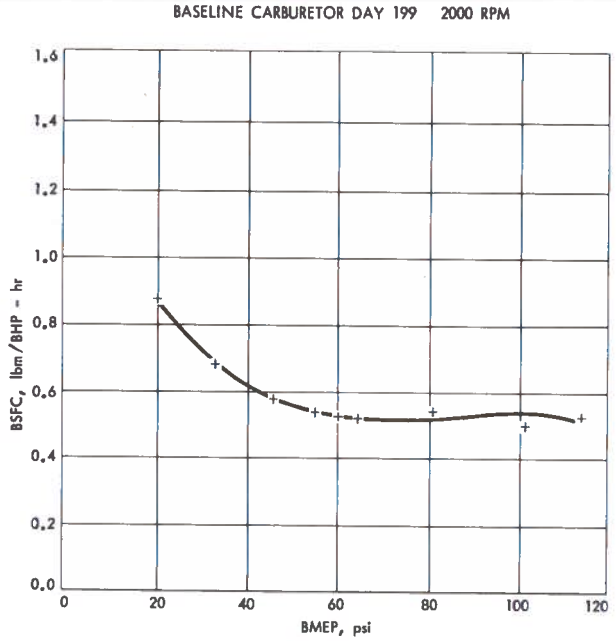

FIGURE 9. BSFC VERSUS LOAD FOR BASELINE ENGINE

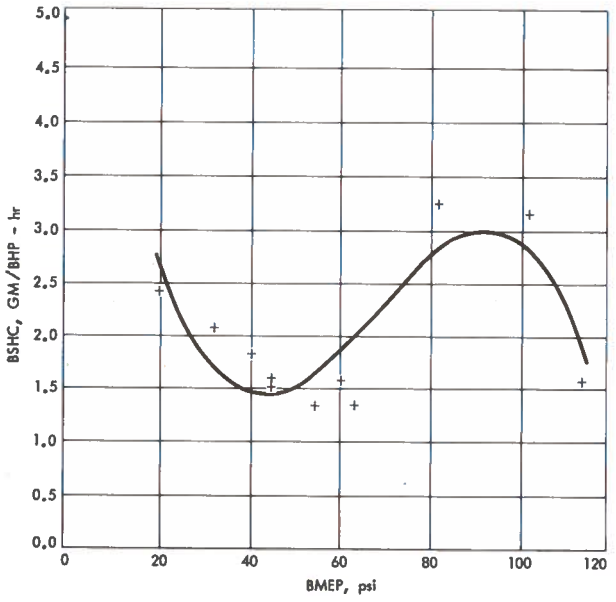

FIGURE 10. BSHC VERSUS LOAD FOR BASELINE ENGINE

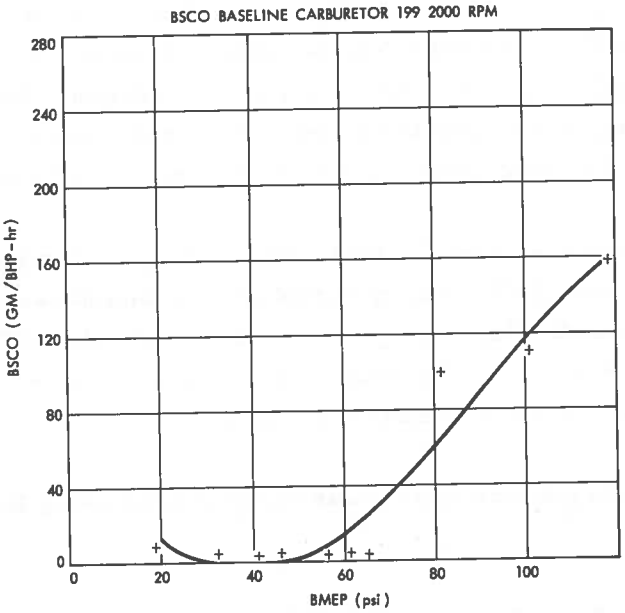

FIGURE 11. BSCO VERSUS LOAD FOR BASELINE ENGINE

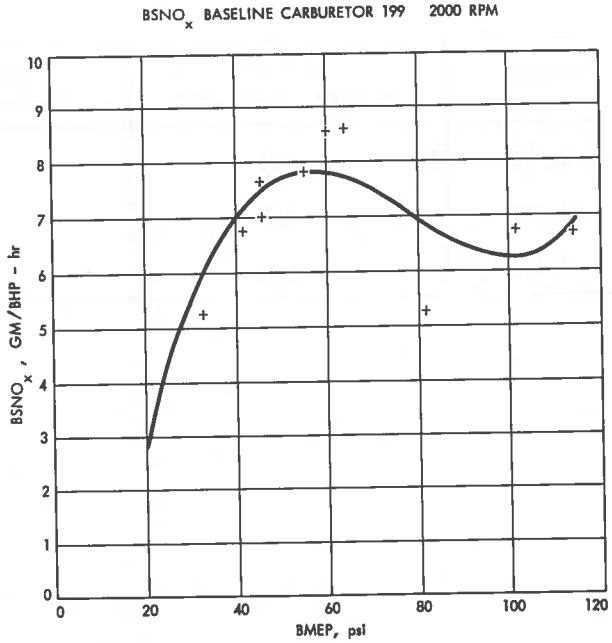

FIGURE 12. BSNO$_X$ VERSUS LOAD FOR BASELINE ENGINE

2.3 Chassis Dynamometer Results

Data were taken on a chassis dynamometer with a 350 CID Chevrolet V-8 engine installed in a 1973 Chevrolet Impala sedan. The car was tuned to factory specifications with all emission control devices in operation. The vehicle was equipped with an automatic transmission and a 2.73 rear axle ratio. This makes an engine speed of 2000 RPM correspond to approximately 55 MPH in high gear.

A CVS emissions test over the EPA urban driving cycle using the 1975 Federal Test Procedure (FTP) was conducted with an inertia wheel simulating a 4500 lbm vehicle mass. Fuel consumption over the simulated 7.5 mile urban driving course was 10.6 MPG. Emissions results are compared with the interim 1977 Federal emission standards in Table 3.

All chassis dynamometer testing was accomplished using Indolene-leaded Motor Fuel No. 30.

TABLE 3. STOCK CVS EMISSIONS

Emissions	Stock	1973 Federal Standard	Interim 1977 Federal Standard
HC (gm/mi)	2.15	3.4	0.41
CO (gm/mi)	36.08	39.0	3.4
NO_x (gm/mi)	2.05	3.0	2.0

3. LEAN BURN ENGINE CONFIGURATION NO. 1 (LBEC-1)

3.1 Description

The modified configuration (LBEC-1) was derived from the baseline configuration by replacing the carburetor and intake manifold with Autotronics equipment consisting of an air-driven atomizer and a single plane Edelbrock Tarantula manifold. The Autotronics equipment is shown installed on the engine in Figure 13. A positive displacement electric fuel pump was added for fuel/air ratio control. Components of this system are listed in Table 4.

Air flow to the engine is sensed by a turbine air flow transducer. Over most of the engine operating range, a baseline air/gasoline ratio is controlled to be constant. A voltage proportional to air flow drives a voltage-controlled oscillator, whose output is compared with the tachometer signal from the positive displacement gasoline metering pump. The resulting error signal is used by the pump power drive circuit to supply more or less electrical power to the pump, hence changing the gasoline flowrate.

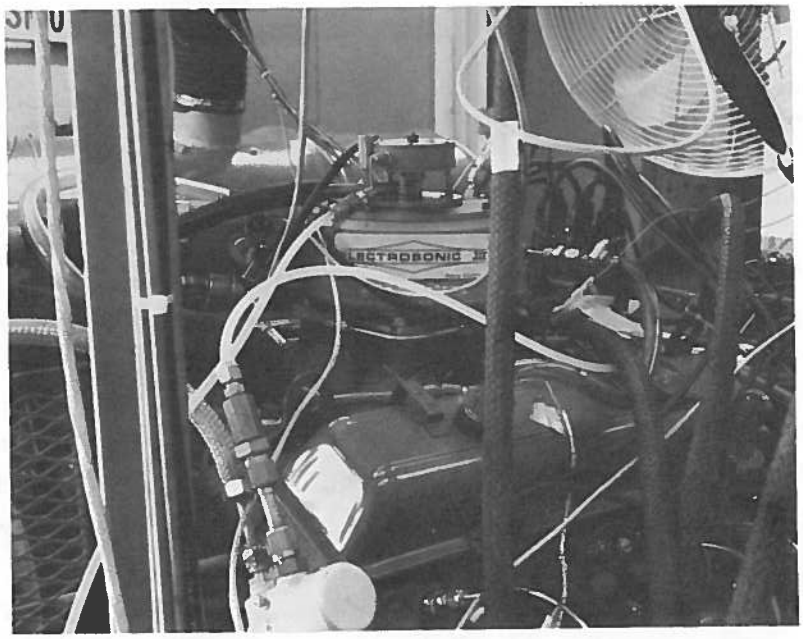

FIGURE 13. AUTOTRONICS INDUCTION CONTROL SYSTEM

TABLE 4. MODIFIED ENGINE COMPONENTS

Induction System:

Air/Fuel Control: Linear airflow transducer series 110 Model 450F. Positive displacement fuel metering pump, Digipump Model 304. Electronic controller Model 253D. Air throttle assembly including throttle valve, throttle position sensors, mixing chamber and pneumatic atomizer Model 200. Fuel valve Model 210B. Flow computer Model 100D. Data terminal box Model 265.*

Intake Manifold: Single plane type.

Ignition System:

Distributor: Delco Remy 1112094 less centrifugal and vacuum advances

Spark Plugs: Champion RBL-17Y @ 0.070-inch gap

Control: Multiple spark discharge Model 405A with CDN coil

Exhaust System: Special headers

Emission Devices: PCV system

*Model numbers refer to Autotronics Controls Corp. of El Paso, Texas.

Air throttling is achieved by rotation of the air butterfly valve located upstream of a mixing chamber. Primary air enters the mixing chamber with a vortex flow pattern and imparts a swirling motion within the plenum. Secondary air flow that bypasses the throttle plate drives a sonic-type atomizer which is shown in Figure 14. The atomizer, which is located directly above the intake manifold and is centered relative to the manifold, receives gasoline from the positive displacement metering pump. In the atomizer a jet of high-velocity air is impinged upon the open end of a small cavity, which resonates to provide acoustic waves in the space between the air nozzle and the cavity. The atomized gasoline is then mixed with the primary airstream as it flows through

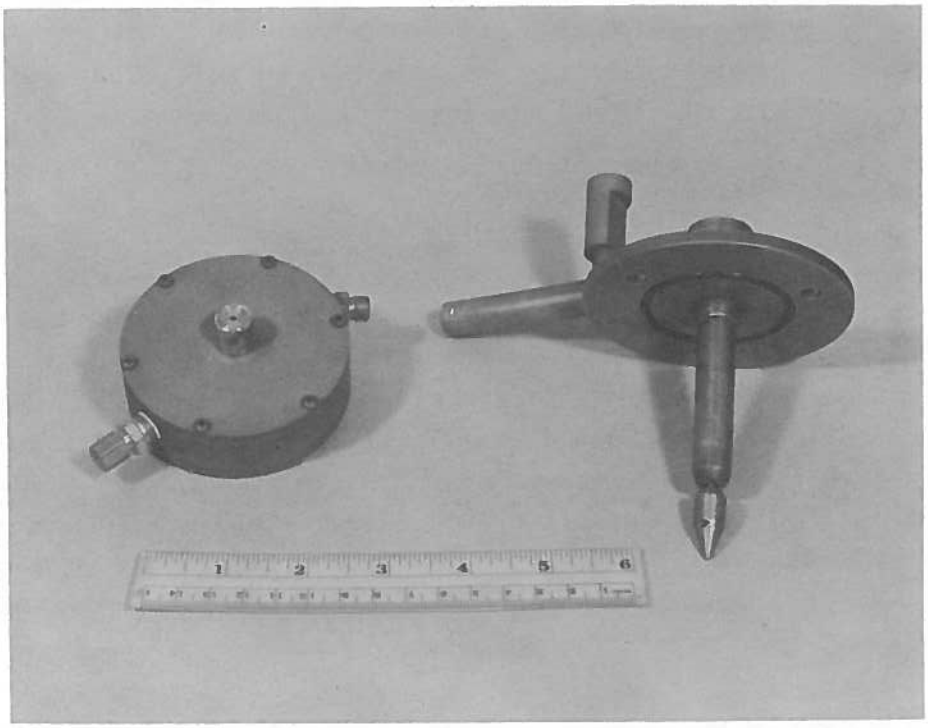

FIGURE 14. COMPONENTS OF AUTOTRONICS INDUCTION CONTROL SYSTEM

the plenum chamber. The precise gasoline/air mixture is then distributed to each cylinder with an aluminum, single-plane intake manifold manufactured by Edelbrock.

The modified ignition system consists of a special coil with a fast rise time, a condenser, and distributor breaker points. Its primary features are multiple striking with external control of the retard and duration of firing. The high energy (60,000 v open circuit voltage) capacitive discharge ignition system provides the multiple spark capability with variable repetition rates extending over as much as 40 crankshaft degrees. It also has the capability of an electronic retard control of 20 degrees maximum. Both the centrifugal and vacuum advance features of the stock distributor have been eliminated.

Champion RBL-17Y spark plugs are used with a gap set of 0,070 inch. Special "mag wire" ignition wires, as recommended by Autotronics, are employed. These include a metallic conductor and a Monel shield wire. The Autotronics electronics require special shielding from the ignition system.

3.2 Engine Dynamometer Results

A series of engine sensitivity tests were conducted to establish the values of equivalence ratio and spark advance which give minimum fuel consumption. The run conditions were selected to be representative of the conditions encountered on the Federal Driving Cycle. For each operating condition (BHP and RPM), several equivalence ratios and spark advances were tested to determine the sensitivity of brake specific fuel consumption (BSFC) to changes in these parameters. Because of the time required for emissions measurements, no exhaust analysis was performed during the sensitivity tests in order to permit a more thorough investigation of the minimum fuel consumption condition.

For each run condition, the minimum fuel consumption condition was identified from wedge plots (gasoline versus air flowrate) of the smoothed data. The data were corrected to the nominal BHP and RPM by assuming that the indicated specific fuel consumption and equivalence ratio are constant for small corrections in BHP and RPM. A typical wedge plot is shown in Figure 15 for 2000 RPM and level-road-load power. Other wedge plots for the sensitivity data are included in Appendix C.

Minimum fuel consumption occurred at an equivalence ratio of 0.85 with a 50° spark advance. The sensitivity data for this modified engine indicated an average 8.7% reduction in BSFC when compared with the stock engine data as shown in Table 5. Contour maps of BSFC and brake specific emissions have been prepared for this modified engine in an effort sponsored by the Environmental Protection Agency[42].

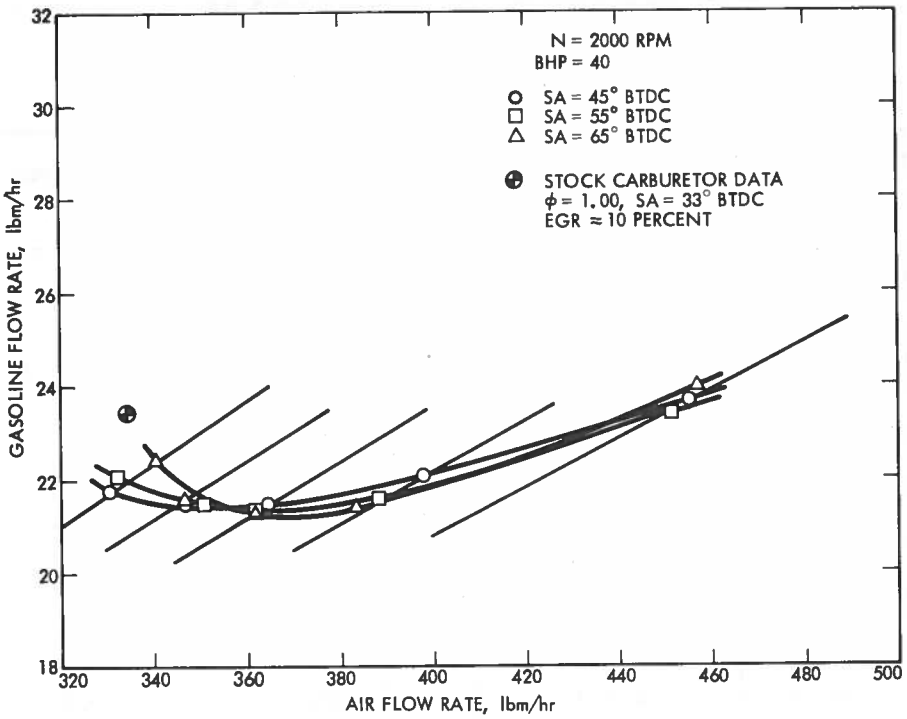

FIGURE 15. WEDGE PLOT FOR LBEC-1

3.3 Chassis Dynamometer Results

Chassis dynamometer data were obtained for an engine identical to the engine dynamometer test engine except that it retained the stock exhaust system. The engine was installed in a 1973 Chevrolet Impala sedan with an automatic transmission and a 2.73 rear axle ratio. The engine was tuned to operate at a primary equivalence ratio of 0.85 and a spark advance of 50°.

A CVS-2 emission test was conducted over the EPA driving cycle using a 4500 lbm inertia wheel. Average fuel consumption over the cycle was 12.8 MPG which is a 20% improvement over the stock baseline data. Emissions results are compared with those for the stock vehicle in Table 6.

TABLE 5. BSFC COMPARISON OF STOCK AND LBEC-1 ENGINES

RPM	BMEP (psi)	Stock BSFC (lbm/BHP-hr)	Modified BSFC (lbm/BHP-hr)	% Decrease in BSFC
1000*	40.7	0.640	0.547	14.5
1000*	40.7	0.640	0.556	13.1
1500	15.1	1.100	0.945	14.1
1500	33.2	0.665	0.598	10.1
1500	34.7	0.655	0.593	9.5
1500	46.8	0.581	0.521	10.3
2000	36.2	0.650	0.592	8.9
2000*	45.3	0.581	0.529	9.0
2000*	45.3	0.581	0.531	8.6
2000	55.4	0.532	0.503	5.5
2000	64.5	0.522	0.482	7.7
2000	70.1	0.526	0.469	10.8
2500	39.8	0.616	0.571	7.3
2500	51.6	0.552	0.524	5.1
2500	55.2	0.534	0.511	4.3
2500	81.5	0.520	0.462	11.2
3000	40.0	0.637	0.589	7.5
3000	64.1	0.540	0.506	6.3
3000	68.6	0.532	0.497	6.6,

*Repeat Points.

TABLE 6. COMPARISON OF CVS EMISSIONS FOR THE STOCK AND LBEC-1 VEHICLE

Emissions	Stock	LBEC-1	1973 Federal Standard	Interim 1977 Federal Standard
HC (gm/mi)	2.15	4.49	3.4	0.41
CO (gm/mi)	36.08	15.04	39.0	3.4
NO_x (gm/mi)	2.05	5.12	3.0	2.0

As expected, the NO_x and HC emissions were worse than the stock vehicle with its emission control equipment in operation. Neither EGR nor AIR was used during vehicle tests with the modified engine.

4. LEAN BURN ENGINE ANALYSIS

4.1 Blumberg-Kummer Cycle Program

The Blumberg-Kummer (B-K) computer program incorporates the modified Zeldovitch kinetics mechanism for NO_x production into a general thermodynamic analysis of a spark-ignited IC engine cycle. It is possible to predict quantitatively the NO_x emissions, mean effective pressure, horsepower, specific fuel consumption and thermal efficiency as a function of the following variables: fuel type, equivalence ratio, percent EGR, compression ratio, intake manifold temperature and pressure, RPM, combustion interval and spark advance. Additional details of the model can be found in Ref. 43.

The calculational method assumes that the instantaneous heat transfer rate is negligible. This assumption should have a minimal effect on the NO_x calculation since most of the NO_x formation occurs over a short time in the cycle. Because of this heat transfer assumption, predicted thermal efficiencies are higher than those achievable in practice; however, they should be acceptable for making comparative analyses.

4.2 Stock Engine

Spark advance data was used to establish the combustion interval information needed for the B-K program. The minimum spark advance for best torque (MBT) as a function of equivalence ratio (ϕ) is shown in Figure 16 for the stock Chevrolet V-8, the LBEC-1 and the single-cylinder CFR engine. In the absence of detailed information about the combustion processes in these engines, the combustion interval was assumed to be 2 times the MBT spark timing for all theoretical calculations. This assumption is consistent with the predictions of the B-K program when the ignition delay is negligible.

The data show no significant difference between the spark timing characteristics for LBEC-1 and the stock engine over the range of available test data. At the same ϕ, the MBT spark timing for the CFR engine was

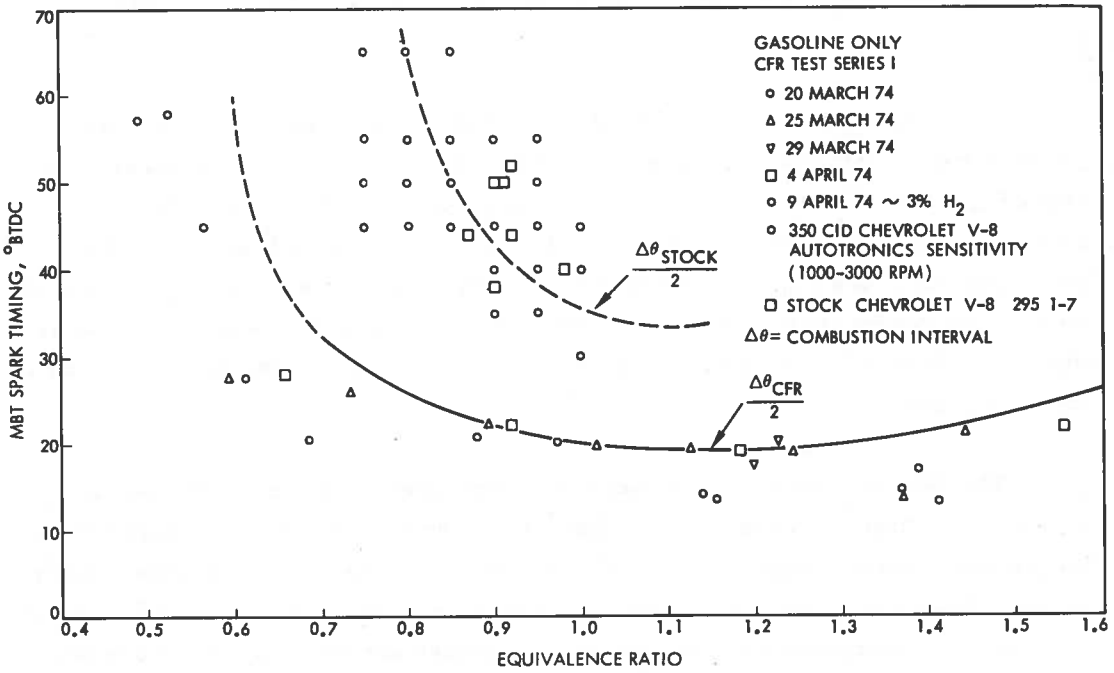

FIGURE 16. SPARK ADVANCE FOR BEST TORQUE VS. EQUIVALENCE RATIO

significantly less than that for the two V-8 configurations. For negligible ignition delay, this characteristic implies a faster burning charge in the CFR engine. The CFR was equipped with shrouded intake valves to increase the combustion chamber turbulence. Very little valve overlap in the CFR engine results in a smaller exhaust residual in the mixture. Although some of these design features produce good results in research engines like the CFR, they cannot be incorporated in the same form in the modern, high-performance, variable-speed V-8 engines in present automobiles.

In the analyses discussed here, the CFR combustion interval characteristic has been used as an upper bound for the improvement in combustion interval for the Chevrolet V-8. Although the ignition delay assumption is probably inaccurate based on subsequent data for a second lean-burn engine configuration

(LBEC-2), it has a similar effect on both the CFR and V-8 characteristics in Figure 16 and should not significantly alter the results of these comparative analyses.

Using the stock combustion interval from Figure 16, the stock spark advance characteristic from Figure 2, and the equivalence ratio characteristic from Figure 3, the B-K model was used to predict the BSFC and $BSNO_x$ emissions for the stock engine at 2000 RPM. As shown in Figure 17, the predicted fuel consumption varies with load in a manner similar to the baseline data. The differences between the predicted curve and the data are primarily due to the fact that heat transfer losses during the combustion are neglected in the B-K model.

The NO_x emissions predictions are compared with the stock data in Figure 18. Predicted curves are shown for zero and 10% EGR. The EGR rate on the stock engine varies from 8-12% for low loads to zero EGR under heavy loads. The exact point for the transition to zero EGR is not known at present; however, measurements of the cracking pressure for the EGR valve are planned. An assumed EGR transition curve is shown for illustration purpose. The predicted curves generally bracket the data except under heavy loads where the prediction falls well below the observed emissions.

In assessing the merits of the lean burn concept, it is important to understand the performance benefits and penalties associated with the stock emission control equipment. In particular, what fuel economy penalties result from the use of EGR and a nonoptimum spark advance characteristic? Predicted fuel economy effects are shown in Figure 19, which indicates a minimal improvement in BSFC results if EGR is removed while retaining the stock spark advance; however, a 3-4% reduction in BSFC is available with MBT spark timing and no EGR. In this comparison 10% EGR is assumed for the stock engine.

The beneficial effects of EGR and retarded spark timing in controlling NO_x emissions are illustrated in Figure 20. The stock engine used as a reference is assumed to have 10% EGR. Removal of EGR results in a factor of

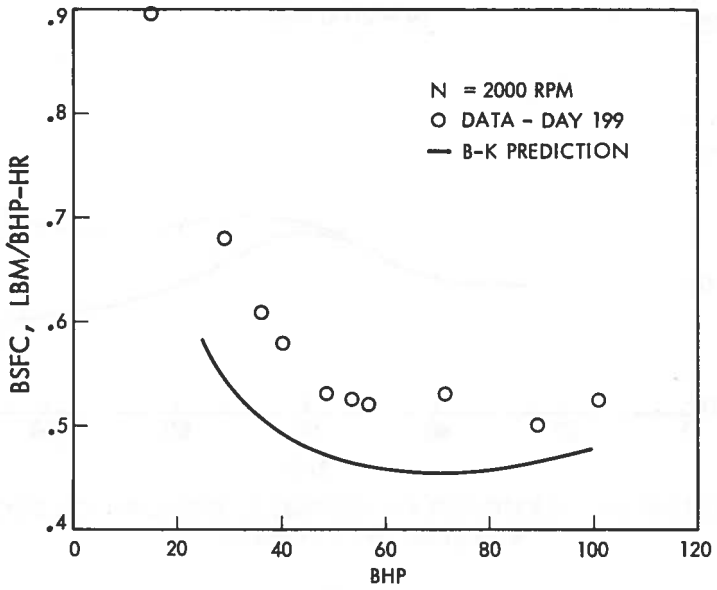

FIGURE 17. FUEL CONSUMPTION CHARACTERISTIC FOR STOCK ENGINE

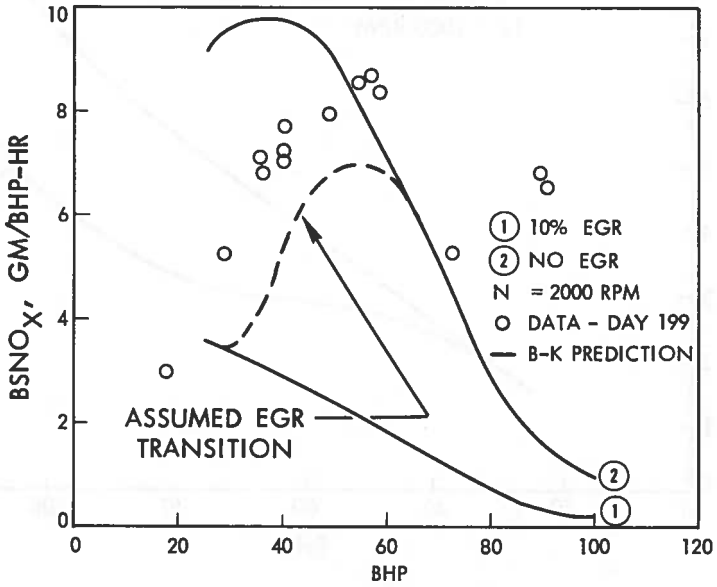

FIGURE 18. NO_x EMISSION CHARACTERISTIC FOR STOCK ENGINE

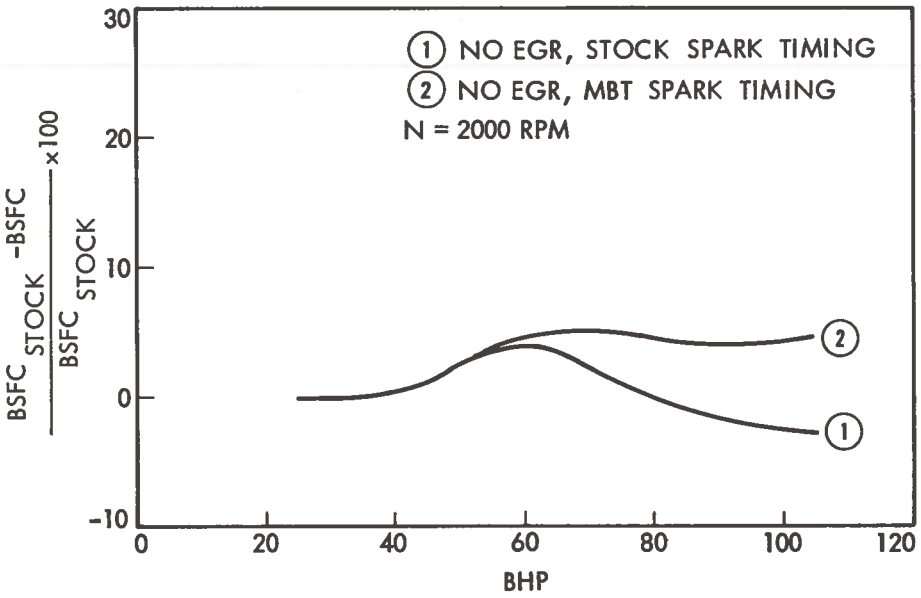

FIGURE 19. EFFECTS OF STOCK EMISSION CONTROL EQUIPMENT ON BSFC

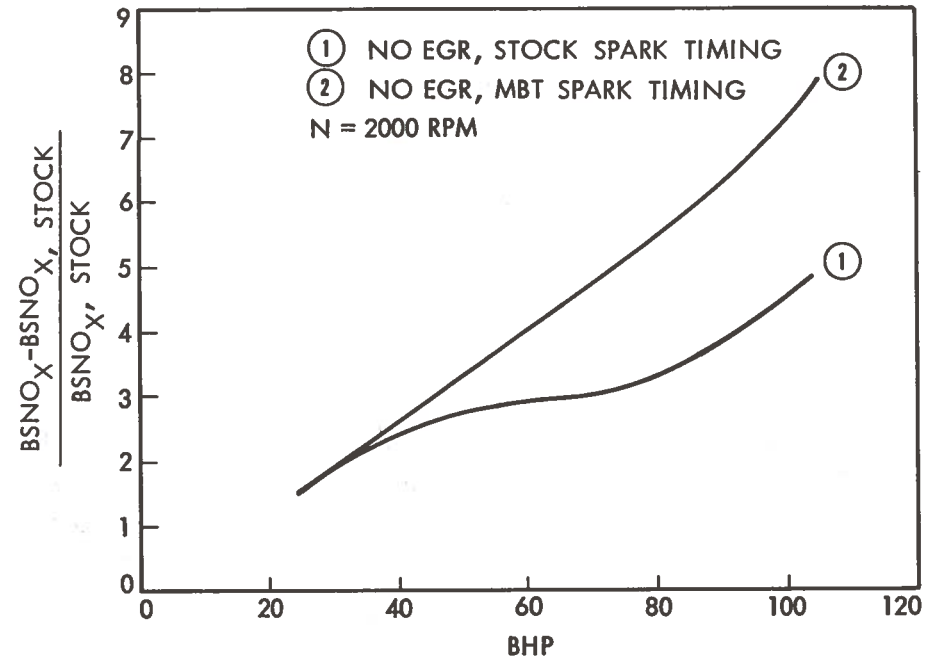

FIGURE 20. EFFECTS OF STOCK EMISSION CONTROL EQUIPMENT ON $BSNO_x$ EMISSIONS

3 increase in the NO_x emissions. If in addition the spark advance is changed to MBT, NO_x emissions increase by a factor of 5 over the stock emission values. Thus, calculations indicate that EGR and a retarded spark are effective means for controlling NO_x and result in only a slight fuel economy penalty.

4.3 Lean Burn Engine Configuration No. 1 (LBEC-1)

As mentioned earlier, the results of the sensitivity tests indicated that the LBEC-1 engine had its minimum fuel consumption at an equivalence ratio of 0.85 and with a 50° spark advance. Using this information and the stock combustion interval from Figure 16, the cycle analysis model was used to predict the BSFC and $BSNO_x$ emissions for the LBEC-1 engine at 2000 RPM.

Again the effect of load on BSFC is adequately predicted by the model as shown in Figure 21, with the differences being caused by the heat transfer present in the actual engine. A prediction of the $BSNO_x$ emissions is given in Figure 22. Emissions maps for the LBEC-1 engine were generated for the Environmental Protection Agency[43] and the NO_x emissions are in general agreement with the predictions of Figure 22.

4.4 Stock and Lean Burn Engine Comparison

To predict the potential performance gains available through the use of lean burn engines, it is necessary to make analytical comparisons of the lean burn engine with some reference engine. To assess the ability of the B-K model to make such studies, a comparison of the stock engine and the LBEC-1 engine was made, since this data is available.

The BSFC comparison of these engines is given in Figure 23. The B-K prediction curve was obtained by using the prediction curves for the stock and modified engines from Figures 17 and 21, respectively. The curve representing the data was generated from computer curve-fits of the stock and modified engine BSFC data. Although the curve shapes are somewhat different, the overall agreement between prediction and data is satisfactory.

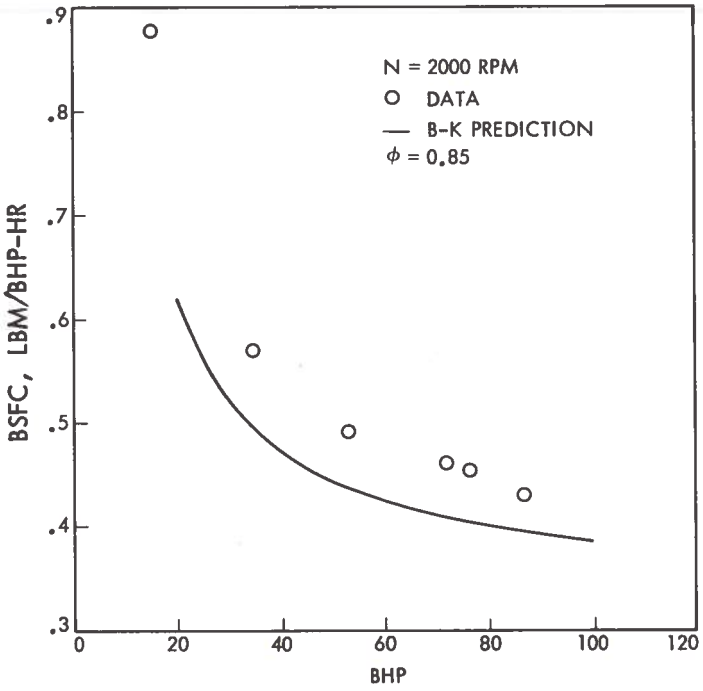

FIGURE 21. FUEL CONSUMPTION CHARACTERISTIC FOR LBEC-1 ENGINE

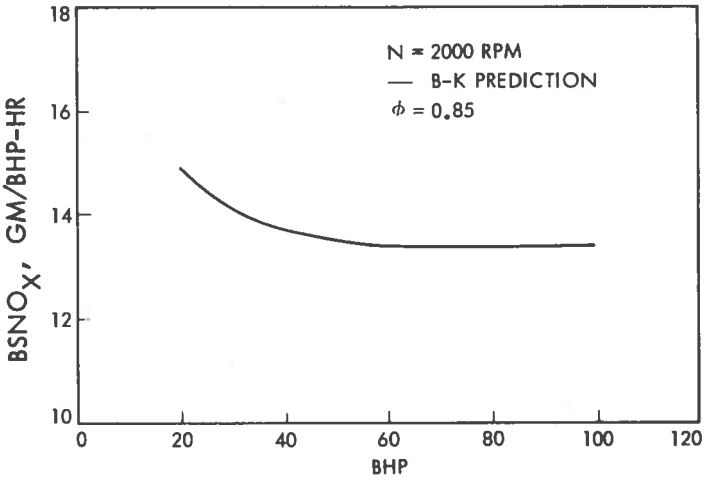

FIGURE 22. NO_x EMISSION CHARACTERISTIC FOR LBEC-1 ENGINE

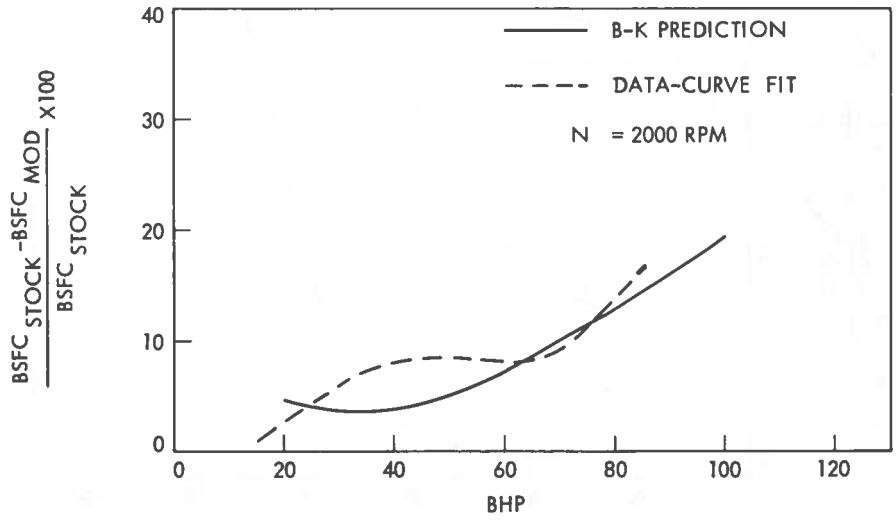

FIGURE 23. BSFC COMPARISON FOR STOCK AND LBEC-1 ENGINES

A similar comparison is made in Figure 24 for the NO_x emissions predictions. The two curves represent the stock engine with 10% EGR and with no EGR. As mentioned earlier, the EGR rate on the stock engine changes from about 10% for low loads to zero under heavy loads. Although no engine dynamometer emissions data was obtained for DOT on the modified engine, results from the EPA driving cycle comparison of the stock and modified engine indicate that the modified engine produced about 2.5 times the NO_x produced by the stock engine. This value falls between the two prediction curves except at heavy load conditions. The steep climb of the prediction curves at heavy loads is probably not too realistic in this case since it results primarily from the lack of agreement between prediction and data for the stock engine under heavy load.

4.5 Combustion Interval Effects

Lean-burn operation offers the potential for improved fuel economy by increasing engine thermal efficiency as shown in Figure 25, which includes

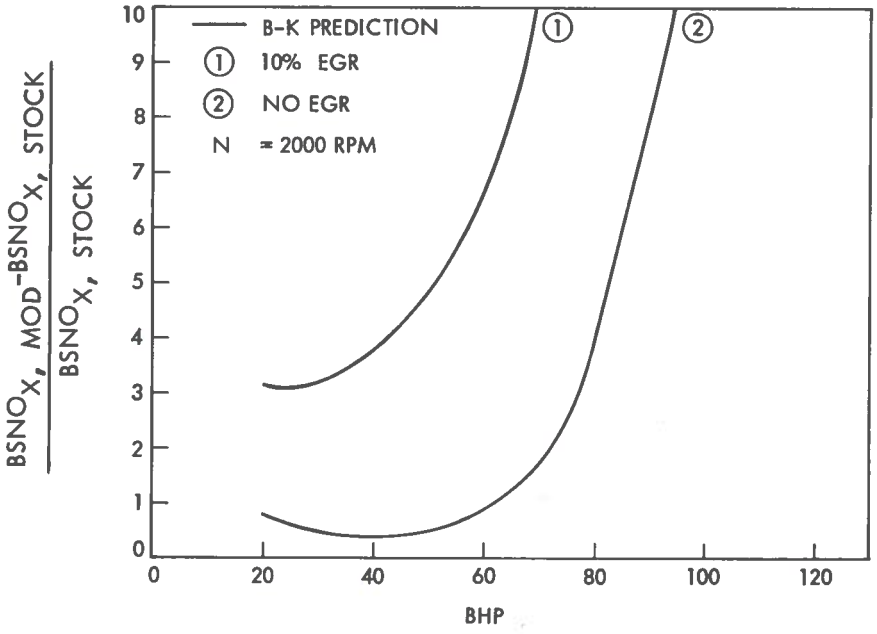

FIGURE 24. $BSNO_x$ COMPARISON FOR STOCK AND LBEC-1 ENGINES

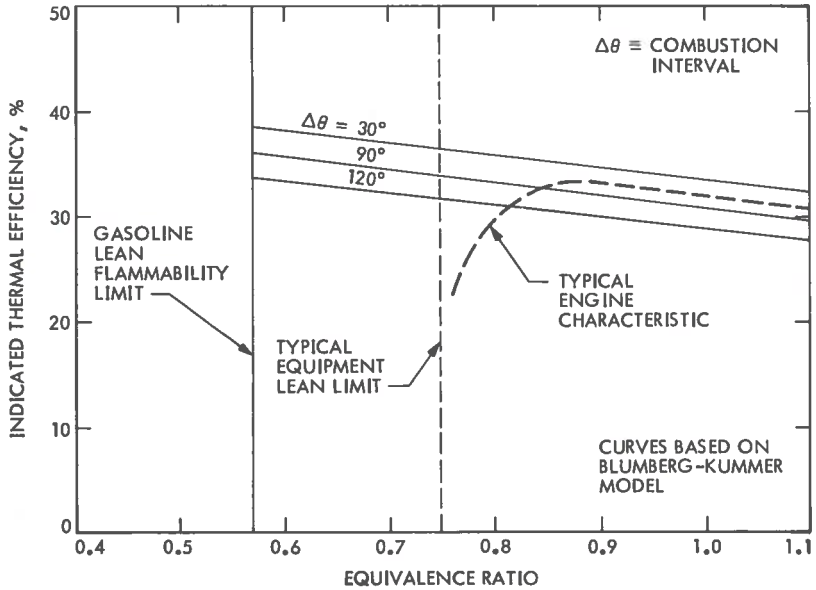

FIGURE 25. THERMAL EFFICIENCY VERSUS EQUIVALENCE RATIO

curves for three combustion intervals. It is observed that higher thermal efficiency is achieved with the shorter combustion interval. If it were possible to maintain a constant combustion interval while lowering the equivalence ratio, then significant improvements in engine thermal efficiency could be achieved until the lean flammability limit of the fuel is reached. It was found that the LBEC-1 engine reached its most efficient operating condition at an equivalence ratio of 0.85, showing a decrease in efficiency for leaner conditions. The MBT spark characteristic in Figure 16 indicates that perhaps this decrease in thermal efficiency is related to an increase in combustion interval as the equipment lean limit is approached. To achieve the potential of lean burn, it is necessary that the engine maintain a fast-burning charge for lean equivalence ratios.

The lean-burn concept also offers potential for controlling NO_x emissions as shown in Figure 26. This analytical curve indicates that NO_x emissions reach a peak for an equivalence ratio of 0.85, however, significant reductions in emissions can be achieved for leaner equivalence ratios. The goal of simultaneously achieving increased fuel economy and reduced exhaust emissions from lean burn operation depends on the success of making engine modifications which permit the efficient use of gasoline at equivalence ratios approaching the lean flammability limit of gasoline.

The effects of decreasing the combustion interval ($\Delta\theta$) from the stock value to the CFR value at the same equivalence ratio were studied using the B-K model. The predicted BSFC characteristics for these two combustion intervals at equivalence ratios of 1.0 and 0.85 are given in Figures 27 and 28. At an equivalence ratio of 1.0, the decrease $\Delta\theta$ results in a 3.4% decrease in BSFC, while a 7.0% decrease in BSFC is predicted for = 0.85. The improvement would be expected to increase as the equivalence ratio is decreased further because of the diverging nature of the stock and CFR characteristics in Figure 16.

Although the decrease in combustion interval produces a significant improvement in fuel economy in the lean regime, it is predicted that slightly more NO_x will be produced as shown in Figures 29 and 30. The shorter

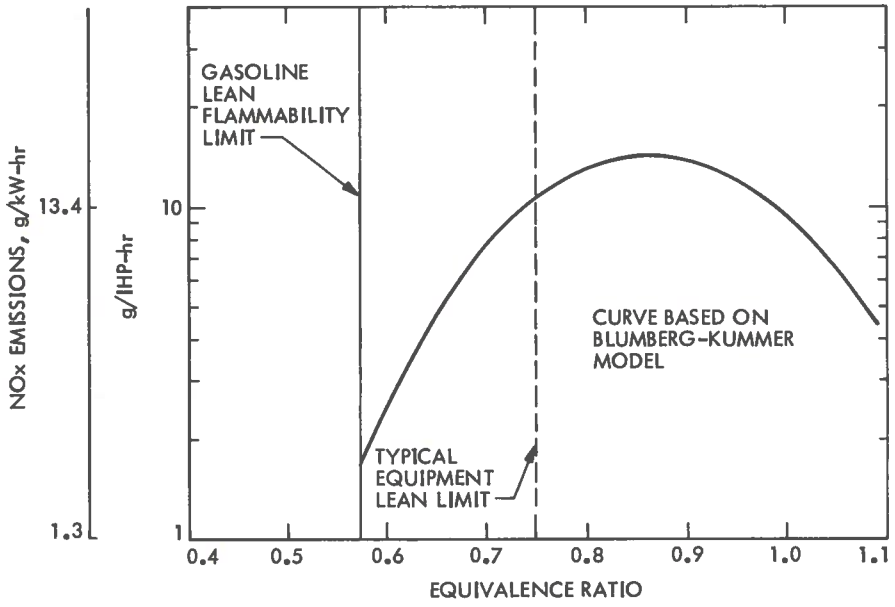

FIGURE 26. NO_x EMISSIONS VERSUS EQUIVALENCE RATIO

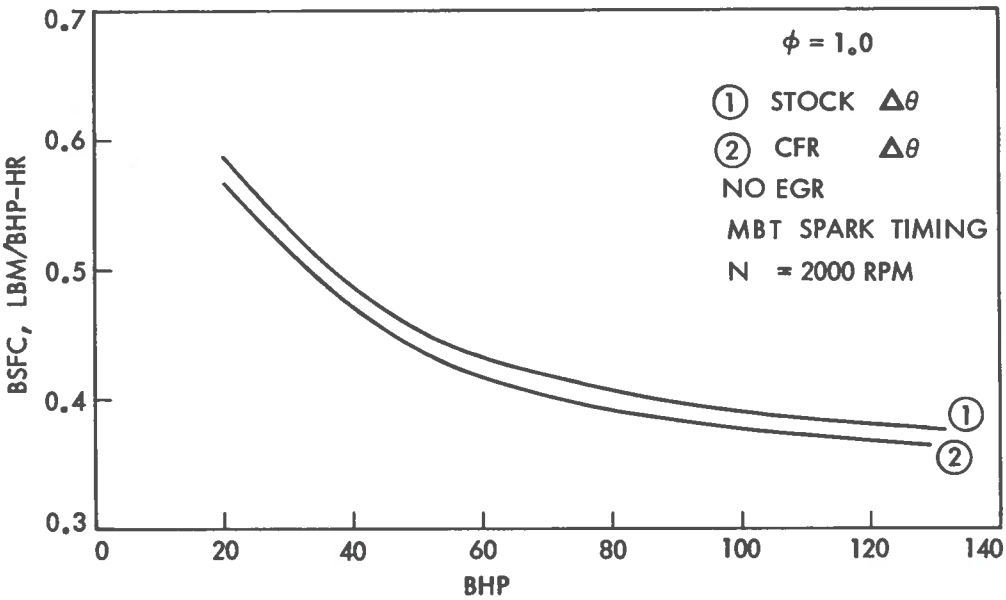

FIGURE 27. EFFECT OF COMBUSTION INTERVAL ON BSFC FOR $\phi = 1.0$

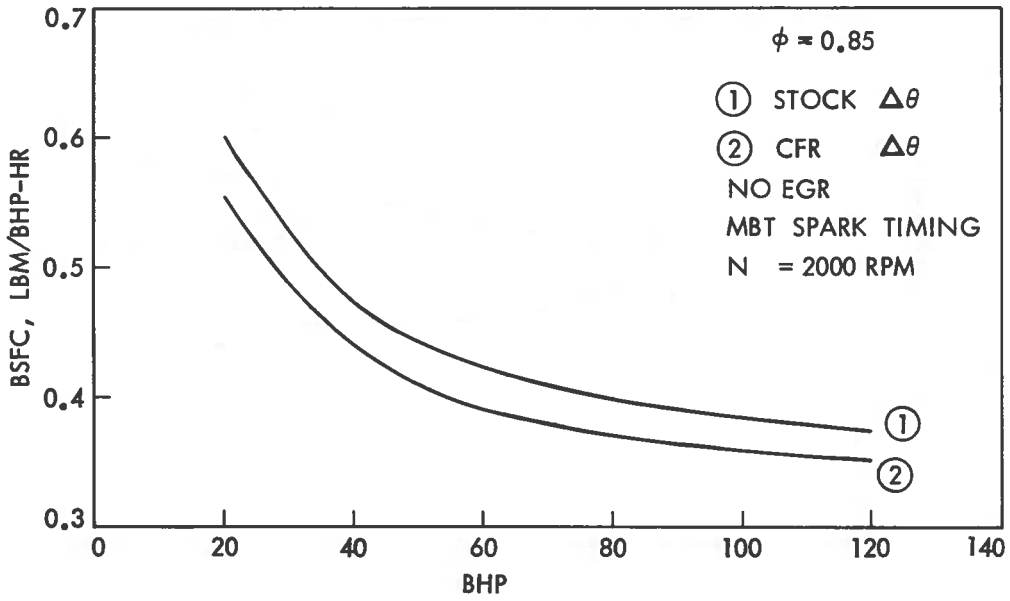

FIGURE 28. EFFECT OF COMBUSTION INTERVAL ON BSFC FOR $\phi = 0.85$

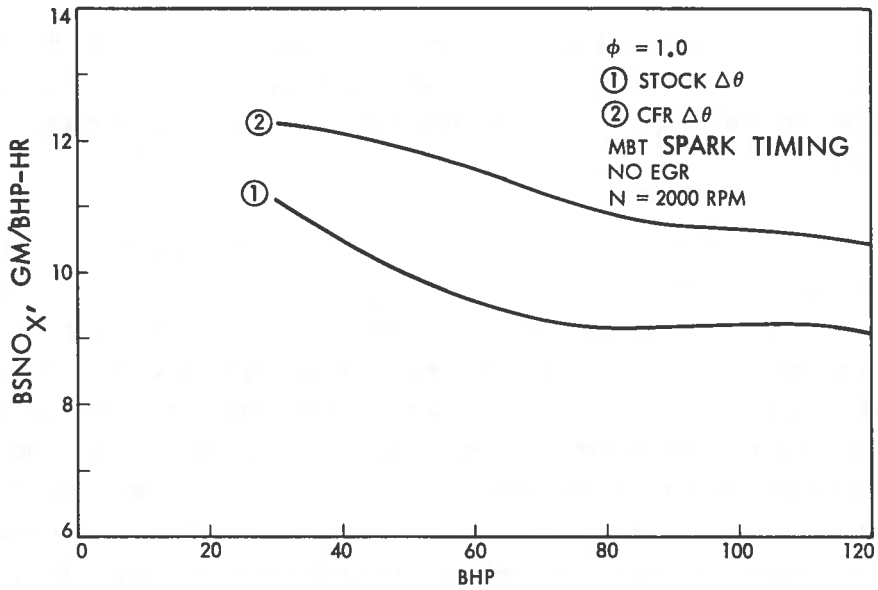

FIGURE 29. EFFECT OF COMBUSTION INTERVAL ON $BSNO_x$ FOR $\phi = 1.0$

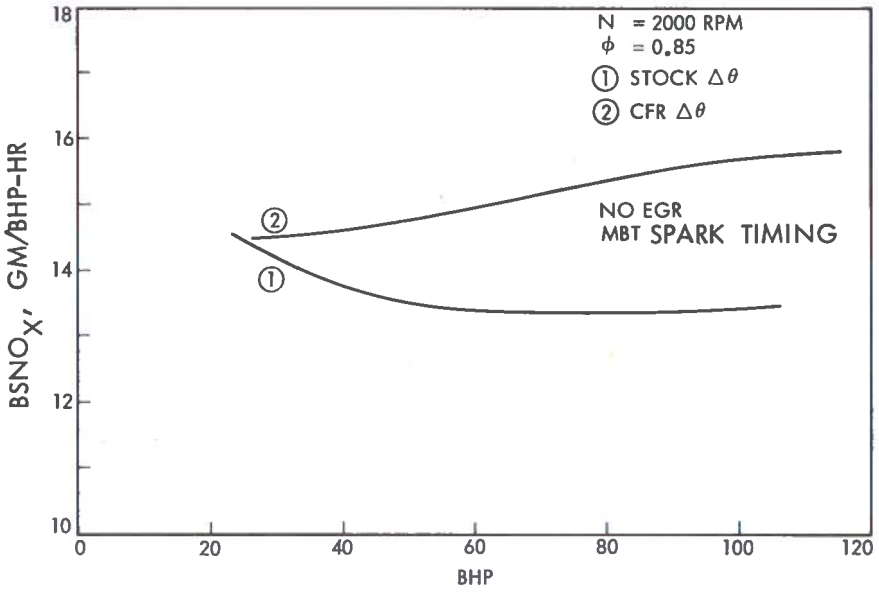

FIGURE 30. EFFECT OF COMBUSTION INTERVAL ON $BSNO_x$ FOR ϕ = 0.85

combustion interval allows less time for NO_x formation; however, the B-K model predicts that the higher peak temperatures associated with the shorter combustion interval more than offset this effect, resulting in an increase in NO_x emissions.

In addition to the effects at the same equivalence ratio, a reduced combustion interval will permit operation at leaner equivalence ratios before the thermal efficiency begins to drop because of sharply increasing combustion intervals as the flammability limit of the fuel is approached. The ability to run at leaner equivalence ratios helps to reduce the NO_x emissions by decreasing peak combustion temperature. Using the stock combustion interval at an equivalence ratio of 0.85 as the basis for comparison, the predicted effects of operating at equivalence ratios of 0.75 and 0.65 with the CFR combustion duration are shown in Figures 31 and 32. In each case, the BSFC is approximately 10% less than the reference engine indicating very little advantage in reducing equivalence ratio from 0.75 to 0.65 from the economy viewpoint.

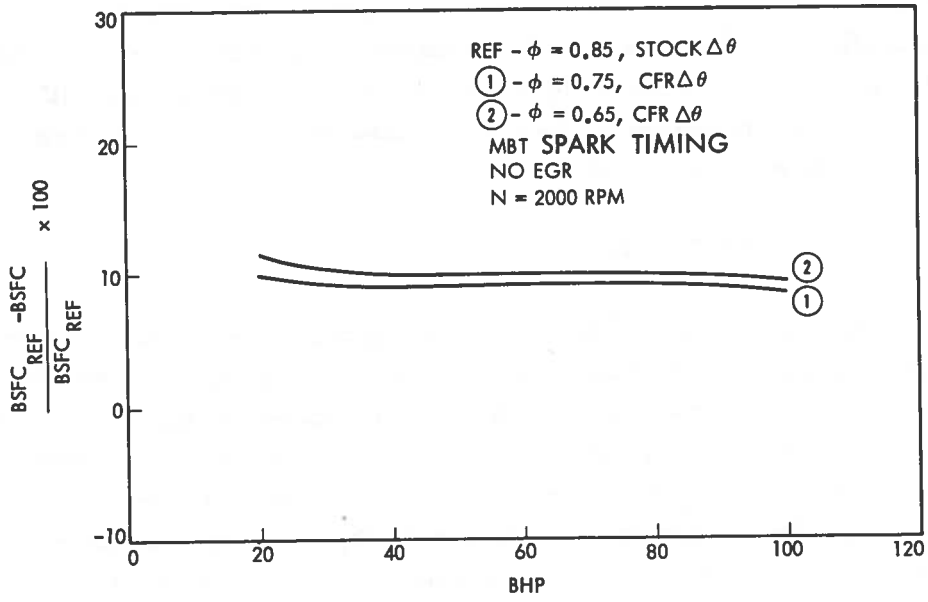

FIGURE 31. COMBUSTION INTERVAL EFFECTS ON BSFC

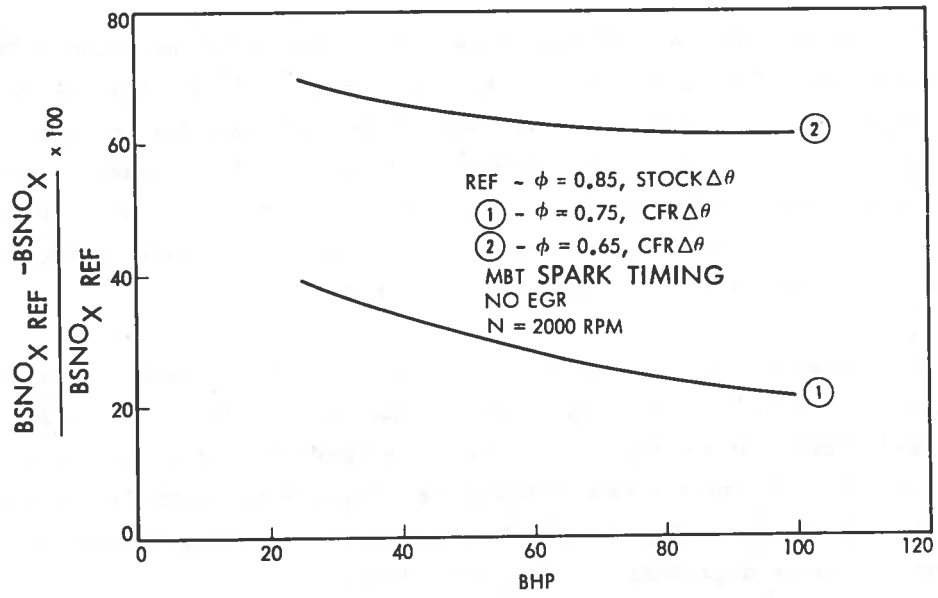

FIGURE 32. COMBUSTION INTERVAL EFFECTS ON $BSNO_x$

This results from the significant increase in CFR combustion interval for equivalence ratios less than 0.7. This effect conforms to experience with existing engine systems; however, improvements in, for example, ignition systems could lead to changes in this situation. It is seen, however, that the lower equivalence ratio has a significant effect on NO_x emissions. It would still be desirable to operate at the lower equivalence ratio considering both NO_x emissions and fuel economy.

4.6 Compression Ratio Effects

Another promising method for improving the performance of lean burn engines is to increase the compression ratio of the engine. It is well known that increasing the compression ratio up to the knock-limiting compression ratio, results in improved thermal efficiency; however, it is important to assess its effect on NO_x emissions as well. The B-K model predictions for the effect of compression ratio on BSFC and NO_x emissions are given in Figures 33 and 34. The stock compression ratio of 8.5 was used as the reference condition. It is assumed that compression ratio has no effect on combustion interval.

Predictions show a 7-8% reduction in BSFC and a 15% increase in NO_x emissions, when the compression ratio is increased to 11.0. Whether or not this compression ratio would be acceptable in practice depends on the knock-limiting compression ratio at an equivalence ratio of 0.75. Sufficient information on limiting compression ratios of lean mixtures is not available at this time; however, it is felt that lean mixtures will be more tolerant of increasing compression ratios than stoichiometric mixtures.

An alternative way of presenting the effect of compression ratio is shown in Figures 35 and 36. The range of B-K predictions includes load conditions from 20-110 Bhp. In the BSFC plot, air cycle predictions for specific heat ratios of 1.2, 1.3, and 1.4 are included for comparison. Increases in compression ratio seem to offer an effective means of improving fuel economy with a relatively minor degradation in NO_x emissions.

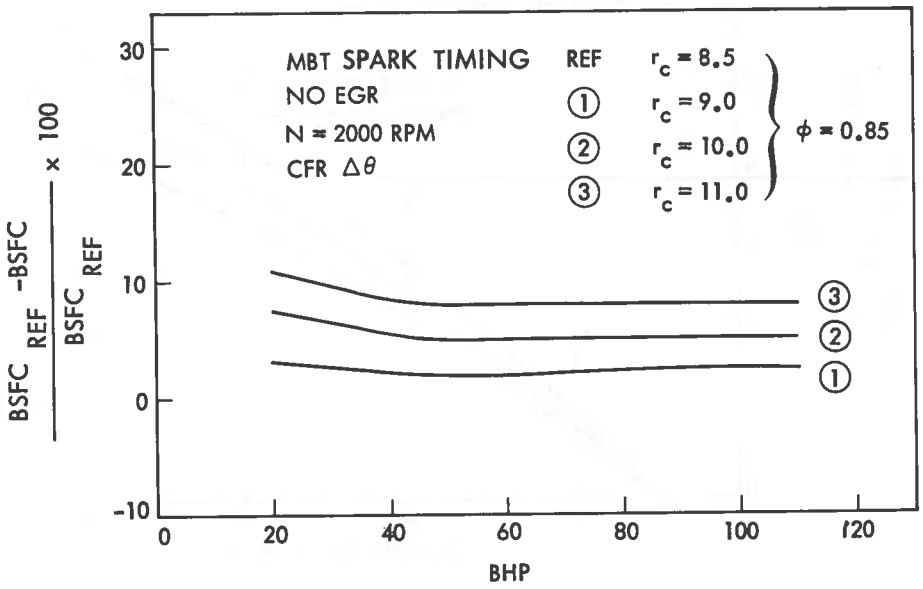

FIGURE 33. COMPRESSION RATIO EFFECTS ON BSFC FOR VARIOUS LOADS

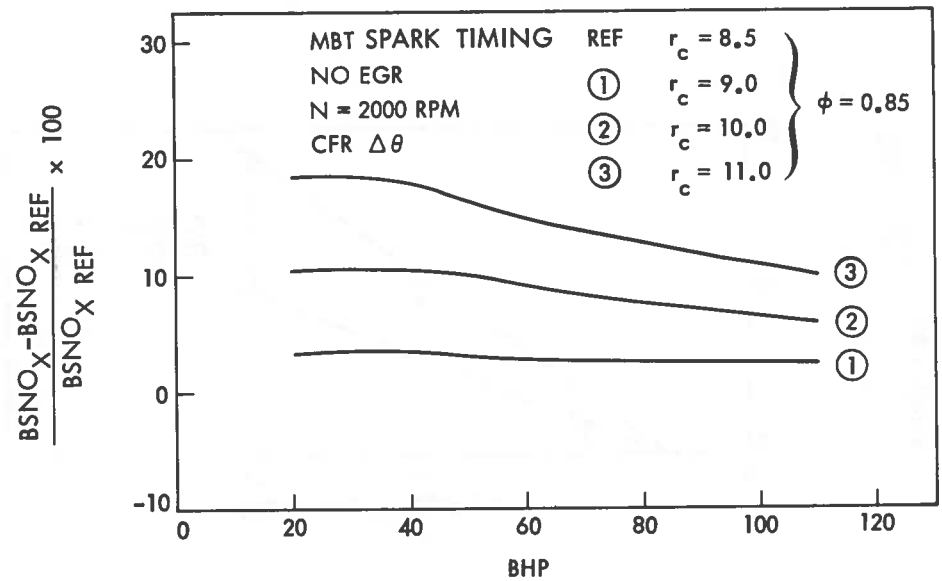

FIGURE 34. COMPRESSION RATIO EFFECTS ON $BSNO_x$ FOR VARIOUS LOADS

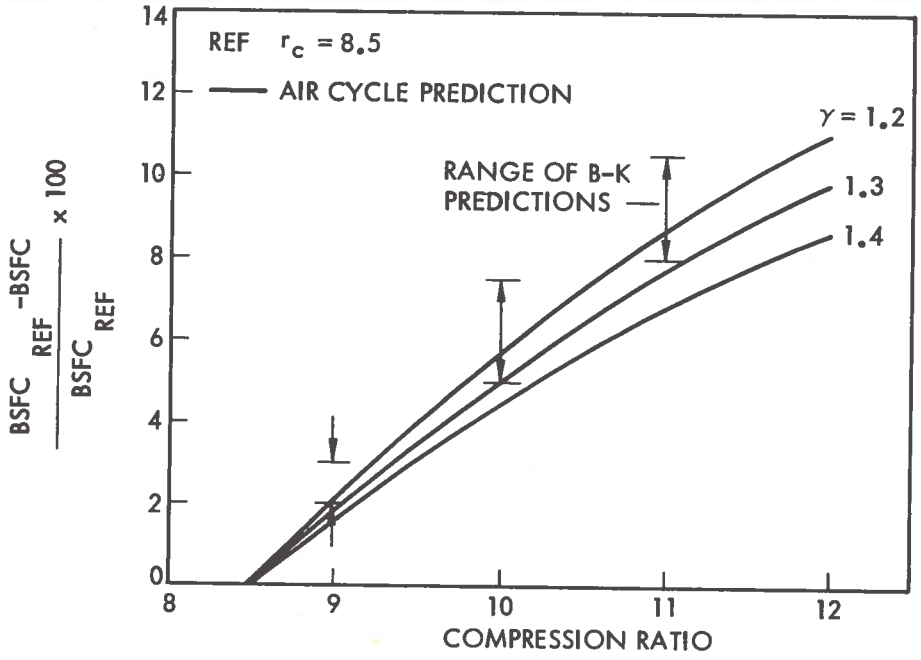

FIGURE 35. COMPRESSION RATIO EFFECTS ON BSFC

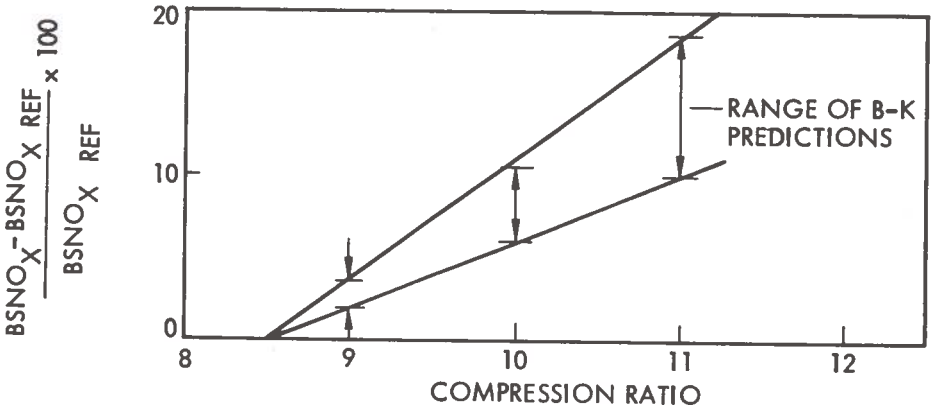

FIGURE 36. COMPRESSION RATIO EFFECTS ON $BSNO_x$

4.7 Hypothetical Lean Burn Engine

To help analytically evaluate the potential of the lean burn approach, consider a comparison of the stock engine with its emission control equipment and a hypothetical lean burn engine with a compression ratio of 10.0 operating at an equivalence ratio of 0.75 and having a combustion interval equal to that of the CFR engine. These characteristics are similar to those of the second lean burn engine configuration discussed in a later section of this report.

Comparisons of the fuel consumption and NO_x emissions predicted for these two engines are given in Figures 37 and 38. For MBT spark timing, the lean burn engine shows an average 21.7% decrease in BSFC over the entire load range when compared with the stock engine. The NO_x emissions comparison is made relative to the first lean burn engine configuration (LBEC-1). For MBT spark timing, the analytical predictions indicate that the hypothetical lean burn engine configuration should have an NO_x emissions performance about midway between that of the stock and LBEC-1 engines. Based on CVS emissions data for the stock and LBEC-1 engines, the prediction indicates that the hypothetical lean burn engine will not meet the interim 1977 Federal Standard for NO_x emissions (2.0 gm/mi). Calculations show that considerable reduction in NO_x emissions can be achieved by retarding the timing from MBT spark timing with only a slight increase in fuel consumption.

Calculations indicate that the interim NO_x standard could probably be met by operating the hypothetical lean burn engine at an equivalence ratio of 0.65 without sacrificing any of the fuel economy benefits of lean operation; that is, without changing from MBT spark timing. Efficient operation at equivalence ratios this close to the lean flammability limit of gasoline will require near-optimum air/fuel distribution, combustion chamber turbulence, and ignition system characteristics. Near the lean limit, control of cylinder-to-cylinder ϕ variations and cycle-to-cycle pressure variations in also required to prevent thermal efficiency losses.

Experimental verification of some of the benefits of lean-burn operation has been achieved using hydrogen/gasoline mixtures[44]. The addition of hydrogen moves the lean flammability limit of the mixture to a lower equivalence

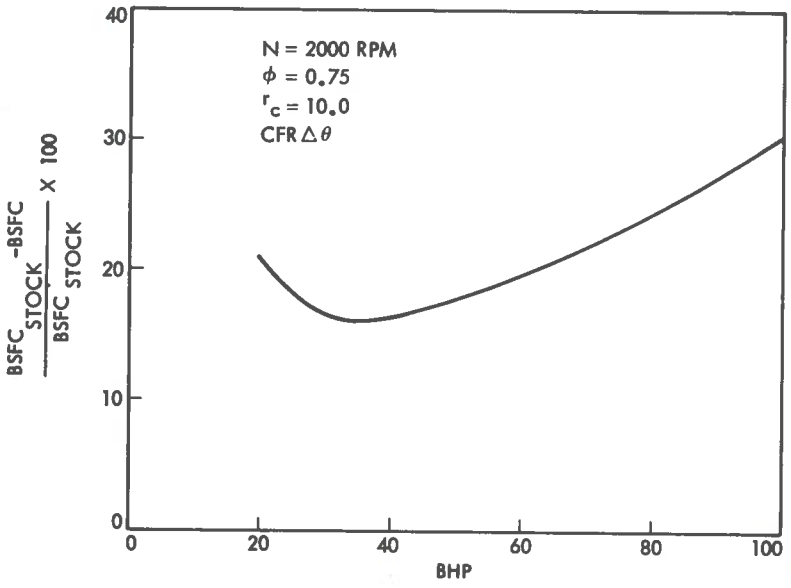

FIGURE 37. PERCENT DECREASE IN BSFC OF HYPOTHETICAL LEAN BURN ENGINE RELATIVE TO STOCK

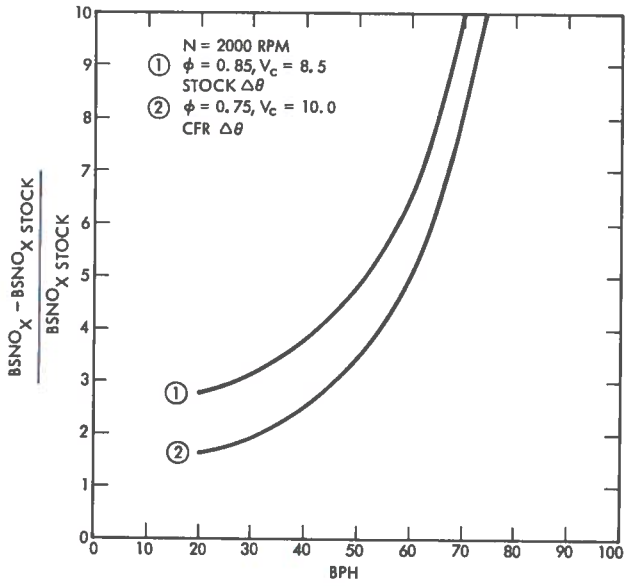

FIGURE 38. $BSNO_x$ COMPARISON OF STOCK AND HYPOTHETICAL LEAN BURN ENGINE

ratio and promotes a faster burning charge. The indicated thermal efficiency of a single-cylinder CFR engine using gasoline, hydrogen and gasoline/hydrogen mixtures is given in Figure 39. The gasoline/hydrogen data is not shown; however, the curves were derived from the mixture data. The addition of hydrogen permits efficient operation at equivalence ratios below the lean flammability limit of gasoline. The NO_x emissions from these CFR tests are given in Figure 40. This data verifies the significant drop in NO_x emissions which is possible at lean equivalence ratios.

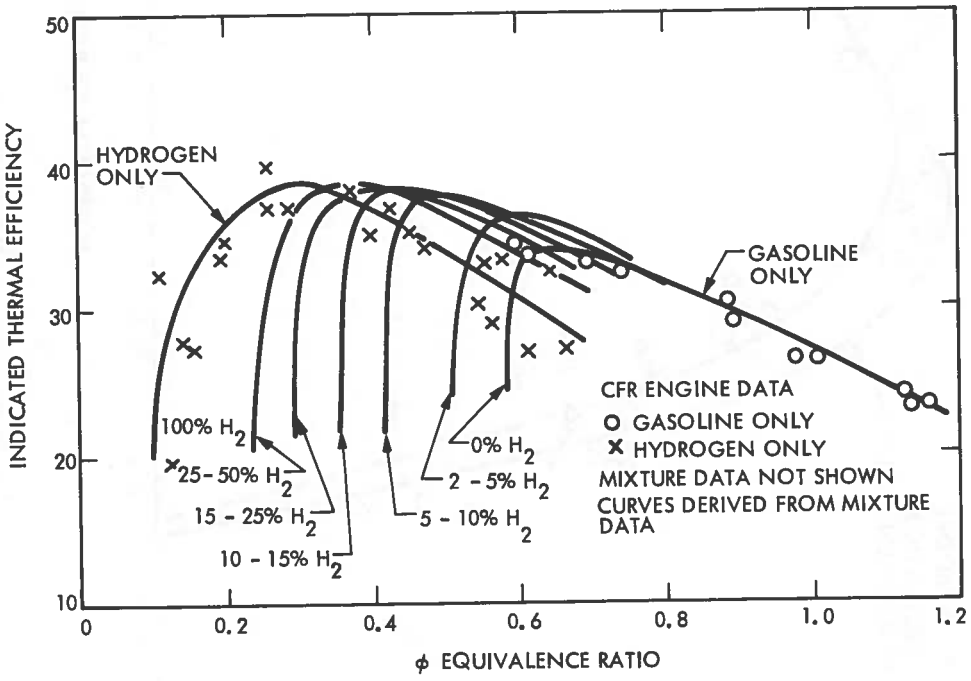

FIGURE 39. THERMAL EFFICIENCY OF THE CFR ENGINE

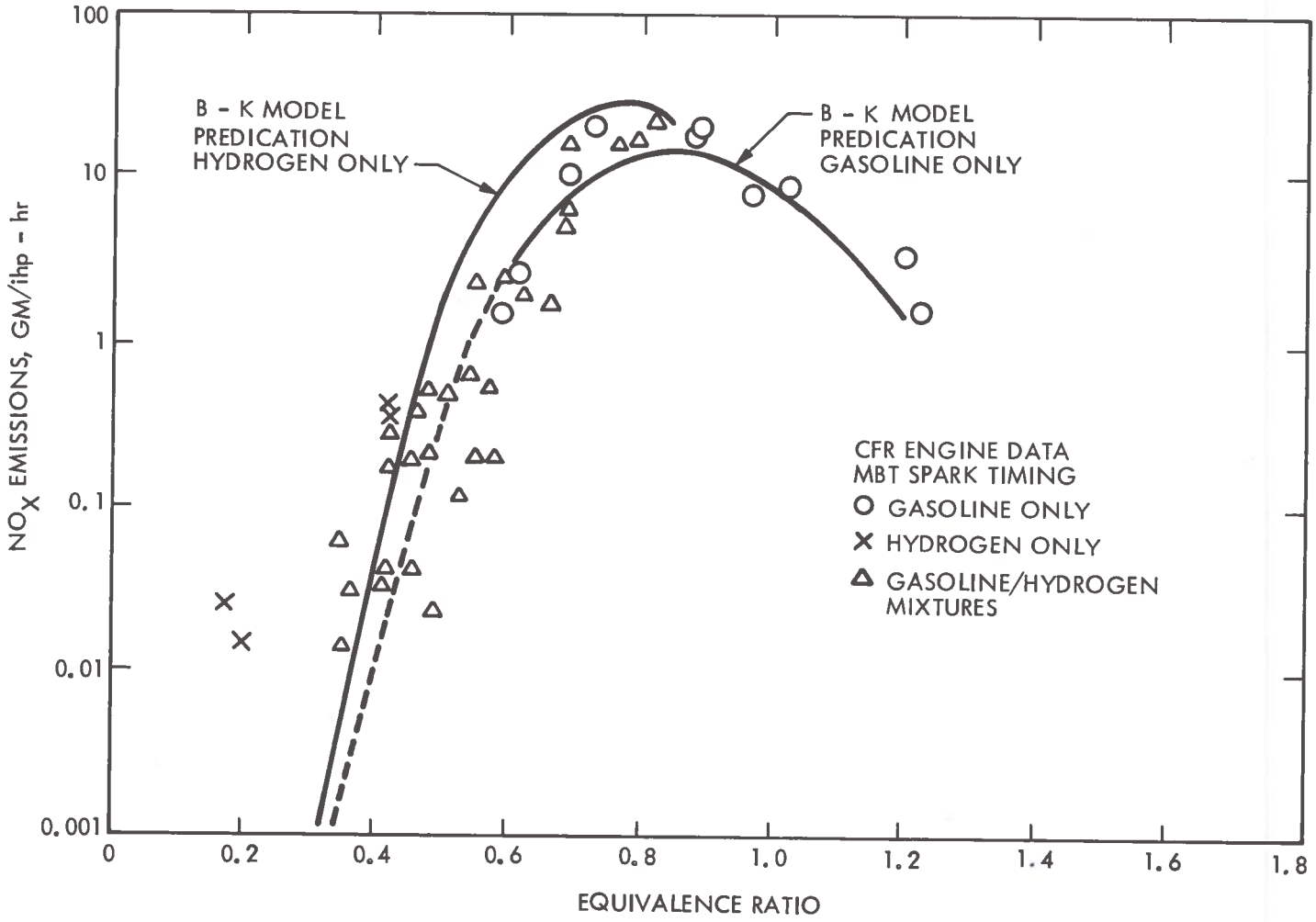

FIGURE 40. NO_x EMISSIONS OF THE CFR ENGINE

5. LEAN BURN ENGINE CONFIGURATION NO. 2 (LBEC-2)

5.1 Description

As previously discussed, the Autotronics-modified engine yielded peak thermal efficiency at an equivalence ratio of about 0.85 which was not sufficiently lean to reduce NO_x emissions or to provide adequate reduction in BSFC. Evaluation of the data suggested that the lean performance of the engine was being limited by cylinder-to-cylinder equivalence ratio variations and long combustion durations.

Individual cylinder data indicated a cylinder-to-cylinder equivalence ratio variation about the median of ±0.05 equivalence ratio units. This places a limit on lean performance by causing the leanest individual cylinder to misfire at a higher average equivalence ratio than an engine with uniform distribution. For example, a reduction in the equivalence ratio variation from ±0.05 to ±0.025 should permit a reduction in average equivalence ratio from 0.85 to about 0.825 while maintaining high efficiency.

From a knowledge of the combustion chamber shape of the 350 CID Chevrolet engine and by comparing the MBT spark timing data of the V-8 and CFR engine, it is possible to infer that the turbulence level in the combustion chamber during combustion is relatively low in the V-8. CFR data taken with shrouded valves indicated that at an equivalence ratio of 0.85 an MBT spark timing of 19° was required compared with 45° to 55° for the V-8.

Within the constraints of this program, it was felt that engine modifications to reduce combustion duration offered the greatest probability of achieving the objective of peak thermal efficiency within the equivalence ratio range from 0.75 to 0.80. Increasing the turbulence in the combustion chamber is one of the most promising techniques for reducing combustion duration because of its effect on flame propagation velocity. It is necessary to increase the turbulence level in the correct region of the eddy size spectrum without incurring an unacceptable reduction in engine volumetric efficiency.

Although there exist many ways to increase combustion chamber turbulence, one of the most common techniques is through using shrouded intake valves. Wentworth in Ref. 36 has shown that shrouded valves potentially increase the HC emissions because the scale of turbulence they introduce is of the order of the cylinder diameter, and the resulting increased heat transfer to the cylinder walls causes the quench layer to grow. JPL tests of shrouded valves in the 350 CID V-8 engine have indicated:

- Increased thermal efficiency.
- Improved lean operation.
- Increased hydrocarbon emissions.
- Reduced spark advance requirement.
- Reduced volumetric efficiency

The advantages resulting from the incorporation of shrouded intake valves were due to the reduction in combustion duration resulting from the increased turbulence level; the disadvantage of poorer hydrocarbon emissions was probably due to increased heat transfer as a result of the large scale eddies introduced by shrouded valves. To obtain these advantages, without the adverse emissions effects, smaller scale eddies are desirable.

Turbulator intake valves similar to the turbulator inserts used successfully in Ref. 3 were designed, fabricated and used in the second lean burn configuration. The design shown in Figure 41 should introduce a minimum of flow losses and result in an insignificant volumetric efficiency penalty.

In addition to the modified intake valves, the stock cylinder heads were replaced with the slant plug heads, shown in Figure 42, which have a slightly modified combustion chamber shape designed to promote combustion chamber turbulence and have an improved spark plug location. Volume measurements indicate that the slant plug heads give the LBEC-2 engine a compression ratio of approximately 9.5.

The Edelbrock Tarantula intake manifold used on the Autotronics modified engine was replaced with an Edelbrock Streetmaster manifold which has smaller diameter runners. The smaller runners result in higher intake velocities and

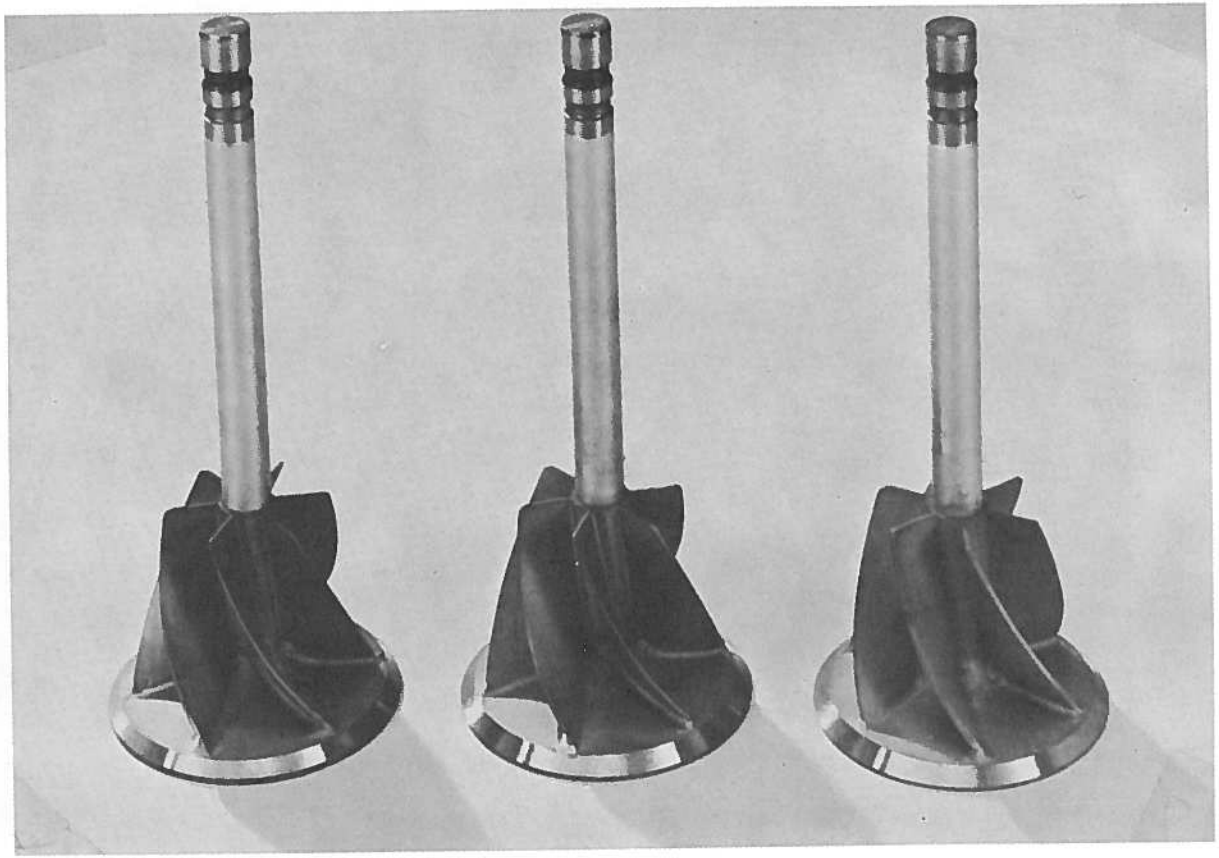

FIGURE 41. TURBULATOR INTAKE VALVES

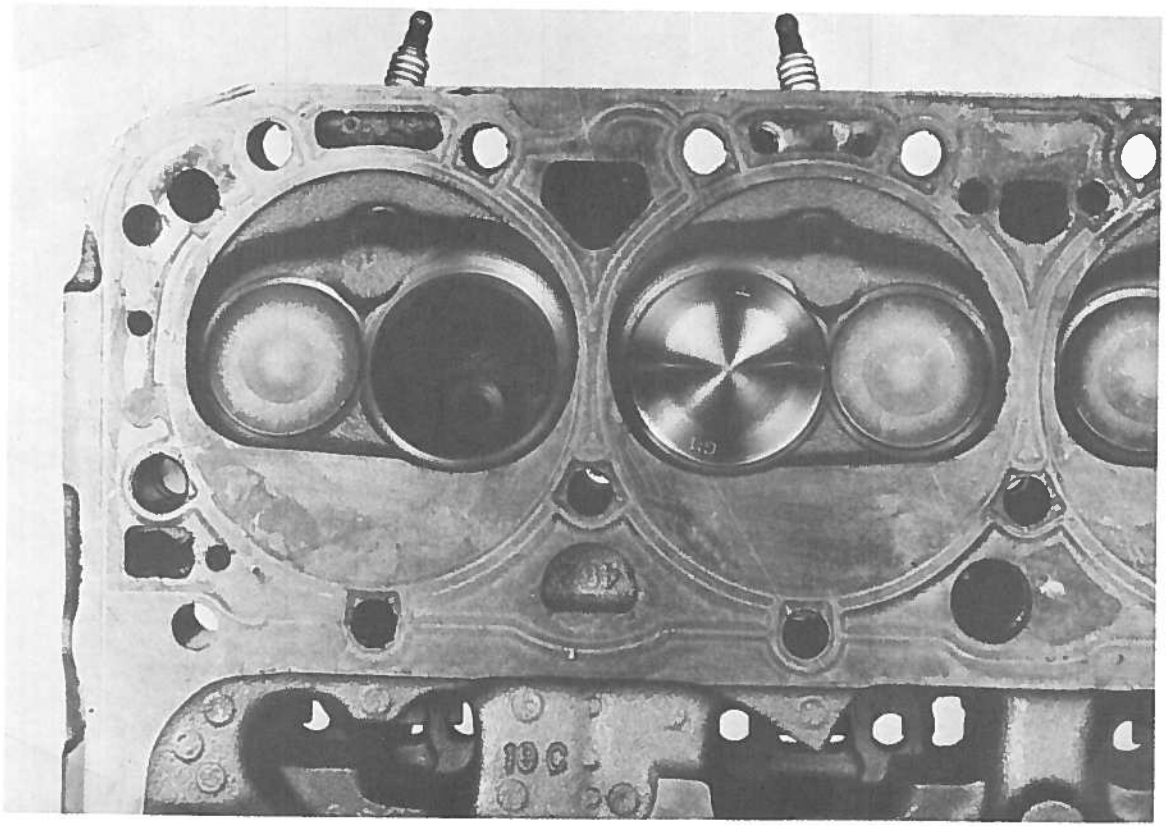

FIGURE 42. SLANT PLUG HEADS

increased turbulence in the incoming charge. The Streetmaster manifold should introduce negligible losses in volumetric efficiency for engine speeds below 4000 RPM.

To promote additional mixing of the gasoline/air mixture, a 4-inch cylindrical standoff was introduced between the Autotronics atomizer system outlet and the intake manifold inlet. The standoff was fabricated from plastic to permit visual observation of the incoming gasoline/air stream.

5.2 Preliminary Tests

A series of preliminary tests were conducted to investigate the effect of induction and ignition system variables on engine performance. These results were required to firmly establish the second lean burn engine configuration to be used for the sensitivity and mapping tests.

The induction system parameters investigated included changes in manifold inlet geometry and orientation of the fuel atomizer relative to the engine air-flow pattern. The ignition parameters studied were the type of ignition system (GM High Energy Ignition versus Autotronics Multiple Spark Discharge), spark plug type (variable heat range and extension), plug gap setting, and ignition timing. Most of these tests were run at 2000 RPM and level-road-load power using the engine dynamometer; however, some selected data were obtained at other engine speeds and loads.

As previously mentioned, special exhaust headers having individual pipes about three feet long were fitted to the engine in place of the stock exhaust manifolds; sample lines were fitted at each exhaust port. The cylinder-to-cylinder distribution results were derived from the analysis of individual exhaust gas samples. The Edelbrock Streetmaster intake manifold was modified by blocking the exhaust hot spot crossover. This prevented mixing of exhaust gases from Cylinders 3 and 4. Heat for the hot spot was supplied by engine coolant flowing through the crossover passage; induction charge temperatures ran only a few degrees above ambient air temperature.

The effect of two different angular positions (θ) of the fuel atomizer on mixture distribution is shown in Figure 43 for θ = 0° and 240°. The Autotronics plenum chamber was in its normal position, i.e., bolted directly to the intake manifold. The ordinate scale is the ratio of the equivalence ratio for each cylinder divided by the overall average equivalence ratio. Points that lie below 1 represent relatively lean firing cylinders and those above 1 indicate rich mixtures. One observation is that for θ = 240°, the left bank of cylinders runs relatively lean while the right side is rich. Rotating the fuel atomizer 120° causes the distribution pattern to shift between the right and left side. A convenient measure of distribution is the standard deviation (σ_{Φ}) of the equivalence ratios for all eight cylinders. As indicated in Figure 43, one sigma varies from 0.035 to 0.060 for these particular tests. The smaller the value of sigma, of course, the better the cylinder-to-cylinder mixture distribution.

Similar experimental results were obtained with the first lean burn engine configuration. These data are presented in Figure 44 for the identical atomizer positions. For this case, σ_{Φ} = 0.101 at = 0°, compared with only 0.035 with the second engine configuration. The same general relationship in distribution was observed, however, between the right and left cylinder banks.

The effect of distribution on engine indicated thermal efficiency (η_t) is shown in Figure 45. Included in this figure are the results of Figure 43 and a second manifold configuration, one in which the air plenum chamber is separated from the engine intake manifold with a 4-inch diameter by 4-inch long standoff pipe. The purpose of installing the standoff pipe was to evaluate the effect of increased induction mixing length on the distribution of the fuel/air charge. As shown in Figure 45, the cylinder-to-cylinder distribution results were similar with and without the standoff distance. There is, however, a slight engine efficiency advantage for the close coupled induction configuration and for this reason the standoff pipe was not used in succeeding tests.

Several additional tests were run at other engine speeds to determine the effect of engine operation on mixture distribution. The results, summarized in Figure 46, show that the best cylinder-to-cylinder distribution (low σ_{Φ}) is achieved at low engine speeds.

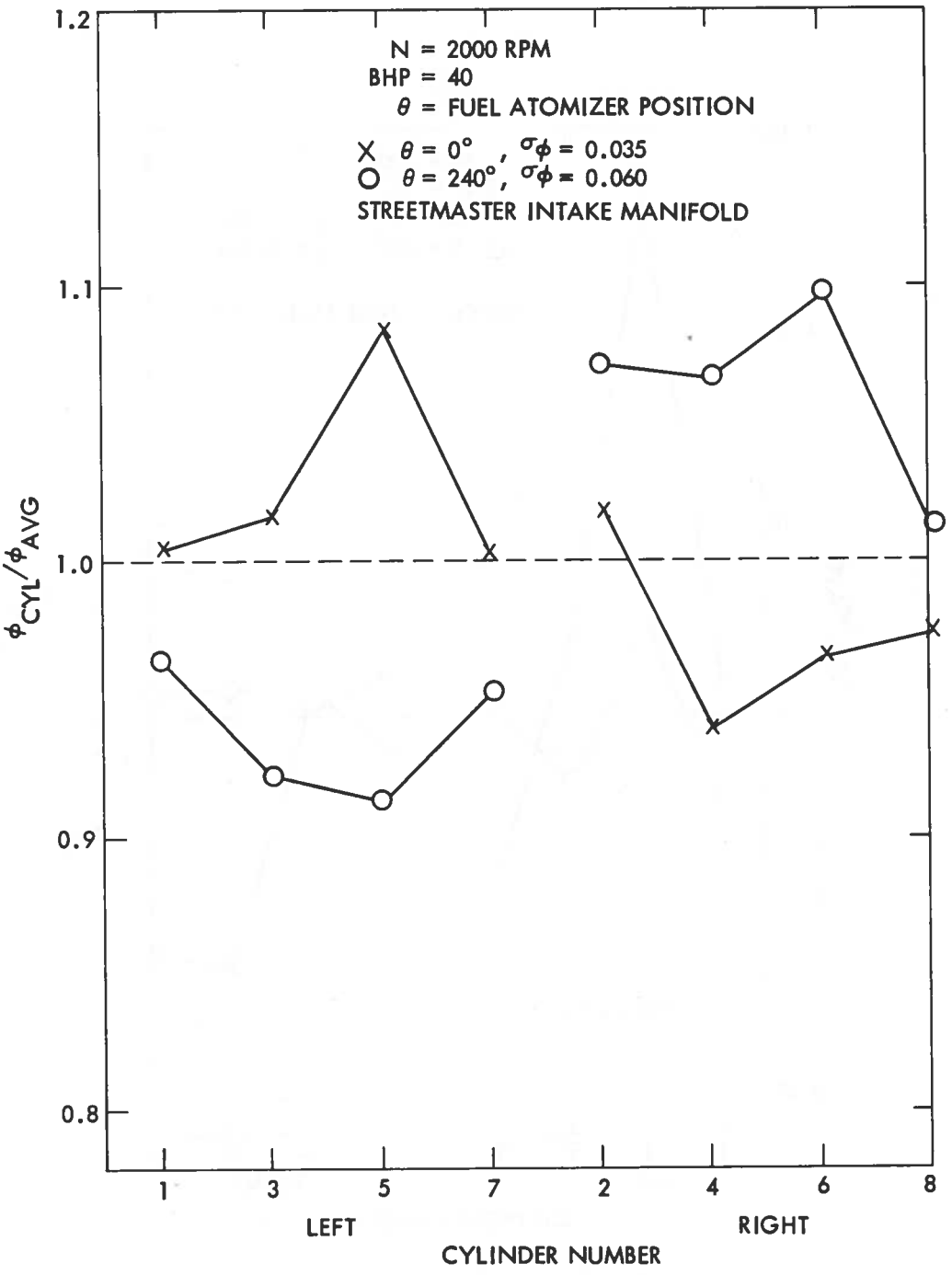

FIGURE 43. MIXTURE DISTRIBUTION FOR LBEC-2

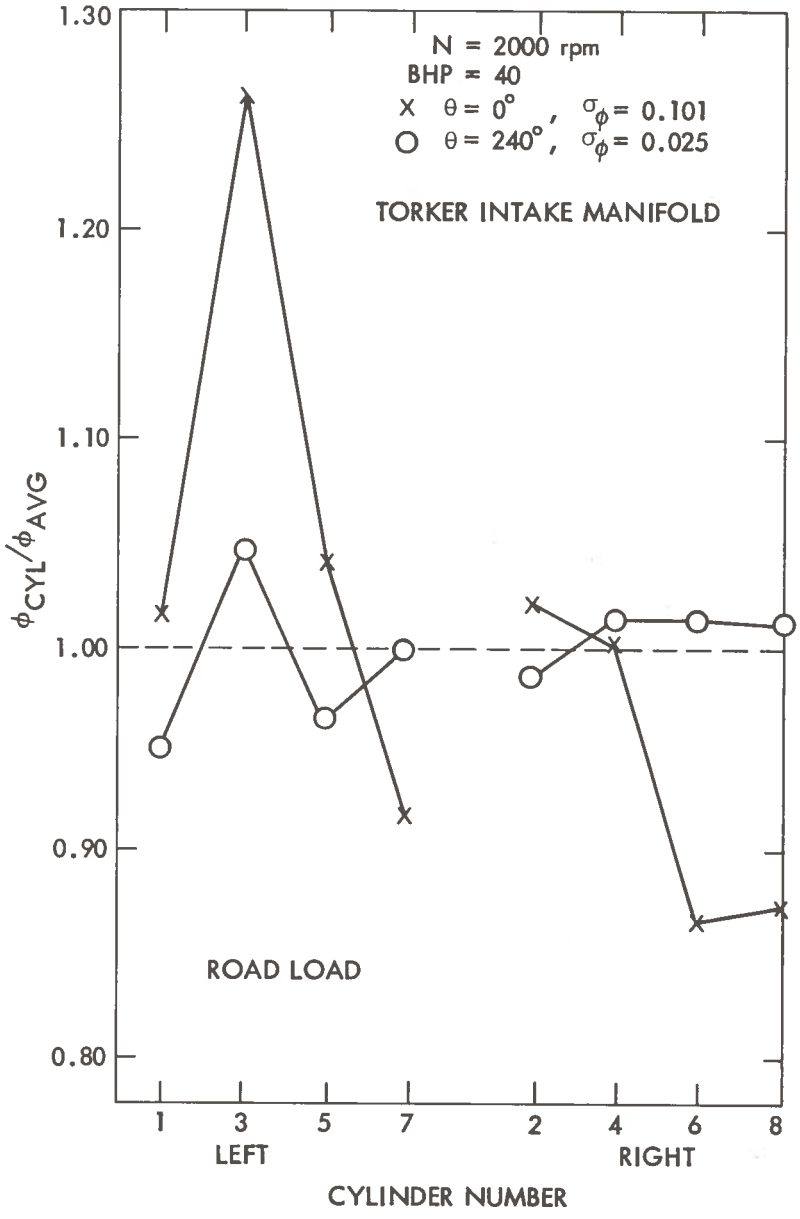

FIGURE 44. MIXTURE DISTRIBUTION FOR LBEC-1

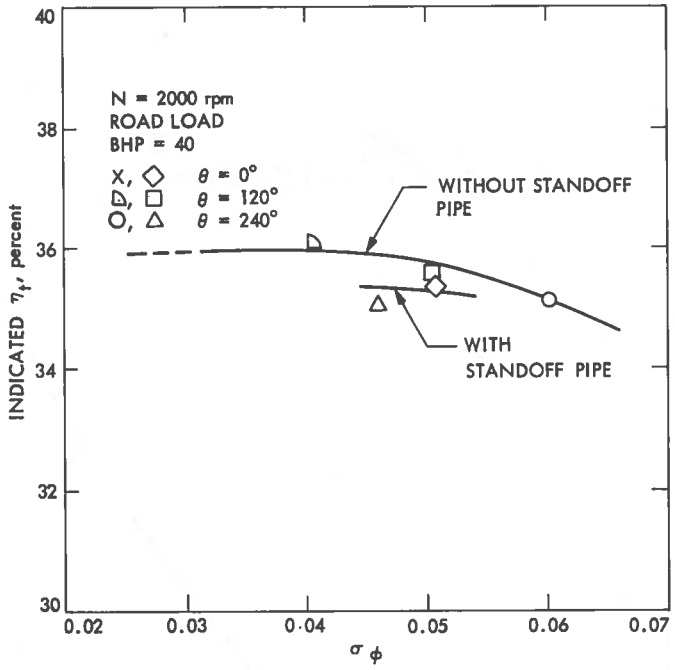

FIGURE 45. EFFECT OF MIXTURE DISTRIBUTION ON ENGINE THERMAL EFFICIENCY

The two different ignition systems evaluated were the Autotronics Multiple Spark Discharge (MSD) system and the stock 1975 GM High Energy Ignition (HEI).

The MSD system consists of a special coil with a fast rise time, a condenser, and distributor breaker points. Its main features are multiple striking with external control of the retard and duration of firing. The high energy (60,000 v open circuit) capacitive discharge system provides multiple spark capability with variable repetition rates extending up to 40 crankshaft degrees. Special shielded "mag wire" ignition wires were employed to prevent electrical interference with the Autotronics control circuits.

The GM HEI system is a breakerless system that has all ignition components, including the coil, contained within the distributor housing. The component parts of the system include a magnetic pickup assembly containing a permanent magnet and pickup coil. An induced voltage in the pickup coil signals

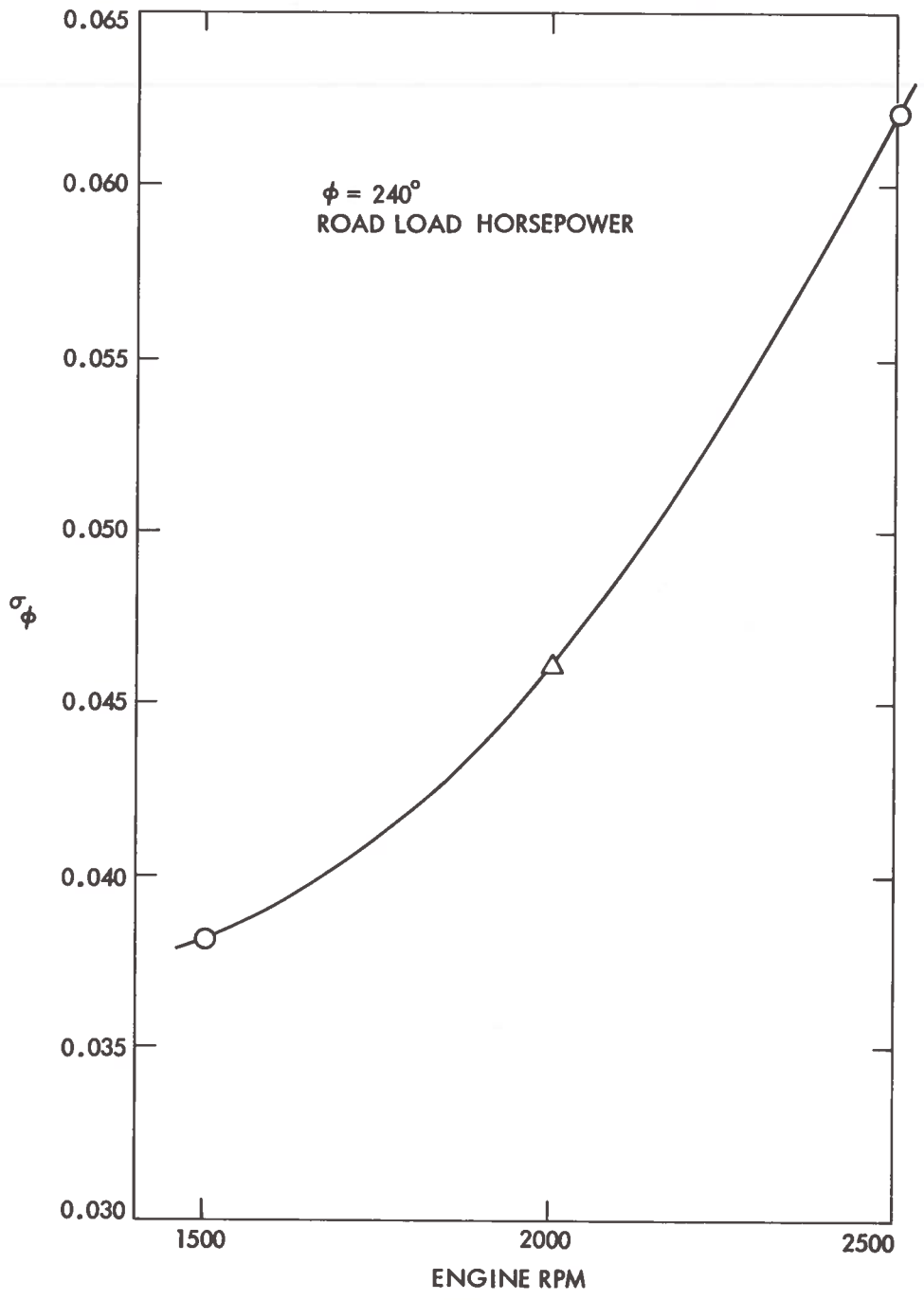

FIGURE 46. EFFECT OF ENGINE SPEED ON MIXTURE DISTRIBUTION

the solid state electronic model to open the ignition primary circuit. This interruption creates the high voltage to the spark plugs as in conventional systems. The system is capable of producing 35,000 v.

Test results with the two different systems are presented in Figure 47. Engine efficiency data are shown as a function of equivalence ratio for a 44° BTDC spark timing and AC-R44TS spark plugs. The results indicate that during relatively rich conditions ($\Phi > 0.80$) when the engine is not misfiring, the engine thermal efficiency does not depend significantly upon the type of ignition system. It is apparent, however, that for lean mixtures the HEI provides improved performance. For this reason, all subsequent tests of the second lean-burn engine configuration were made with the HEI ignition system.

Four sets of spark plugs with different heat ranges were evaluated using the HEI Ignition System. The plugs were identified as AC 43, 44, 45, and 46; the heat range increases with increasing plug numbers. In addition, three of the plugs were evaluated with both a normal tip extension (Type T) and extended tip (Type TS). The test results are presented in Figure 48 using a constant Φ of 0.75 and gap setting of 0.070 inches. The results show an improvement in engine efficiency using the extended reach plugs with a colder heat range. For this reason, the AC plug type R43LTSX was selected for the remaining tests.

Using the R43LTSX plugs of the previous test series, additional gap settings of 0.080, 0.090 and 0.100-inches were evaluated. The test data are shown in Figure 49 for three different spark advance settings from 50 to 60° BTDC. The results show that engine performance is relatively insensitive to both parameters. Since a 0.080-inch spark plug gap is recommended by GM for use with the HEI ignition system, this setting was used with the AC R43LTSX spark plugs for the remaining tests.

Several of the engine modifications used in the second lean burn configuration affect the breathing capacity of the engine. Some restriction to air flow is introduced by use of the turbulator intake valves. The larger intake valve ports in the slant plug heads, on the other hand, produce the opposite effect. To determine the combined effect of these changes in breathing capacity, a series

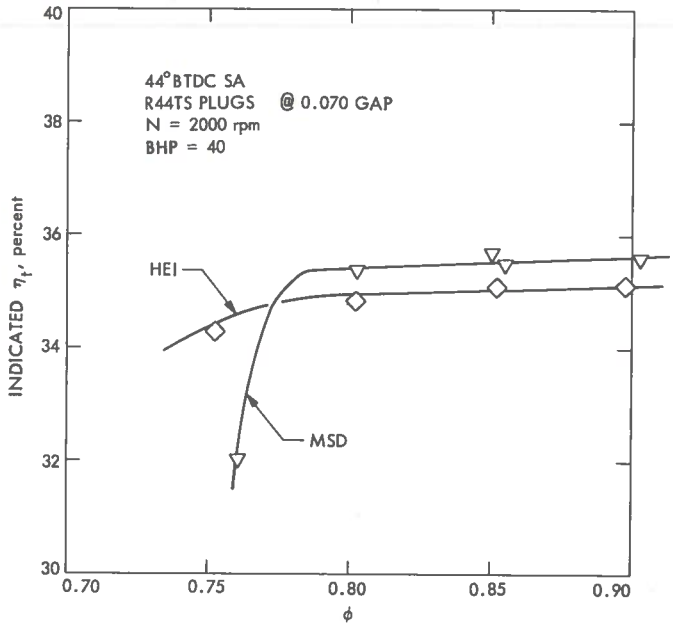

FIGURE 47. EFFECT OF IGNITION SYSTEM ON ENGINE THERMAL EFFICIENCY

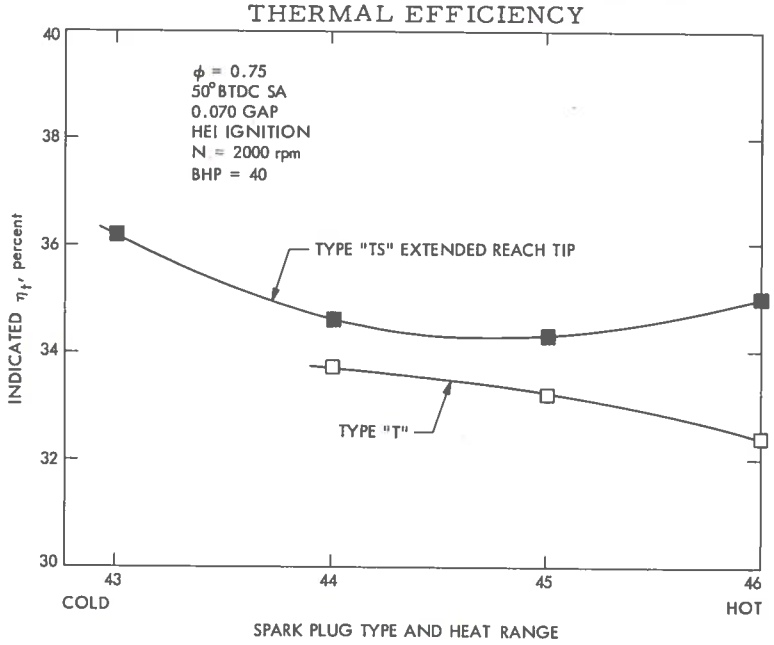

FIGURE 48. EFFECT OF SPARK PLUG TYPE ON ENGINE THERMAL EFFICIENCY

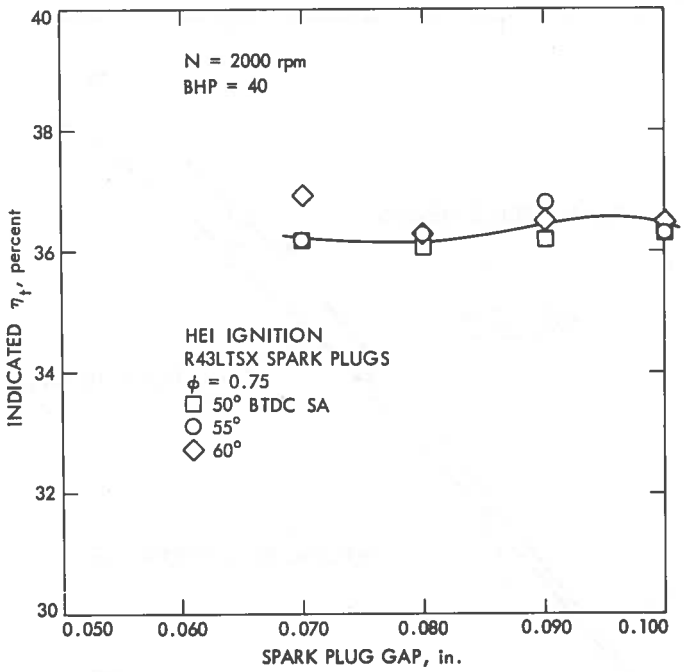

FIGURE 49. EFFECT OF PLUG GAP ON ENGINE THERMAL EFFICIENCY

of tests were conducted at wide-open-throttle (WOT). The results are presented in Figure 50 in terms of actual mass air flow consumption and maximum developed engine brake horspower as a function of engine speed.

The breathing capacity of the modified engine is shown to be about 5 percent greater than the stock engine. This result suggests that the flow restriction produced by the turbulator intake valves is more than compensated for by the increased flow area of the larger intake port openings.

The improved breathing characteristics of the modified engine can be directly related to the brake horsepower as shown by the lower curves of Figure 50. At an equivalence ratio of 1.0, for example, the modified engine produces about 5 percent more brake horsepower than the stock engine. For comparison purposes, a second power curve is presented for the stock engine operating at an equivalence ratio of 0.75. As expected, the WOT power is reduced approximately 25 percent.

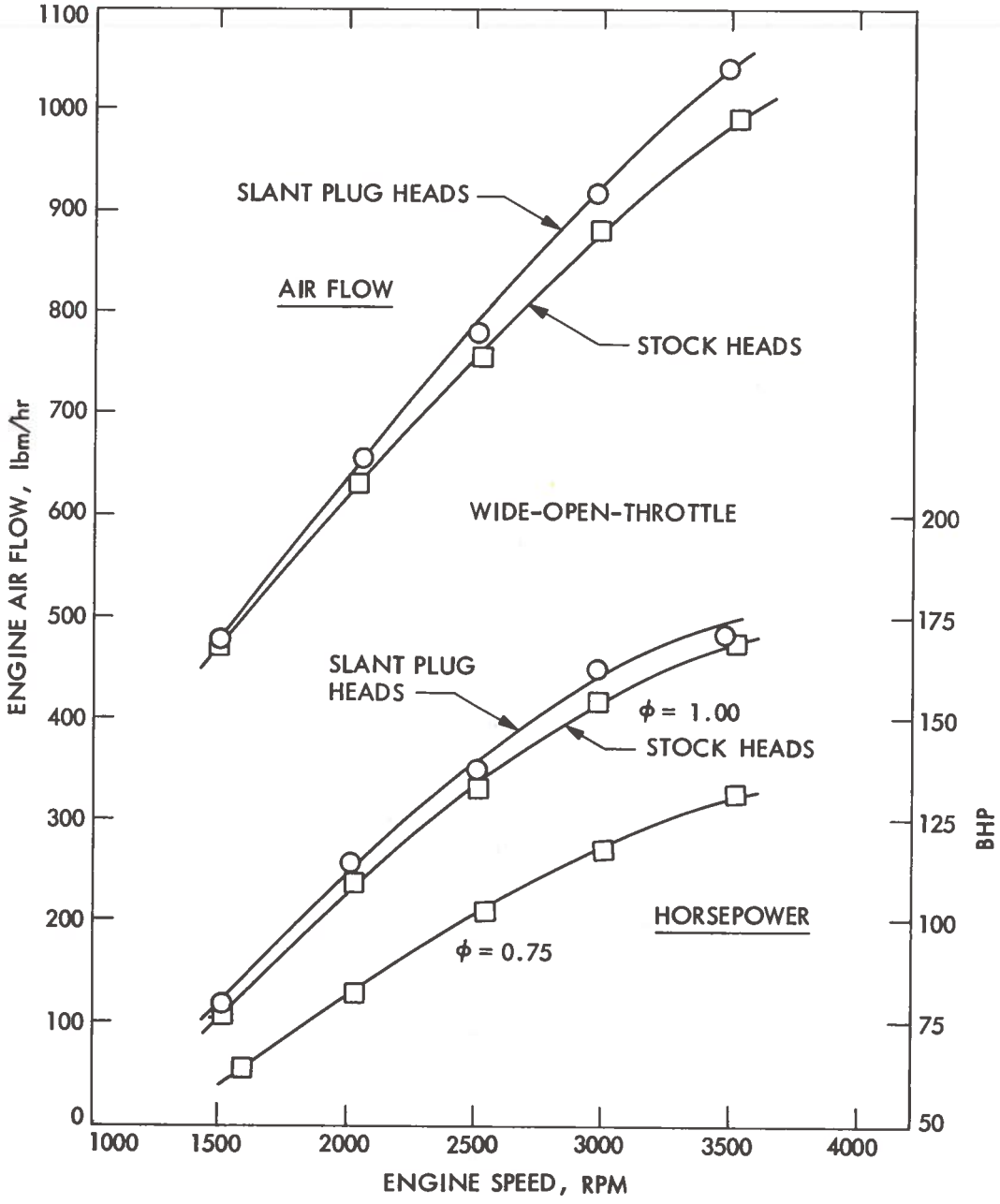

FIGURE 50. EFFECT OF SLANT-PLUG HEADS ON MAXIMUM ENGINE PERFORMANCE

5.3 Sensitivity Tests

A series of engine tests were conducted to establish the equivalence ratio and spark advance which give the minimum fuel consumption for a given operating condition. Run conditions were selected to be representative of the conditions encountered on the Federal Driving Cycle. For each operating condition (BHP and RPM), several equivalence ratios and spark advances were tested to determine the sensitivity of brake specific fuel consumption (BSFC) to changes in these parameters. No exhaust emissions measurements were made during the sensitivity tests.

For each run condition, the minimum fuel consumption conditions were identified from wedge plots of the smoothed data. The data were corrected to the nominal BHP and RPM by assuming that the indicated specific fuel consumption and equivalence ratio are constant for small corrections in BHP and RPM. Wedge plots for the sensitivity data are included in Appendix D.

A typical wedge plot is shown in Figure 51 for 2000 RPM and level-road-load power. For comparison purposes, a stock carburetor data point from the JPL baseline tests is shown for an equivalence ratio of 1.00 and a spark advance of 35° BTDC. The second lean burn engine configuration required less fuel than the stock configuration for all equivalence ratios and spark advances tested. Minimum fuel consumption was reached at an equivalence ratio of 0.75 with a spark advance of 60° BTDC. This compares with a minimum fuel consumption condition at $\Phi = 0.85$ with a 50° BTDC spark advance for the Autotronics-modified engine. The minimum fuel consumption condition at $\Phi = 0.85$ with the second lean burn engine required a 40° BTDC spark advance indicating a shorter combustion duration and/or ignition delay than the Autotronics-modified engine.

Minimum fuel consumption occurred generally at an equivalence ratio between 0.75 and 0.80 which is somewhat leaner than the $\Phi = 0.85$ that was obtained with the Autotronics-modified engine. The sensitivity data for the second lean burn engine indicated an average 11.6 percent reduction in BSFC when compared with the JPL stock engine data for this engine, as shown in Table 7.

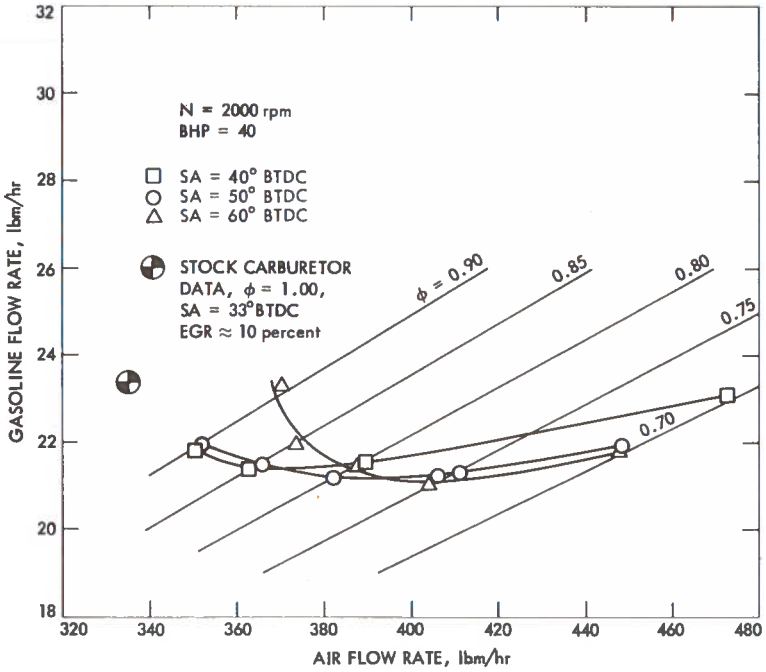

FIGURE 51. WEDGE PLOT FOR LBEC-2

5.4 Mapping Tests

To provide data for establishing brake specific fuel consumption and brake specific emissions contour maps for comparison with the baseline data, a complete engine map of the second lean burn engine configuration was obtained. The points shown in Figure 52 were selected to provide adequate coverage of the engine operating range for making accurate contour maps. The data point density was reduced for run conditions above 3000 RPM and for power levels less than level-road-load power because of the less frequent use of this portion of the operating regime. Because of their significance, additional data were taken for level-road-load power and for the maximum power needed on the Federal Driving Cycle. Measurements of fuel consumption and HC, CO and NO_x emissions were taken for each operating point.

The original plan was to select the equivalence ratio and spark advance for each operating point in the engine mapping matrix based on the minimum fuel

TABLE 7. BSFC COMPARISON OF STOCK AND SECOND LEAN BURN ENGINE CONFIGURATION

RPM	BMEP	Stock BSFC	Modified Engine		% Decrease in BSFC
			Φ	BSFC	
1000	10.0	--	0.805	1.242	--
1000	41.0	0.640	0.754	0.550	14.1
1500	15.8	1.100	0.797	0.861	21.7
1500	32.0	0.665	0.760	0.594	10.6
1500	48.1	0.581	0.812	0.521	10.4
2000	35.0	0.650	0.796	0.582	10.5
2000	45.6	0.581	0.754	0.522	10.1
2000	55.3	0.532	0.740	0.489	8.1
2000	63.7	0.522	0.750	0.471	9.8
2500	40.0	0.616	0.803	0.562	8.8
2500	55.6	0.534	0.756	0.491	8.1
3000	63.1	0.540	0.766	0.470	12.9
3000	69.0	0.532	0.769	0.459	13.7

consumption settings obtained in the sensitivity tests. After evaluating some early mapping results, it became clear that the modified engine could not be operated with these settings and produce NO_x emissions consistent with the 2.0 gm/mi NO_x standard. It was decided that sensitivity tests with emissions measurements were required at each operating point to provide the data needed for fuel economy and emissions tradeoffs.

The typical engine operating point at 2000 RPM and level-road-load power, corresponding to 55 MPH in the 1973 Chevrolet Impala Vehicle, was chosen for detailed discussion in this part of the report; however, plots of other mapping data are included in Appendix E. In all plots, comparisons are made with the stock carburetor data from the JPL stock baseline map. As previously discussed, the stock data was obtained with the stock emissions control devices in operation.

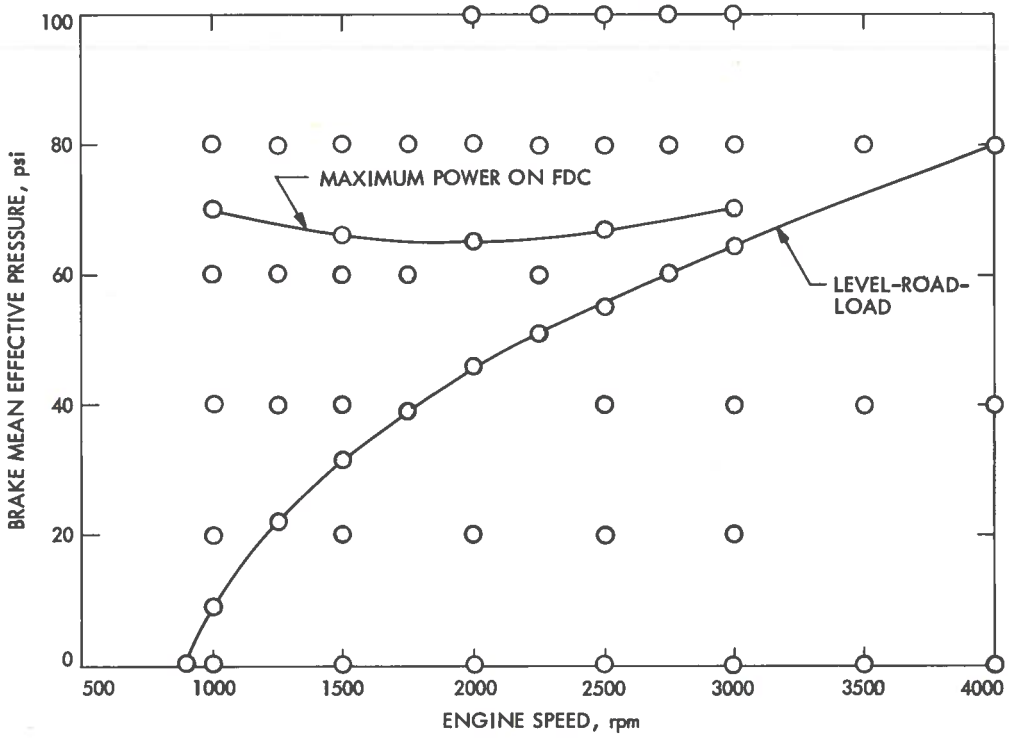

FIGURE 52. ENGINE MAPPING TEST CONDITIONS

The effect of equivalence ratio and spark advance on the brake specific fuel consumption (BSFC) is shown in Figure 53. These data are consistent with the data obtained in the sensitivity test series. For this modified engine, the BSFC decreases with decreasing equivalence ratio, reaching a minimum for $\Phi = 0.75$ and a spark advance of 60° BTDC. Further decreases in equivalence ratio result in a loss of fuel economy. Indications that the combustion interval and/or ignition delay are increasing as the equivalence ratio is decreased are implied by the spark advance required for minimum fuel consumption as a function of equivalence ratio.

As shown in Figure 54, brake specific NO_x ($BSNO_x$) emissions are quite sensitive to variations in equivalence ratio and spark advance. For a given spark advance, decreasing the equivalence ratio is effective in reducing $BSNO_x$ emissions. This is probably a result of decreasing peak temperatures and

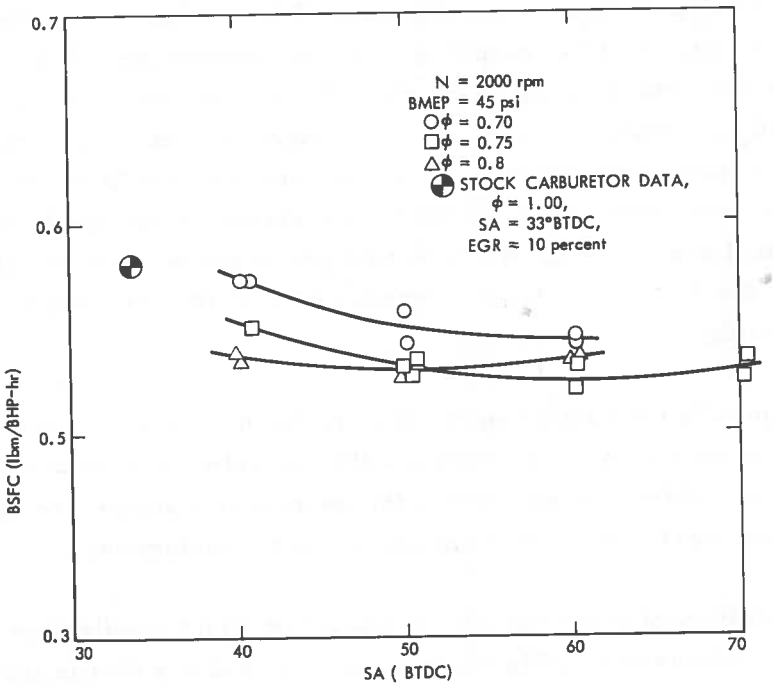

FIGURE 53. BSFC VERSUS SPARK ADVANCE

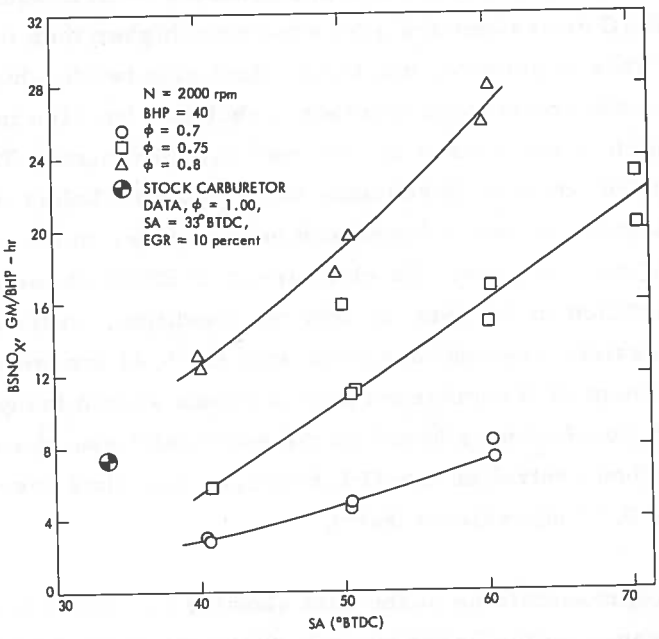

FIGURE 54. BSNO$_x$ EMISSIONS VERSUS SPARK ADVANCE

decreasing time at peak temperature because of the increase in combustion duration and/or ignition delay resulting with lean combustion. For a given equivalence ratio, retarding the spark timing is also an effective means for reducing $BSNO_x$ emissions since it results in reduced peak temperatures and reduced time at peak temperatures. For this operating condition, the modified engine is equal to or better than the $BSNO_x$ emissions for the stock vehicle with emission control equipment for $\Phi = 0.70$ with spark advances of 40, 50, or 60° BTDC and for $\Phi = 0.75$ with a spark advance of 40°BTDC (20° retarded from MBT spark timing).

Brake specific CO (BSCO) emissions are found to be rather insensitive to equivalence ratio and spark advance for this operating condition as shown in Figure 55. The BSCO emissions levels for the modified engine are about equivalent to the stock vehicle with emission control equipment.

The sensitivity of brake specific hydrocarbon (BSHC) emissions to equivalence ratio is illustrated in Figure 56. There is a sharp rise in BSHC emissions as the equivalence ratio is decreased from 0.8 to 0.7 with all values being higher than those for the stock vehicle with emissions control equipment in operation. The BSHC emissions are also somewhat higher than the Autotronics-modified engine. This is probably due to the slant plug heads which increase the squish area to promote combustion chamber turbulence but also increase the crevice volume which is one source of unburned hydrocarbons. The particular turbulator valves used could be introducing large scale turbulent eddies similar to shrouded valves which result in increased heat transfer to the cylinder walls causing the quench layer to grow. No clear trend of BSHC emissions with spark advance can be identified in the data for this run condition. Although these levels of hydrocarbon emissions are not consistent with the 0.41 gm/mi standard, catalytic aftertreatment of the unburned hydrocarbons should bring them down to the standard. This conclusion is based on the successful use of a catalytic converter for hydrocarbon control on the JPL hydrogen-enriched gasoline vehicle which operates at a 0.53 equivalence ratio.

Alternative representations of the data showing the effect of equivalence ratio and spark advance on the brake specific fuel consumption and brake specific emissions are shown in Figures 57 and 58.

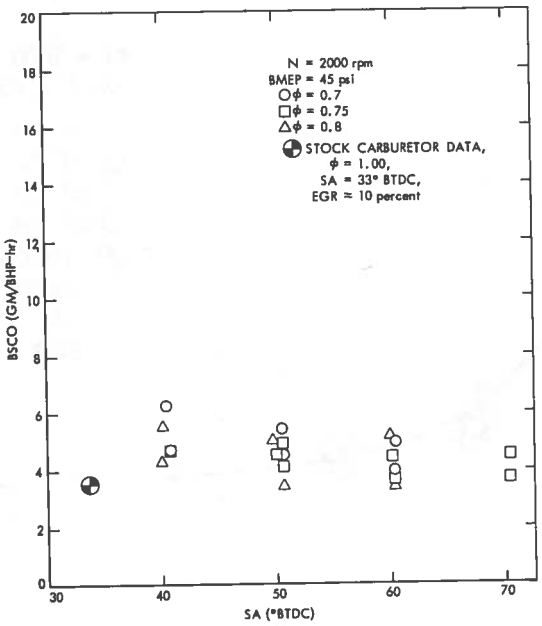

FIGURE 55. BSCO EMISSIONS VERSUS SPARK ADVANCE

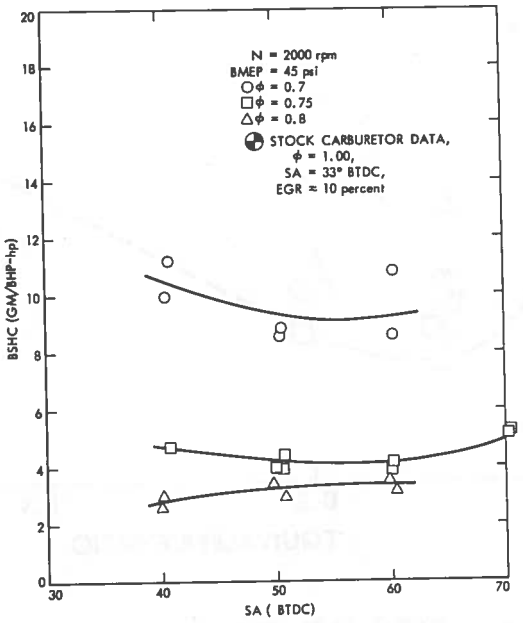

FIGURE 56. BSHC EMISSIONS VERSUS SPARK ADVANCE

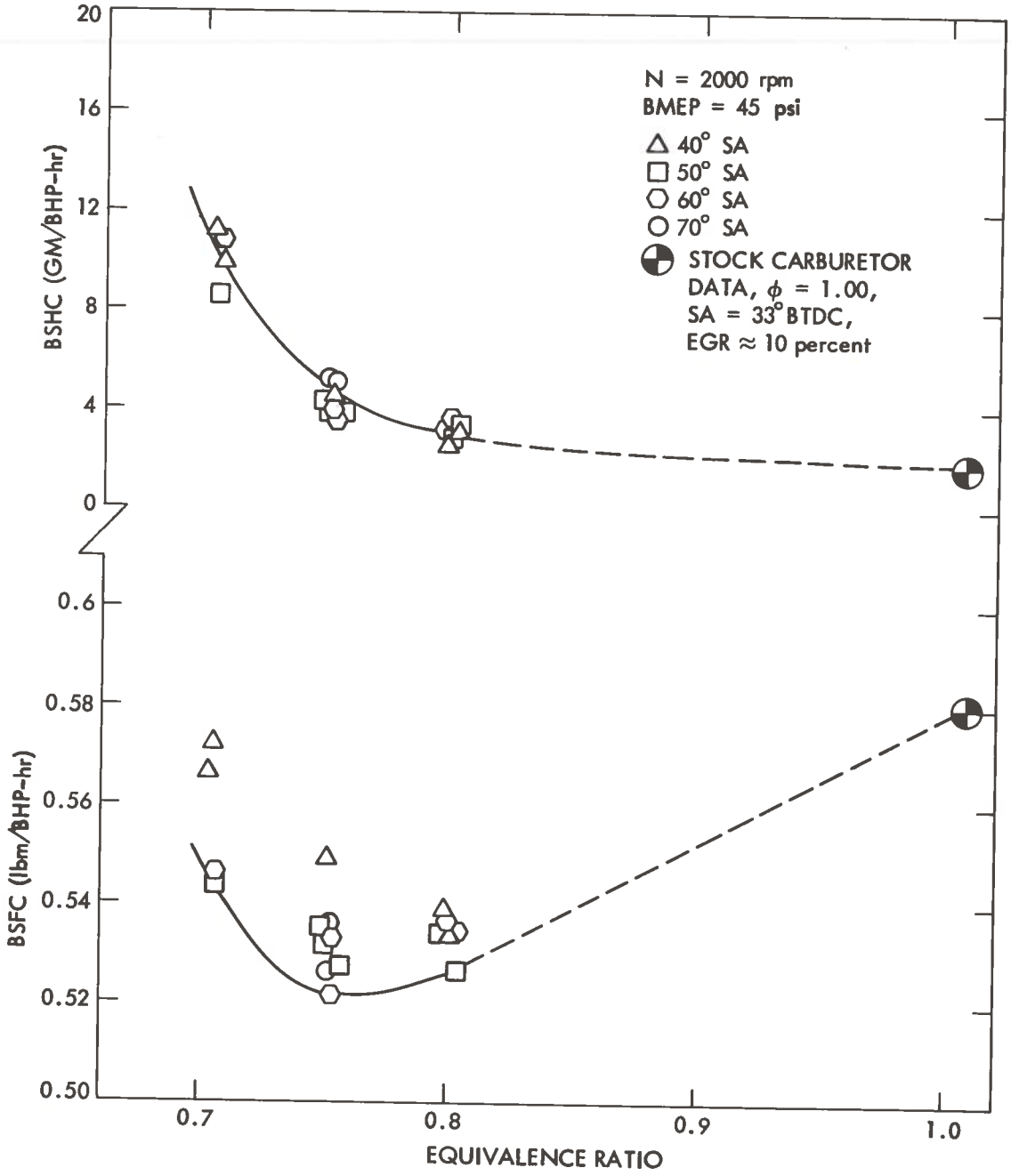

FIGURE 57. BSFC AND BSHC EMISSIONS VERSUS EQUIVALENCE RATIO

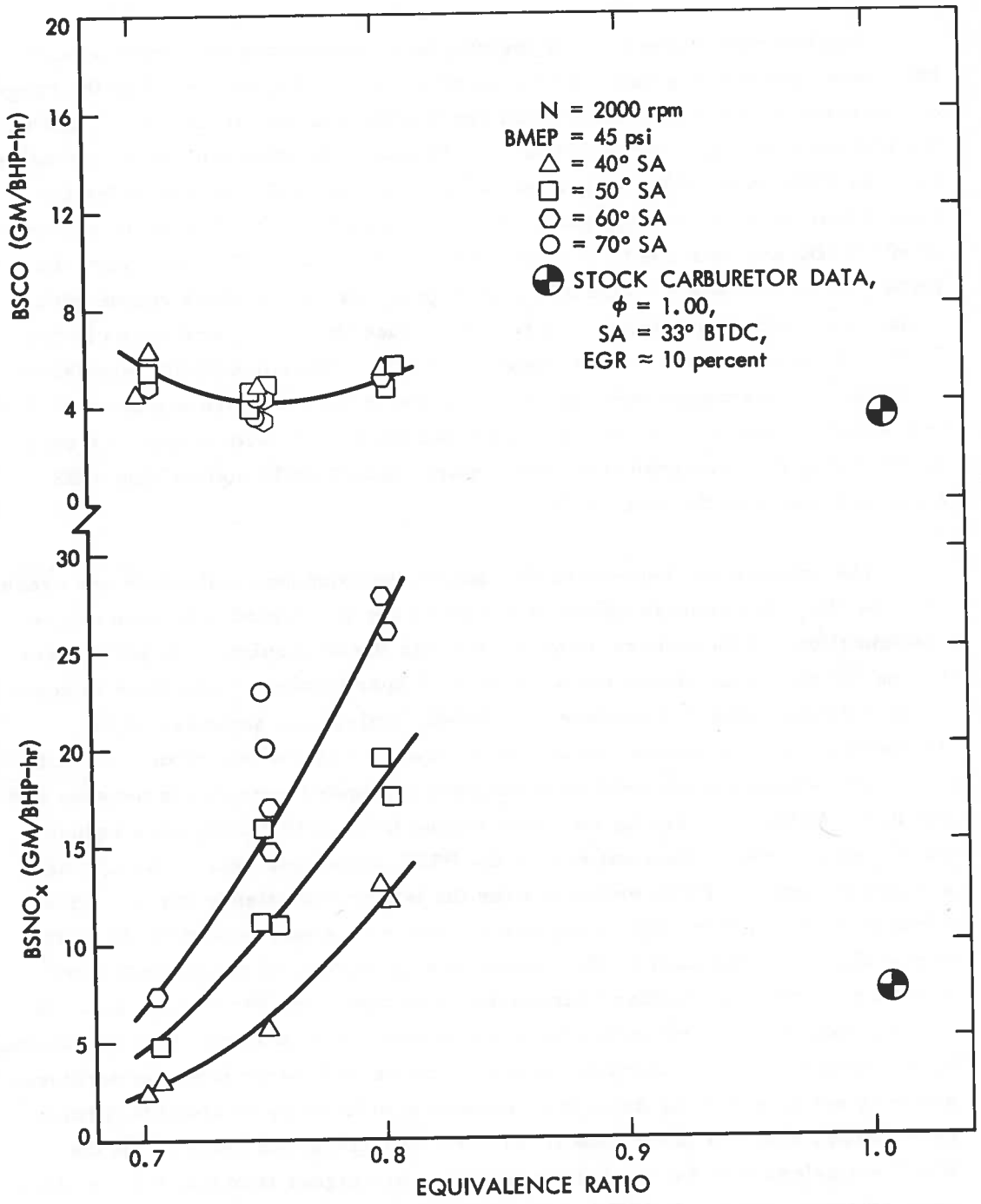

FIGURE 58. BSCO AND $BSNO_x$ EMISSIONS VERSUS EQUIVALENCE RATIO

The tradeoff between brake specific fuel consumption and brake specific NO_x emissions for this run condition is illustrated in Figure 59. For the range of equivalence ratios (0.7 to 0.9) and spark advances (40° BTDC to 70° BTDC) of the test data, a single curve can be used to generally represent the relationship between BSFC and $BSNO_x$ emissions. The minimum BSFC condition for the second lean burn engine configuration occurs for $\Phi = 0.75$ with a spark advance of 60° BTDC and is about 10 percent less than the stock BSFC; however, the $BSNO_x$ emissions are a factor of 2 higher than that for the stock engine with emissions control equipment. To further reduce the $BSNO_x$ emissions in the lean burn engine results in an increase in BSFC. The stock $BSNO_x$ emissions level for this operating condition can be met with the lean burn engine at $\Phi = 0.70$ with spark advances of 50° or 60° BTDC and for $\Phi = 0.75$ with a spark advance of 40° BTDC (20° retarded from MBT spark timing) while maintaining a BSFC 6 percent less than the stock value.

The relationship between brake specific hydrocarbon emissions and brake specific NO_x emissions is shown in Figure 60 for the second lean burn engine configuration. A dashed line is drawn through the data points with MBT spark timing for each equivalence ratio. For MBT spark timing, reductions in equivalence ratios below 0.9 produce less $BSNO_x$ emissions; however, BSHC emissions begin increasing rapidly for equivalence ratios less than about 0.8. The BSHC emissions are relatively constant for equivalence ratios between 0.8 and 0.9. Although retarding the spark timing from MBT timing does reduce $BSNO_x$ emissions, it does not reduce the BSHC emissions and, in fact, causes a slight increase in BSHC emissions for the leaner equivalence ratios. This effect is different from that in engines running rich where retarding the spark timing decreases the hydrocarbon emissions by increasing the exhaust temperatures to promote further hydrocarbon reaction in the exhaust system. In lean burning engines, retarding the spark timing leads to an increase in unburned hydrocarbons in the combustion chamber because of lowered peak temperatures and does not increase the exhaust temperature sufficiently to promote further hydrocarbon reaction in the exhaust system. As discussed earlier, all the BSHC emissions data for the lean burn engine are higher than that for the stock data; however, the stock $BSNO_x$ emissions performance can be met with the lean burn engine using lean equivalence ratios and/or retarded spark timing.

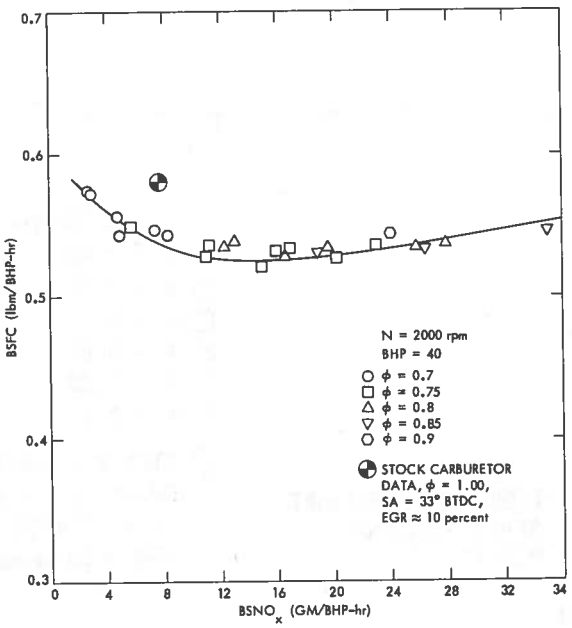

FIGURE 59. BSFC VERSUS BSNO$_x$ EMISSIONS

A plot of brake specific fuel consumption versus brake specific hydrocarbon emissions is given in Figure 61. A dashed line is drawn through each equivalence ratio point with MBT spark timing. For MBT timing, decreasing the equivalence ratio to 0.75 reduces the fuel consumption; however, below $\Phi = 0.8$ the BSHC emissions start to increase. Further reductions in Φ below 0.75 produce increases in both BSFC and BSHC emissions. Compared with the stock baseline engine, the second lean burn engine configuration gave less fuel consumption and higher BSHC emissions for all data points at this run condition.

Individual cylinder exhaust temperatures were measured for all test conditions and provide a good indicator for brake specific hydrocarbon emissions. BSHC emissions are shown plotted versus average exhaust temperature in Figure 62. For average exhaust temperatures less than about 1200°F, the BSHC emissions increase sharply. A similar trend is seen when hydrocarbon emissions are plotted against the minimum exhaust temperature of the eight

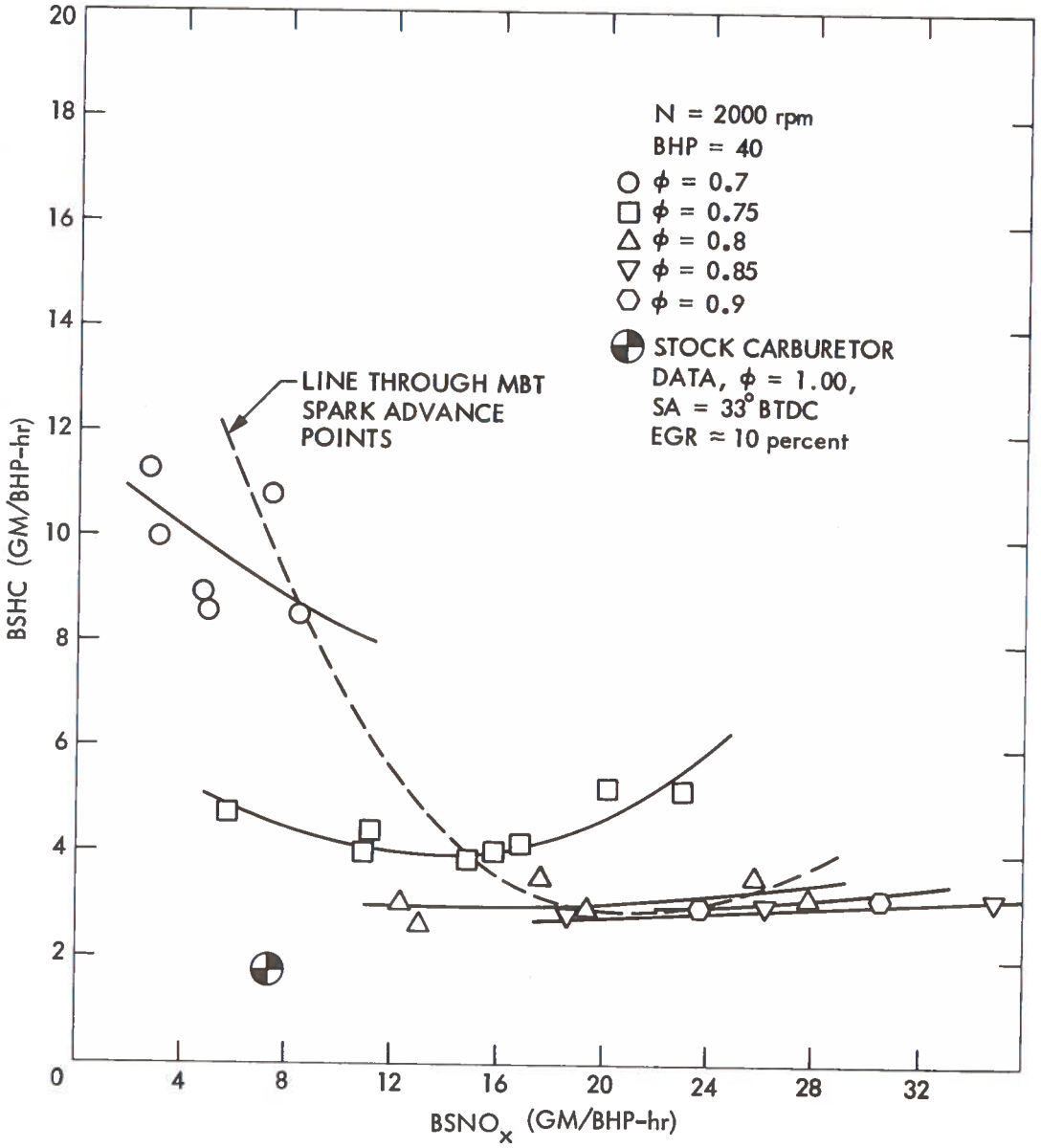

FIGURE 60. BSHC EMISSIONS VERSUS $BSNO_x$ EMISSIONS

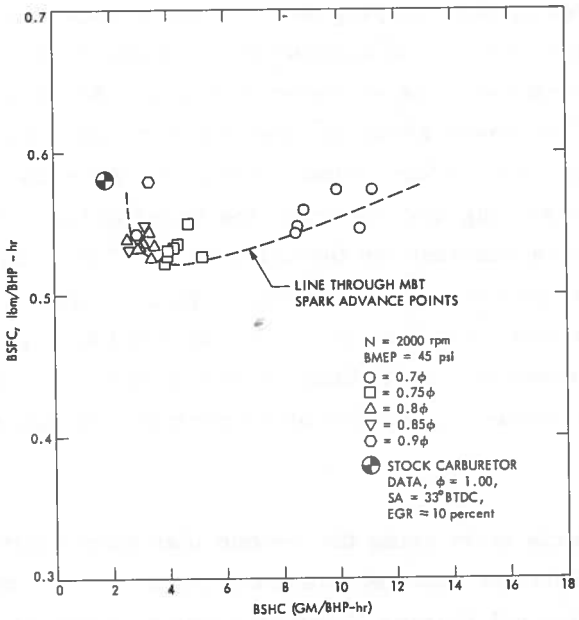

FIGURE 61. BSFC VERSUS BSHC EMISSIONS

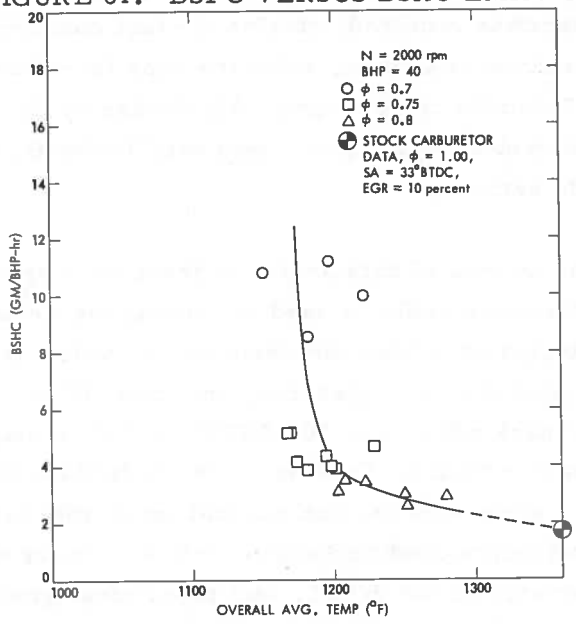

FIGURE 62. BSHC EMISSIONS VERSUS OVERALL AVERAGE TEMPERATURE

cylinders as shown in Figure 63. The sharp increase in BSHC emissions occurs in this case at an exhaust temperature of about 1140°F.

In its final form, the mapping data for the second lean burn engine configuration is presented in terms of contour plots of BSFC and brake specific emissions on the BMEP-RPM plane as shown in Figures 64, 65, 66, and 67 for Φ = 0.75 and a 50° BTDC spark advance. Several data smoothing operations are used in processing the data for contour plots. All data are corrected to the nominal RPM by assuming that the indicated specific fuel consumption and equivalence ratio are constant for the correction. The corrected data is then curve-fitted by a third order polynominal. Typical curve-fit plots of BSFC and brake specific emissions are shown in Figures 68, 69, 70, and 71. The contour plots are made by interpolating only within the bounds of the test data. Contour plots and curve-fit plots for other control strategies are given in Appendix E.

Since no vehicle tests using the second lean burn engine configuration were included in this effort, an attempt was made to predict the response of such a vehicle over the Federal Driving Cycle by using a computer simulation of the cycle. The computer program breaks the cycle up into one-second increments, calculates the horsepower required, obtains the fuel consumption and emissions from engine dynamometer map data, sums the time increments over the cycle and divides by the 7.5-mile cycle length. All driving cycle calculations were made for a 1973 Chevrolet Impala (4500 lbm) with Turbo-Hydromatic transmission and a 2.73 rear axle ratio.

Because of the amount of data available from the mapping tests, many different control strategies could be used in running the Federal Driving Cycle. Three control strategies have been run through the cycle: (1) a map using the best economy data point for each operating condition, (2) a map for an equivalence ratio of 0.75 and a spark advance of 50° BTDC, and (3) a map with Φ = 0.75 and a 40° BTDC spark advance. Driving cycle predictions for these three cases are given in Table 8 along with predictions and actual measurements for the stock vehicle and the Autotronics-modified engine with a primary equivalence ratio of 0.85 and a spark advance of 50° BTDC. All three strategies yield better than 20 percent higher fuel economy than the stock vehicle and meet the 3.4 gm/mi

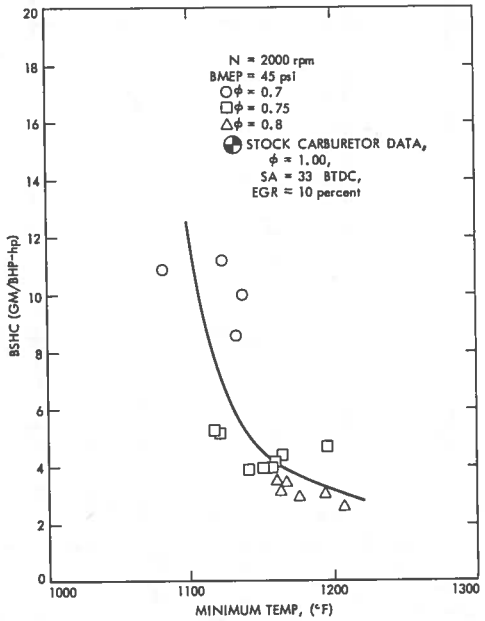

FIGURE 63. BSHC EMISSIONS VERSUS MINIMUM TEMPERATURE

CO emissions standard. The NO_x emissions show the most variation with the strategy selection, being smallest for the case with $\Phi = 0.75$ and a spark advance of 40° BTDC. For this case, the NO_x emissions are 4.2 gm/mi which falls between the values for the stock vehicle and the Autotronics modified engine, but it is a factor of 2 higher than the 2.0 gm/mi NO_x standard. The standard could probably be met by retarding the spark another 10° with a slight decrease in fuel economy. Hydrocarbon emissions for all three cases are higher than the stock values; however, by using a catalytic converter, the 0.41 gm/mi standard could probably be met.

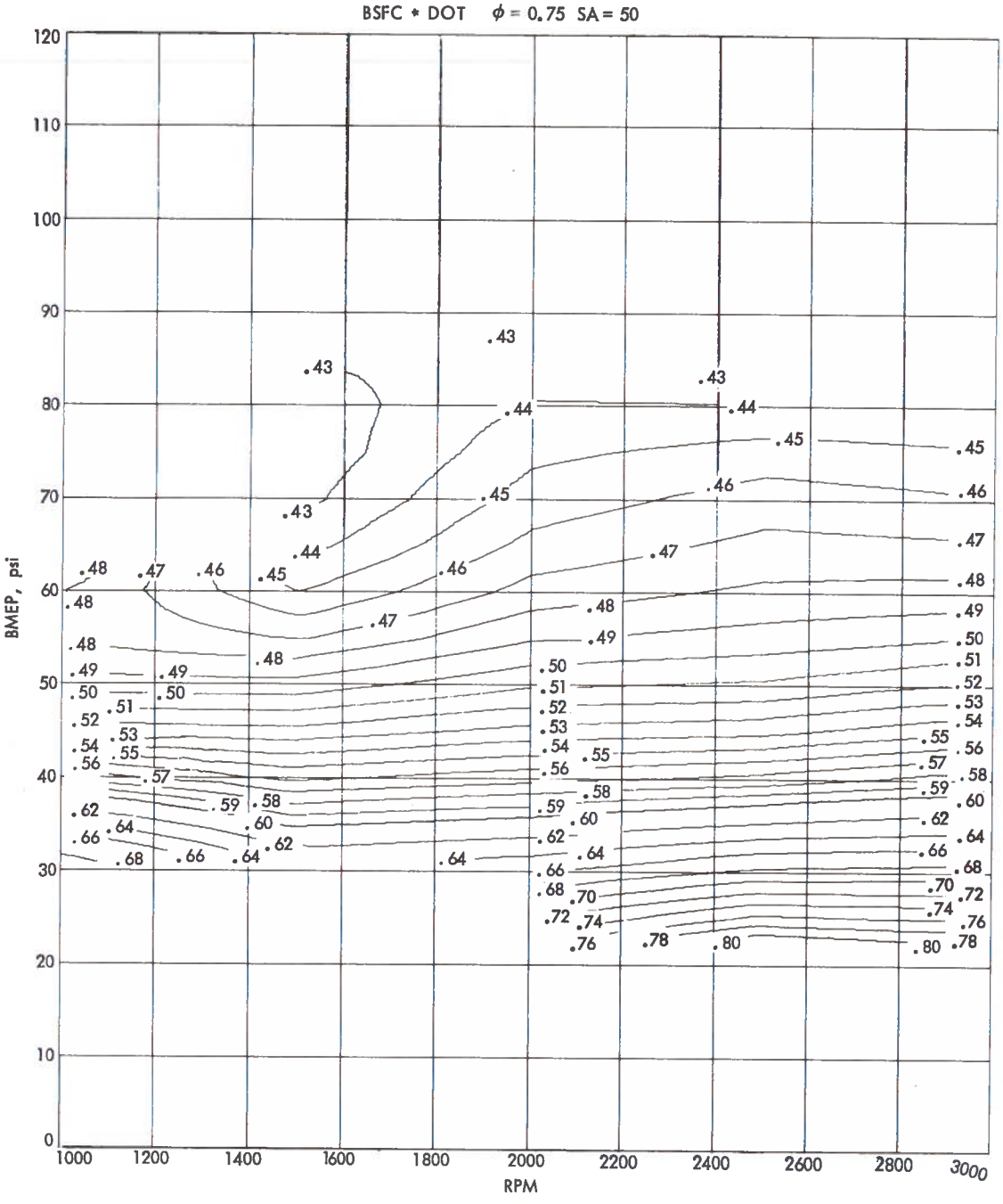

FIGURE 64. BSFC CONTOUR MAP FOR SECOND MODIFIED ENGINE CONFIGURATION

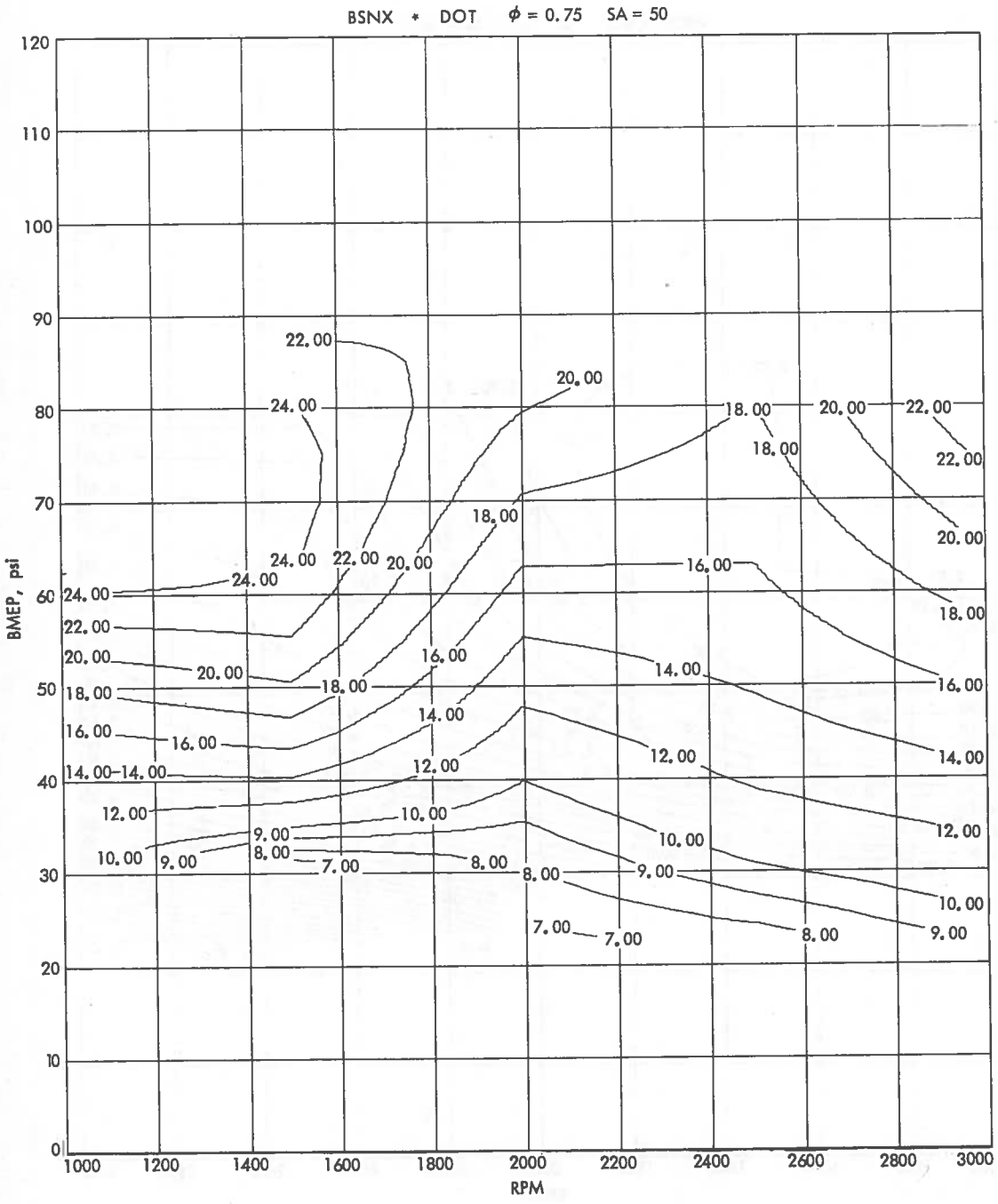

FIGURE 65. BSNO$_x$ CONTOUR MAP FOR SECOND MODIFIED ENGINE CONFIGURATION

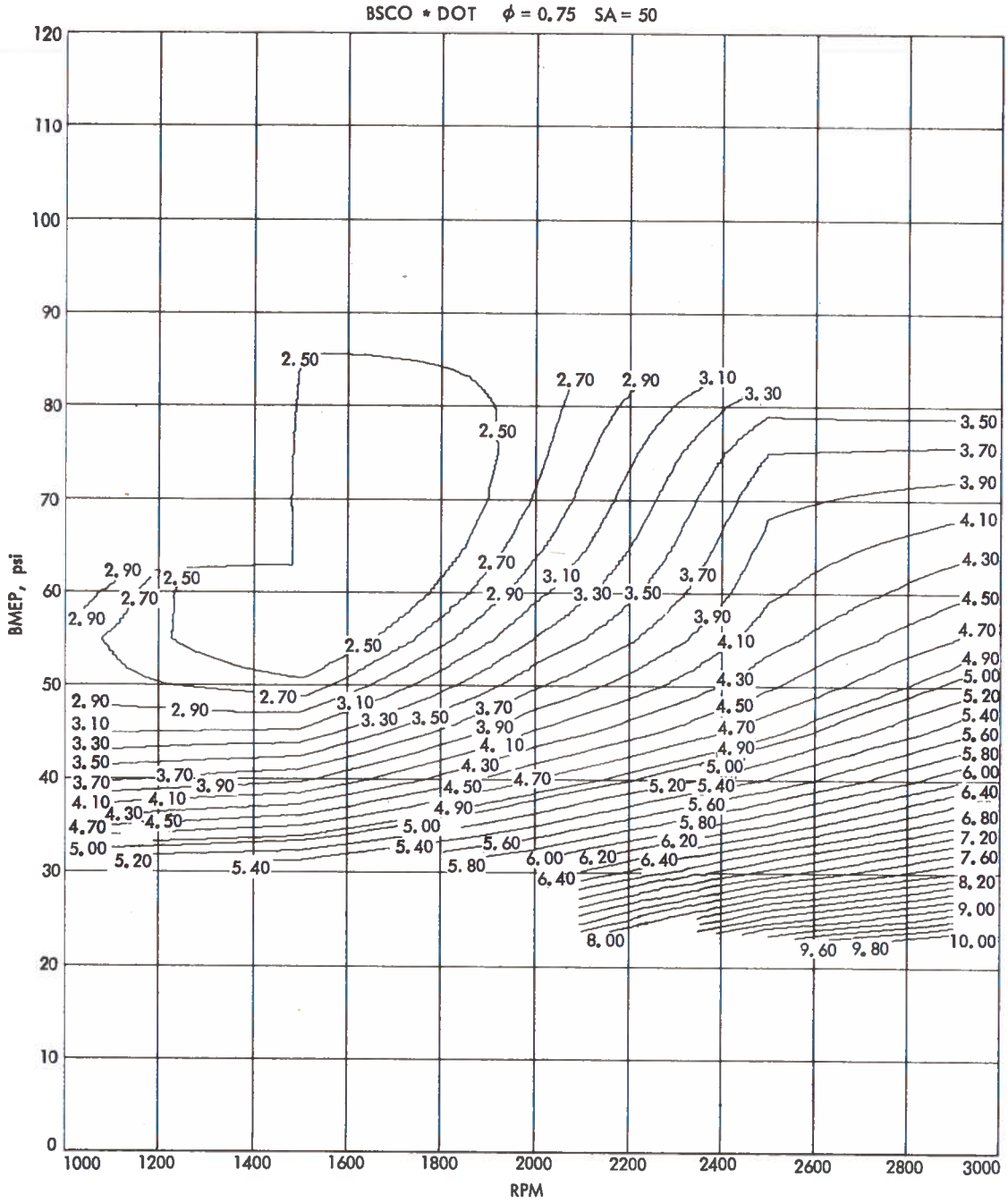

FIGURE 66. BSCO CONTOUR MAP FOR SECOND MODIFIED ENGINE CONFIGURATION

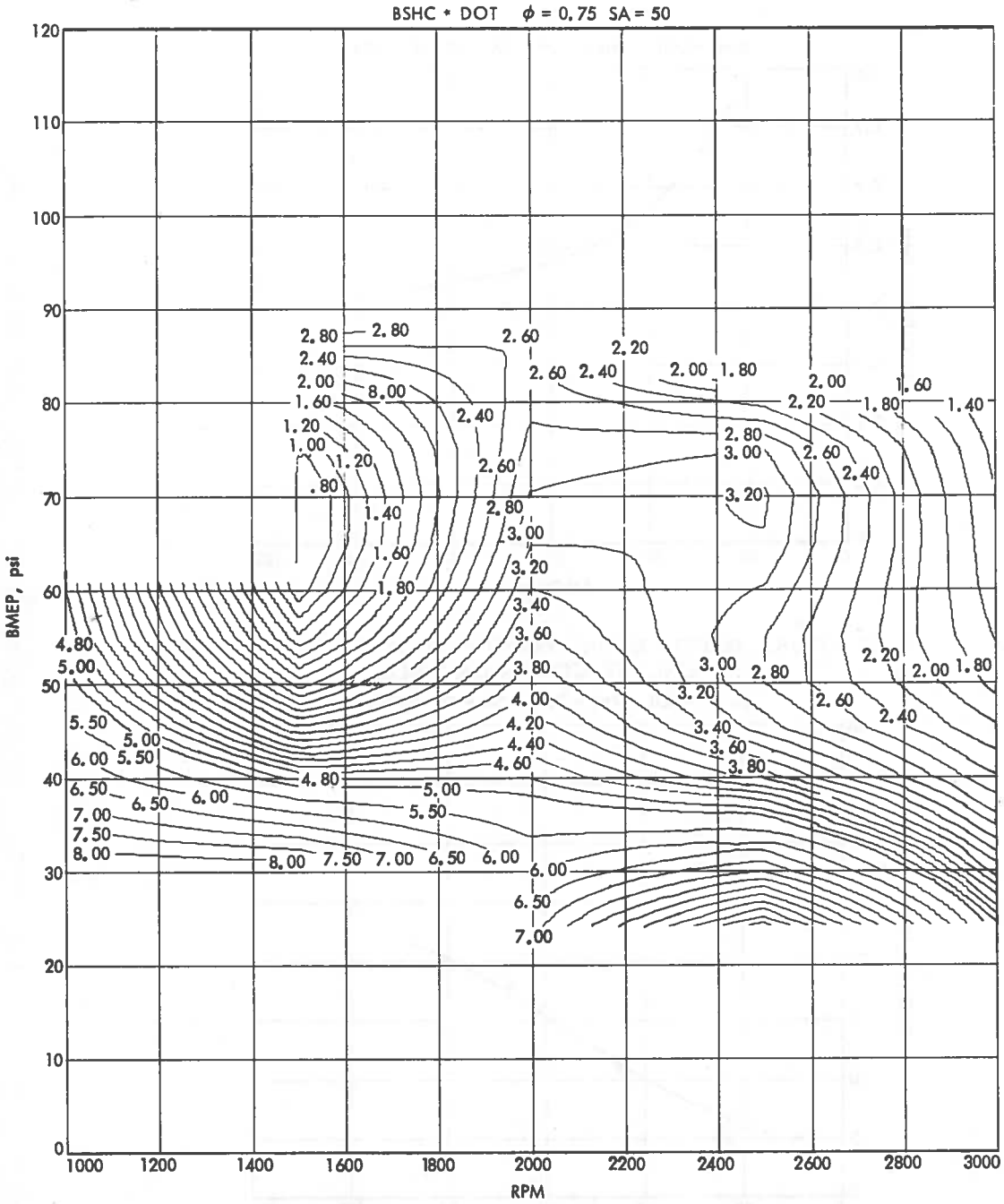

FIGURE 67. BSHC CONTOUR MAP FOR SECOND MODIFIED ENGINE CONFIGURATION

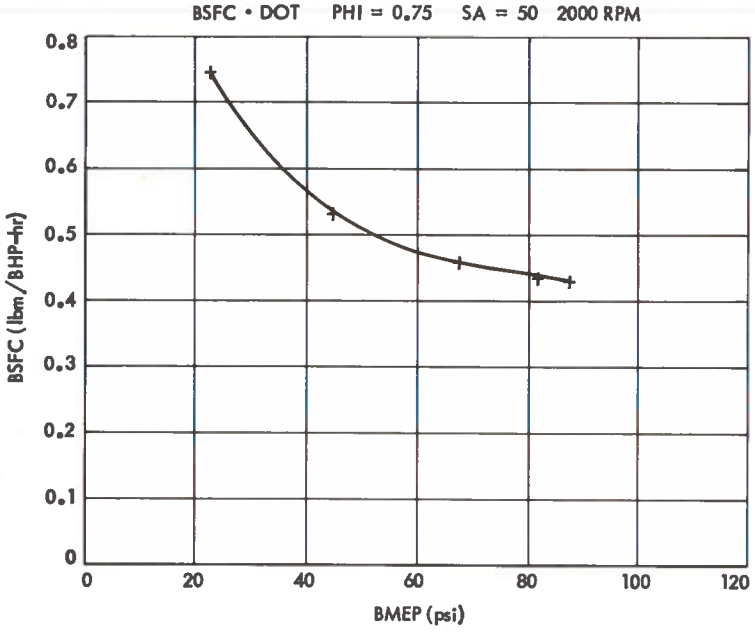

FIGURE 68. BSFC VERSUS LOAD FOR SECOND MODIFIED ENGINE CONFIGURATION

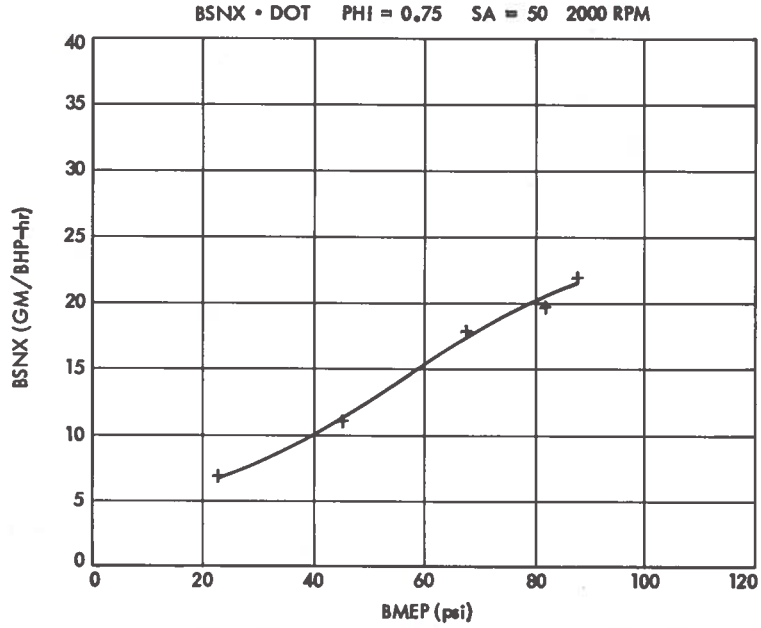

FIGURE 69. BSNO$_x$ VERSUS LOAD FOR SECOND MODIFIED ENGINE CONFIGURATION

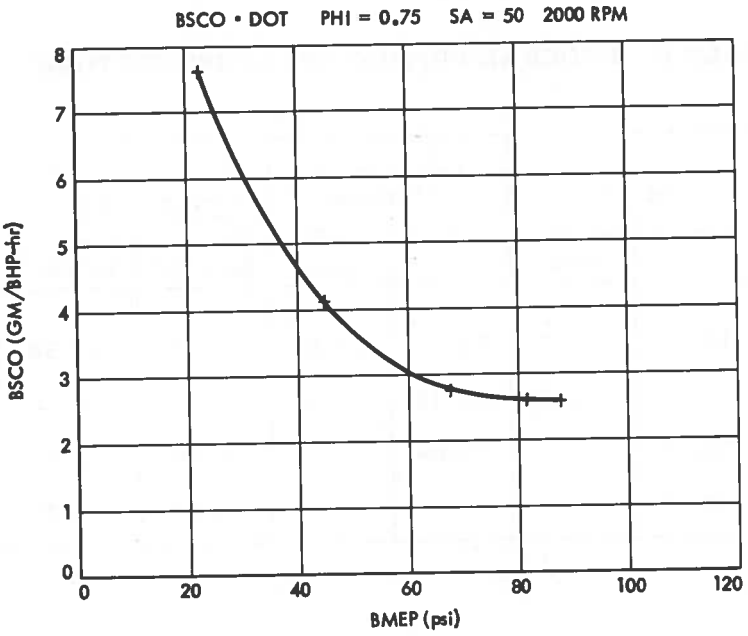

FIGURE 70. BSCO VERSUS LOAD FOR SECOND MODIFIED ENGINE CONFIGURATION

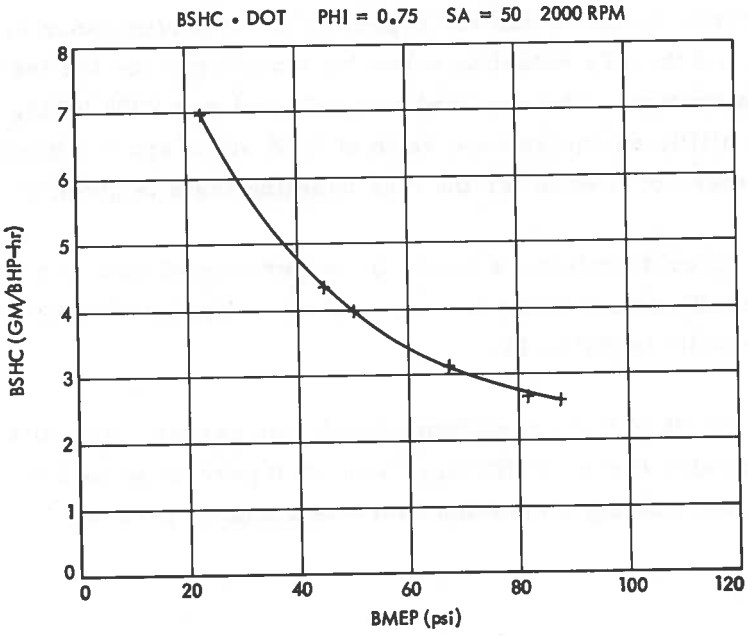

FIGURE 71. BSHC VERSUS LOAD FOR SECOND MODIFIED ENGINE CONFIGURATION

TABLE 8. FEDERAL DRIVING CYCLE PREDICTIONS

Parameters	Stock		Autotronics - Modified		Second Lean Burn Engine Configuration Predictions		
	Actual	Prediction	Actual	Prediction	Φ=0.75, SA = 50°	Φ=0.75, SA = 40°	Best Economy
MPG	10.6	12.11	12.8	13.82	14.68	14.54	14.85
NO_x (gm/mi)	2.05	2.16	5.12	5.54	6.66	4.20	8.29
CO (gm/mi)	36.08	---	15.04	---	2.90	3.02	2.87
HC (gm/mi)	2.15	---	4.49	---	3.68	4.20	4.15

5.5 Data Repeatability

A baseline test condition was periodically run with the second lean burn engine configuration to determine the repeatability of performance and emissions measurements and thereby establish a level of confidence for the test engine and data acquisition system. The run condition selected was 2000 RPM, level-road-load power (40 BHP), an equivalence ratio of 0.85 and a spark advance of 44° BTDC. A summary of results for the nine baseline tests is given in Table 9.

For a 95 percent confidence level, the experimental data can be expected to lie within a $\pm 1.86\ \sigma$ band of the average. A statistical evaluation of the test data yield the results in Table 10.

Based on the 95 percent confidence level, the percent deviation in the measurement of indicated thermal efficiency was ±1.0 percent while the corresponding deviation in the exhaust emissions data was about 15 percent.

TABLE 9. EXPERIMENTAL BASELINE TEST RESULTS

Test Number	RPM	BMEP	Φ	η_{t_I}	RPM NO_x	PPM HC	% CO	Point
304.1	2006	45.235	0.849	0.3632	2970	1321	0.1	1
310.1	2024	45.28	0.851	0.3627	2550	1173	0.1	2
311.1	2004	44.828	0.85	0.3600	3370	1321	0.09	3
312.1	1992	44.985	0.853	0.3610	3430	1334	0.09	4
315.1	2018	45.190	0.851	0.3625	3330	1243	0.09	5
316.1	1994	45.734	0.851	0.3626	3100	1336	0.1	6
317.1	2037	45.213	0.852	0.3655	3190	1255	0.09	7
218.1	2015	45.369	0.854	0.3646	3130	1270	0.09	8
$\bar{x}$	2011	45.23	0.8514	0.3628	3134	1282	0.09	---
σ	14.29	0.250	0.0015	0.0017	263.2	53.5	0.007	---

TABLE 10. STATISTICAL ANALYSIS OF BASELINE DATA

Parameter	Confidence Range at 95% Probability	Percent Deviation at 95% Probability $\left(\frac{1.86\ \sigma}{\bar{x}} \times 100\right)$
RPM	1984 - 2038	1.32
BMEP	44.8 - 45.7	1.03
Φ	0.848 - 0.854	0.33
η_{t_I}	0.360 - 0.366	0.87
NO_x, PPM	2644 - 3624	15.6
HC, PPM	1182 - 1382	17.8
CO, %	0.077 - 0.103	14.5

6. HIGH-RESPONSE PRESSURE-TIME DATA

6.1 Description

High-response pressure measurements were made for selected operating conditions to help understand the performance of the second lean-burn engine configuration. Pressure-time traces yield information about ignition delay, combustion duration and cycle-to-cycle pressure variations for individual cylinders. This kind of detailed information is needed for the Blumberg-Kummer cycle analysis calculations. The 4 operating points in Table 11 were selected to provide information about the sensitivity of individual cylinder pressure characteristics to engine speed, load and equivalence ratio. All tests were made with MBT spark timing.

TABLE 11. OPERATING POINTS FOR PRESSURE-TIME DATA

RPM	BHP	EQUIVALENCE RATIO
1500	21.0	0.7, 0.75, 0.8, 0.85, 0.9, 0.95, 1.00
2000	40.0	0.7, 0.75, 0.8, 0.85, 0.9, 0.95, 1.00
2000	57.5	0.7, 0.75, 0.8, 0.85, 0.9, 0.95, 1.00
2500	61.5	0.7, 0.75, 0.8, 0.85, 0.9, 0.95, 1.00

Pressure taps were drilled in the slant plug heads adjacent to the spark plug locations for measuring cylinder pressures. A Kisler pressure transducer was mounted close to the engine to provide high-response measurement capability. All pressure data reported in this work are for cylinder #3. Pressure measurements were made for every 1 degree of crank rotation on the compression and expansion strokes. Ignition delay and combustion duration information were obtained from averaged motoring and firing pressure-time traces which were computed and stored during the test. The motoring pressure traces for the operating points were obtained by electrically shorting cylinder #3 while maintaining engine RPM and load with the remaining 7 cylinders. The average motoring pressure trace was based on 50 successive motoring cycles while 100 successive firing cycles were used for the average firing pressure trace.

In addition, the pressure difference between the average firing trace and the average motoring trace was computed and stored. The average motoring trace, the average firing trace and the average pressure difference trace were then plotted versus crank angle along with an indicator of when the spark was initiated. This mechanized data handling was quite useful in reducing the data processing required after the test. Average motoring and firing pressures were digitally recorded for every 1 degree of crank rotation on the compression and expansion strokes.

To obtain an indication of the cycle-to-cycle pressure variations, photographs were made of multiple pressure traces using a storage oscilloscope. For each operating point, approximately 10 successive cycles were recorded for both the motoring and firing mode.

6.2 Pressure-Time Characteristic

To help in analyzing pressure-time data, several parameters are normally defined, as illustrated in Figure 72. The combustion interval is the period from the initiation of the spark to the peak cylinder pressure. Ignition delay is defined as the period from spark initiation to the first measurable rise in cylinder pressure above the motoring pressure trace. The ignition delay period corresponds to the time required for transition from the spark kernel to a developed flame front. The effective combustion interval is defined as the combustion interval minus the ignition delay period. The effective combustion interval is the parameter needed for use in the Blumberg-Kummer cycle analysis program.

For level-road-load power at 2500 RPM, pressure-volume characteristics are given in Figures 73 and 74 for near stoichiometric operation ($\Phi \approx 0.95$) and for lean operation ($\Phi \approx 0.70$). The diagrams are drawn for the compression and expansion strokes only and are based on the digitized data for the averaged firing pressure traces. During the compression stroke, the data define a straight line equivalent to an isentropic compression of the fuel-air mixture until the development of a flame front when it begins to deviate from the

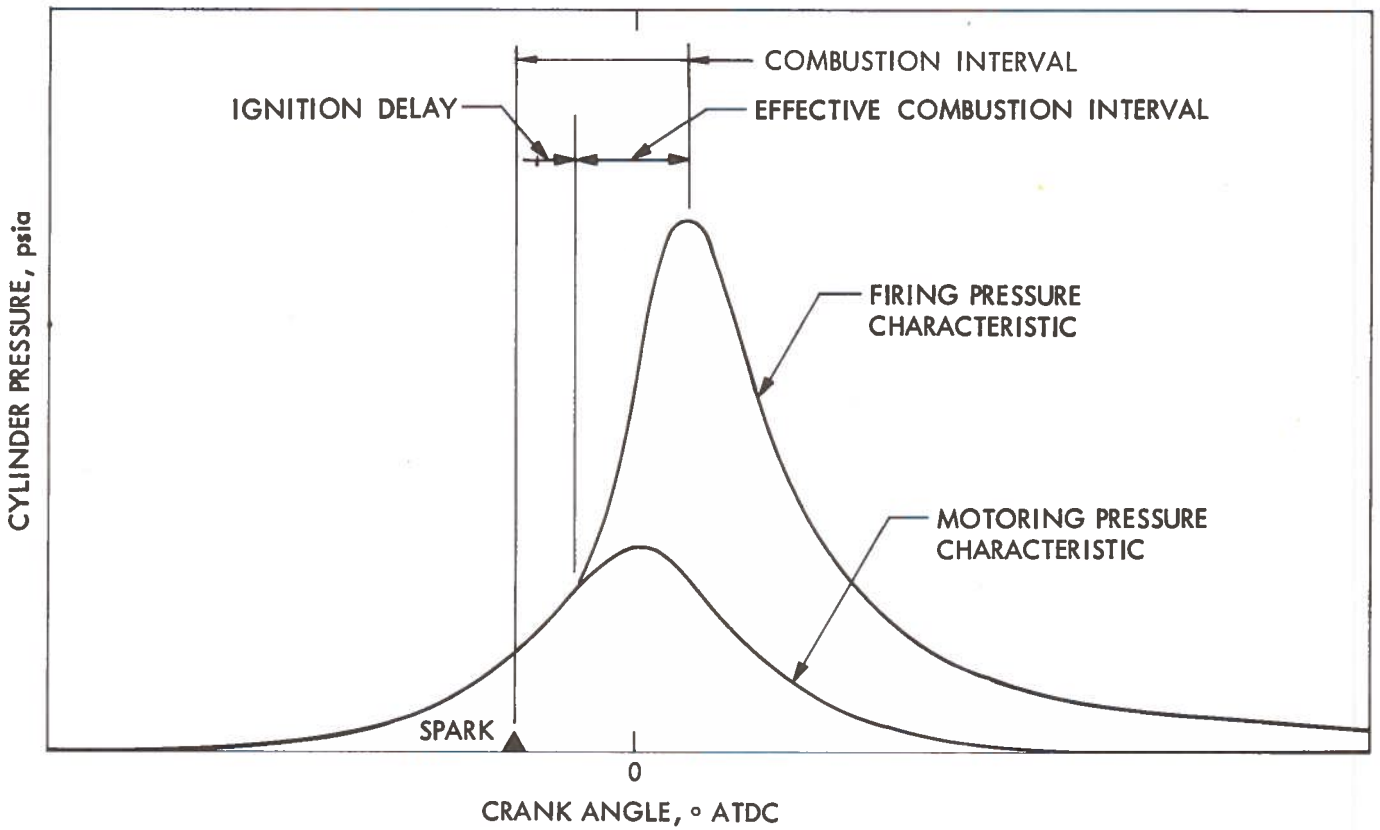

FIGURE 72. CYLINDER PRESSURE CHARACTERISTIC

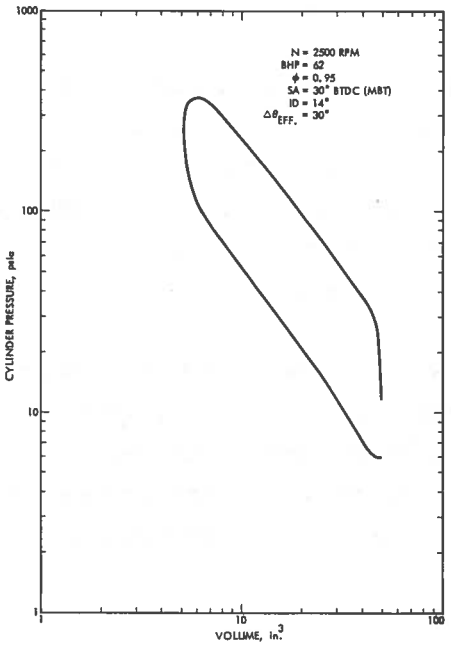

FIGURE 73. PRESSURE-VOLUME CHARACTERISTIC FOR NEAR STOICHIOMETRIC OPERATION

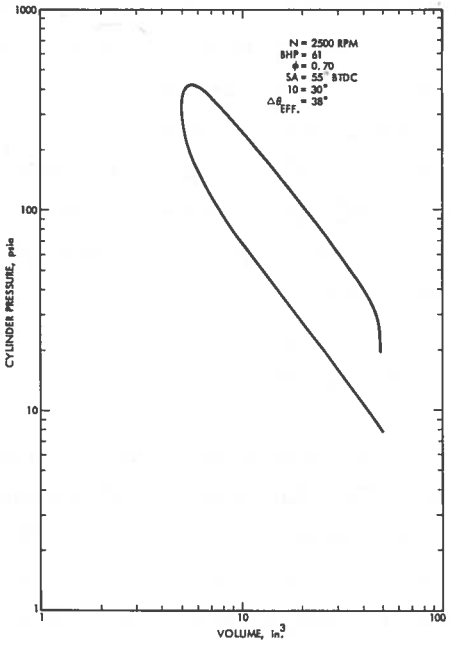

FIGURE 74. PRESSURE-VOLUME CHARACTERISTIC FOR LEAN OPERATION

straight-line relationship. From an examination of the pressure difference plot generated during the test, it is found that the point where the pressure-volume data begins to deviate from a straight line corresponds to the first measurable deviation of the pressure from the motoring pressure trace. Also identified on the diagrams are the point of spark initiation and the point where peak cylinder pressure is achieved.

Values of ignition delay (ID) and effective combustion duration ($\Delta\theta_{EFF}$) were obtained from the pressure-volume characteristics and the average pressure plots which were made during the tests. For MBT spark timing, lean operation is seen to require more spark advance than stoichiometric operation because of an increase in both ignition delay and effective combustion duration.

Significant errors in ignition delay and effective combustion duration can arise because of the difficulty in accurately determining the crank angle where cylinder pressure first rises above the motoring pressure characteristic. To avoid this difficulty, two additional parameters are defined, as illustrated in Figure 75. The plot shows the normalized pressure difference between firing, and motoring pressure traces versus crank angle. An ignition delay parameter (α) is defined as the period from spark initiation until the cylinder pressure reaches 10 percent of the peak pressure difference between firing and motoring traces. A flame speed parameter (β) is defined as the period when cylinder pressure moves from 10 percent to 95 percent of the peak pressure difference between firing and motoring traces.

6.3 Ignition Delay and Flame Speed Data

The ignition delay parameter is shown plotted versus the equivalence ratio of cylinder #3 in Figure 76. The individual cylinder equivalence ratio was derived from an exhaust gas analysis of cylinder#3. The ignition delay parameter is seen to increase significantly as the equivalence ratio is decreased. This indicates that lean mixtures require a much longer time than stoichiometric mixtures for establishing a flame front. The long ignition delays with this lean burn configuration could be the result of excessively high turbulence in the

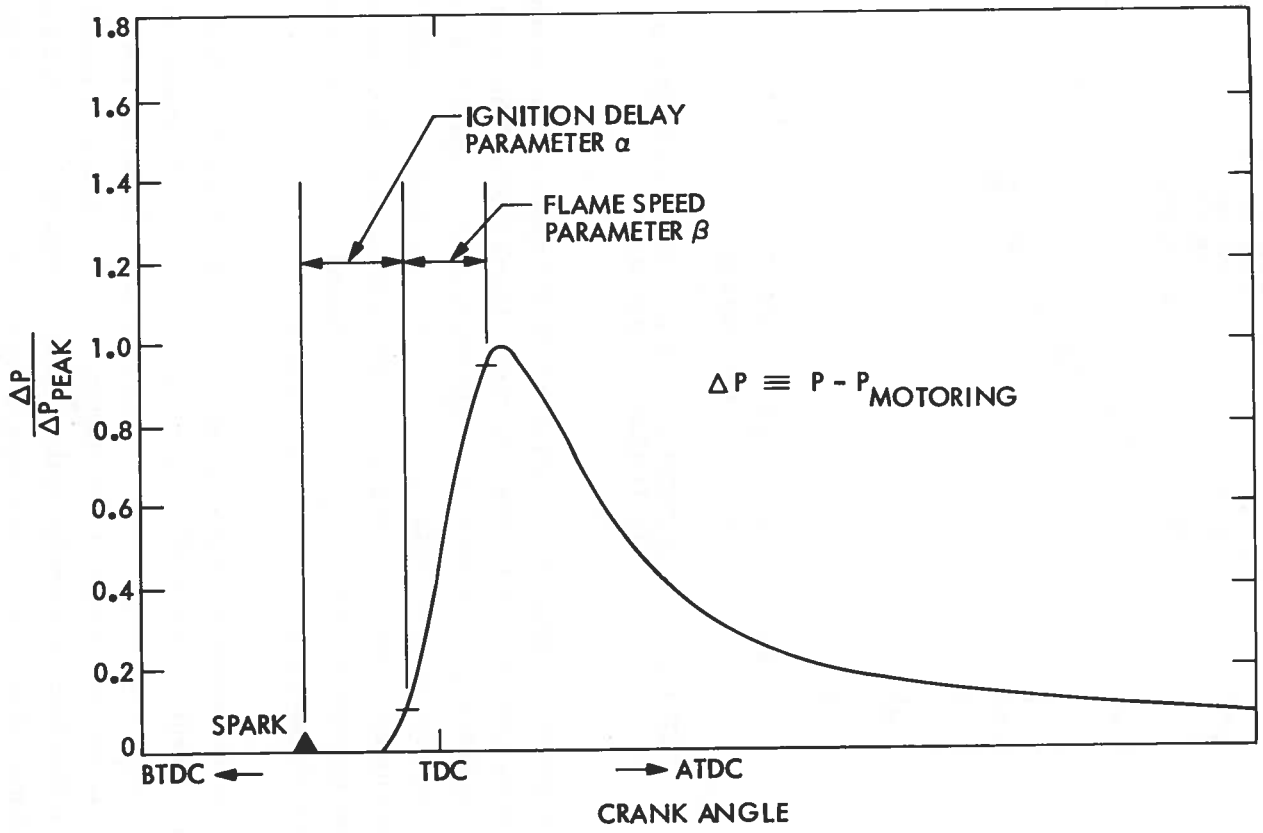

FIGURE 75. DEFINITION OF IGNITION DELAY AND FLAME SPEED PARAMETERS

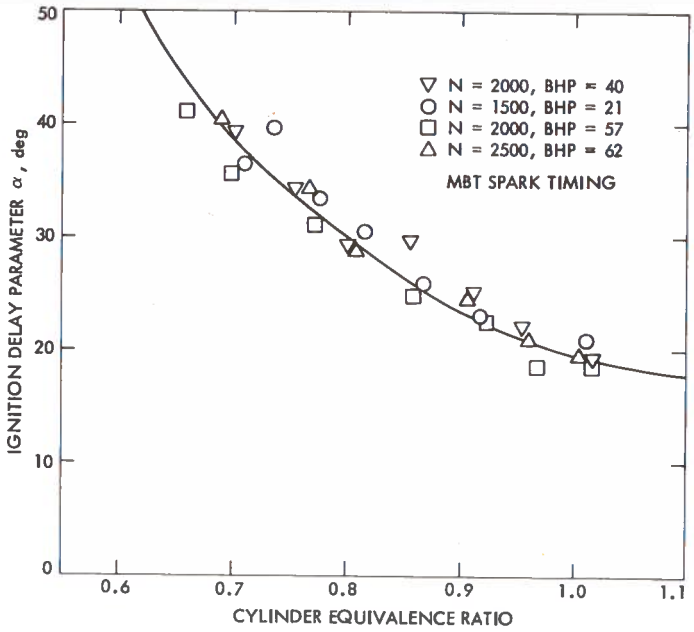

FIGURE 76. IGNITION DELAY PARAMETER VERSUS EQUIVALENCE RATIO

vicinity of the spark plug which interacts with the spark kernel to inhibit development, quench, or produce a distorted flame front. The slant plug heads, turbulator intake valves, and long-reach spark plugs which were used to increase burning velocity could have resulted in the spark gap being located in a high turbulence region. No significant dependence of the ignition delay parameter on engine RPM and load can be established from the test data with all data being adequately correlated with a single curve.

The flame speed parameter is shown plotted versus the cylinder #3 equivalence ratio in Figure 77. Flame speed is seen to decrease only sightly as the equivalence ratio is decreased. This indicates that once a flame front is established, the lean mixtures are burning almost as fast as a stoichiometric mixture in this lean burn configuration. The combination of slant plug heads and turbulator intake valves have apparently been successful in producing a high

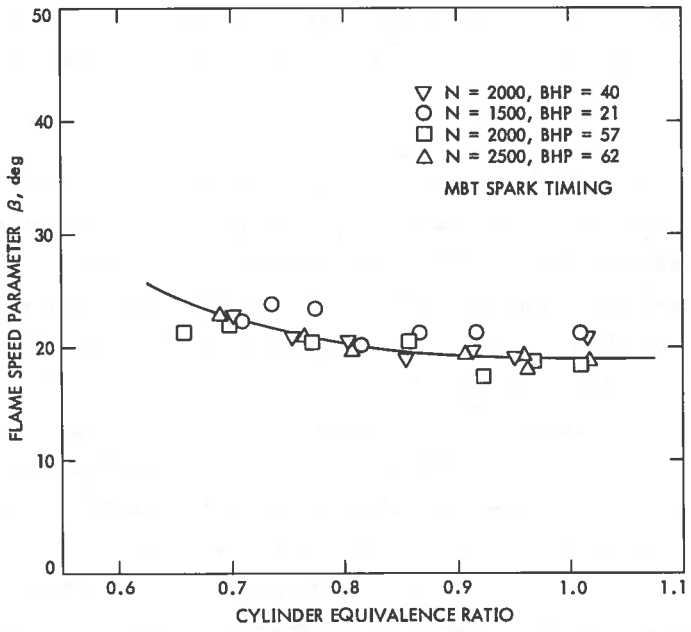

FIGURE 77. FLAME SPEED PARAMETER VERSUS EQUIVALENCE RATIO

turbulence level in the combustion chamber to maintain a rather constant burning velocity for a broad range of equivalence ratios based on the analysis of data presented here. Although the flame speed parameter as defined does not provide a direct measure of flame speed, it is useful in evaluating the effects of equivalence ratio on the combustion process. The test data show no significant dependence of the flame speed parameter on engine RPM and load, with all data being adequately correlated by a single curve.

6.4 Cycle-to-Cycle Pressure Variations

It is well known that the details of the combustion process change in succeeding firing cycles leading to fluctuations in the pressure-time characteristics of individual cylinders. To understand how significant these variations are in the modified lean burn engine, multiple pressure traces were compared

using a storage oscilloscope. For each test condition, the evaluation was based on approximately 10 successive cycles of data for both the motoring and firing modes. The measured fluctuations were characterized by computing the standard deviation of the peak cylinder pressures measured from photographs of multiple pressure traces.

The influence of equivalence ratio on cycle-to-cycle pressure variations is illustrated in Figure 78 for one operating condition. Note the much larger spread in peak pressures for the leaner equivalence ratio point. The standard deviation of peak pressures increased from 19.1 to 31.2 for a decrease in equivalence ratio from 0.95 to 0.72. Photographs for other operating conditions are included in Appendix F. No significance can be attached to the apparent variation in time when peak pressure occurred on the photographs since ignition delay and RPM effects are inseparable because of the measurement system used. A composite plot of all the data showing the effect of equivalence ratio on cycle-to-cycle peak pressure variations is given in Figure 79. The individual cylinder equivalence ratios were based on exhaust gas composition measurements on individual cylinders. For the range of conditions tested, cycle-to-cycle pressure variations remained fairly constant until the sharp increase for equivalence ratios less than about 0.75. It is not possible to detect any effect of engine speed and load from this data. The data scatter is partially due to inaccuracies in making measurements from photographed data.

6.5 Emissions Measurements

For the pressure-time data points, individual cylinder emissions measurements were made for cylinder #3. If it is assumed that cylinder #3 produces one-eight of the brake horsepower while consuming one-eighth of the gasoline and air, the ppm emissions measurements can be calculated on a brake specific basis. This assumption is probably not too bad since in Figure 43 the equivalence ratio of cylinder #3 is seen to be approximately equal to the average equivalence ratio for 2000 RPM and level-road-load power. Reduced on this basis, the brake specific NO_x emissions from cylinder #3 is shown plotted versus the cylinder equivalence ratio in Figure 80. For each of the operating conditions shown, the peak in $BSNO_x$ emissions occurs at an equivalence ratio

N = 2000
BHP = 57
ϕ = 0.72
SA = 56° BTDC

$$\frac{\sigma_{P_{PEAK}}}{\langle P_{PEAK} \rangle} = 0.0751$$

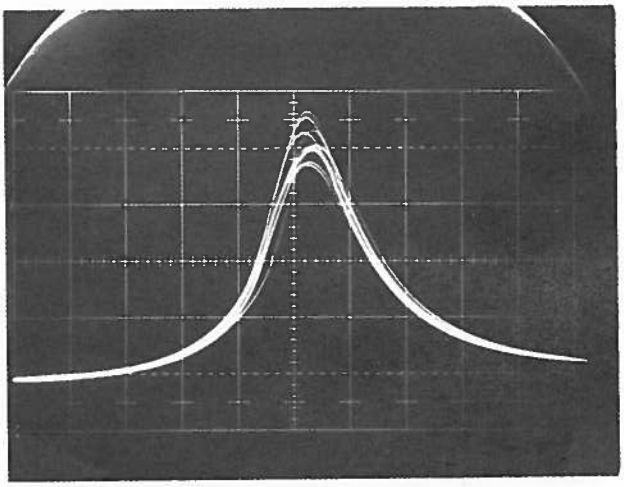

(a) LEAN OPERATION

N = 2000
BHP = 57
ϕ = 0.95
SA = 30° BTDC

$$\frac{\sigma_{P_{PEAK}}}{\langle P_{PEAK} \rangle} = 0.0462$$

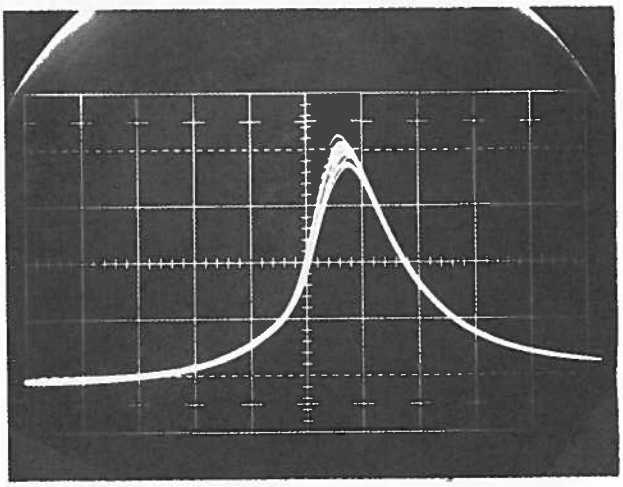

(b) NEAR -STOICHIOMETRIC OPERATION

FIGURE 78. COMPARISON OF CYCLE-TO-CYCLE CYLINDER PRESSURE VARIATIONS

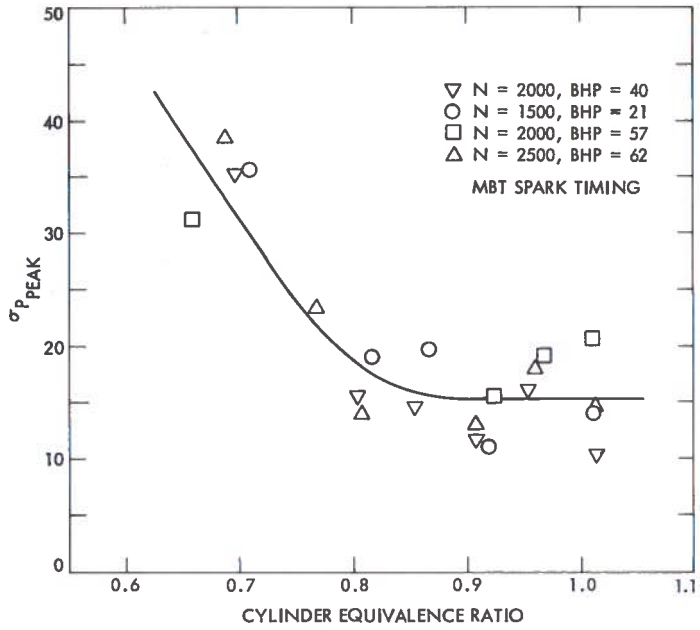

FIGURE 79. PEAK CYLINDER PRESSURE STANDARD DEVIATION VERSUS EQUIVALENCE RATIO

of about 0.85. There are three distinct curves for the three operating conditions indicating a further dependence of $BSNO_x$ emissions on RPM and/or load.

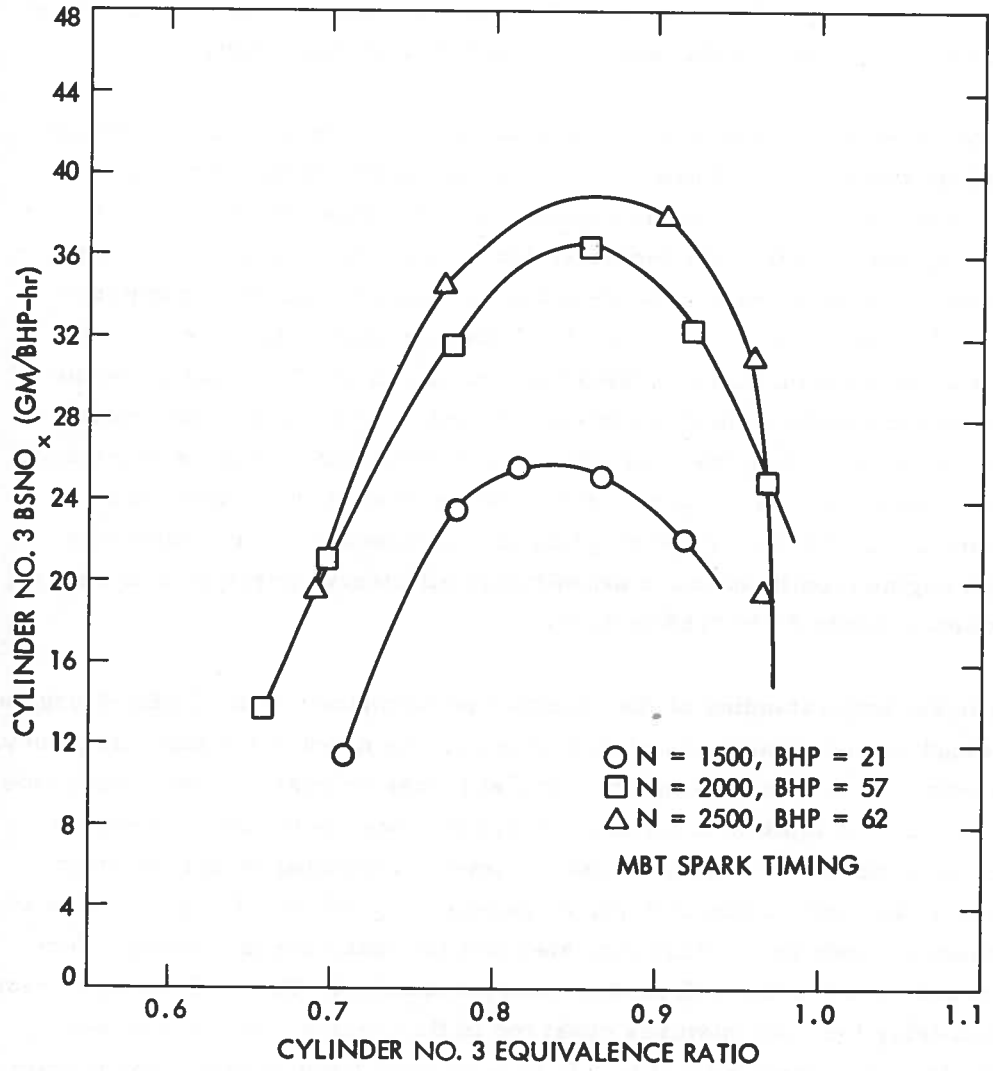

FIGURE 80. BRAKE SPECIFIC NO_x EMISSIONS VERSUS EQUIVALENCE RATIO

7. CONCLUSIONS

Certain conclusions can be made regarding the potential of the lean burn approach for improving fuel economy and reducing exhaust emissions based on the analytical and experimental work accomplished on this effort.

It has been successfully demonstrated on two lean burn engine configurations that operating lean can provide significant improvements in fuel economy over the stock engine. During the sensitivity test series, the second lean burn engine configuration (LBEC-2) demonstrated an average 12 percent reduction in BSFC at an equivalence ratio of 0.75 and MBT spark timing when compared with the stock version of the same engine. Using mapping data for the LBEC-2 engine, a 22 percent increase in MPG over the urban driving cycle is predicted using the driving cycle computer simulation model. For equivalence ratios less than 0.75, the engine thermal efficiency of the LBEC-2 engine decreased; however, it was possible to operate the engine without misfire down to an equivalence ratio of 0.70. Further gains in fuel economy are possible with additional engine modifications to permit peak efficiency operation in the range of equivalence ratios from 0.65 to 0.70.

A better understanding of the observed performance of the LBEC-2 engine was obtained through diagnostic measurements. As noted in the high-frequency, pressure-time data, the drop in efficiency at leaner equivalence ratios coincides with an increase in ignition delay and a sharp increase in the cycle-to-cycle pressure variations. The flame speed parameter remained rather constant down to an equivalence ratio of 0.70, increasing only slightly from the value at stoichiometric conditions. This indicates that the lean charge is being effectively burned once the flame front has been established. The significant increase in ignition delay for lean mixtures observed in this engine implies a slower transition from the spark kernel to a fully developed flame front. This transition is perhaps slowed by the high turbulence level in the spark gap region resulting from the slant plug heads, turbulator intake valves, and extended reach spark plugs used in the LBEC-2 engine to promote a faster burning charge.

In addition to the high turbulence level, an improperly mixed charge (fuel, air, and residual) can also contribute to cycle-to-cycle pressure variations. Individual-cylinder exhaust gas composition measurements indicate a rather large cylinder-to-cylinder equivalence ratio variation (± 0.05 equivalence ratio units) in the LBEC-2 engine which also contributes to the drop in thermal efficiency for equivalence ratios less than 0.75.

The ability of the lean burn approach to meet the 1977 interim emissions standards has not been experimentally demonstrated in this work; however, certain conclusions can be made regarding the potential of this approach. The LBEC-2 engine clearly does not meet the 2.0 gm/mi NO_x emissions standard when operated at its peak efficiency point of an equivalence ratio of 0.75 and MBT spark timing. As shown earlier in the tradeoff plot for fuel economy and NO_x emissions, the 2.0 gm/mi NO_x standard can be met by operating at a slightly leaner equivalence ratio and/or using spark retard with some reduction in the fuel economy gains over the stock engine. Additional engine modifications to allow efficient operation in the equivalence ratio range from 0.65 to 0.70 would be effective in meeting the NO_x requirement while retaining the fuel economy benefits of lean burn.

The lean burn approach is effective in meeting the 3.4 gm/mi CO emissions standard as demonstrated by the performance of the LBEC-2 engine.

As previously discussed, the HC emissions of the lean burn engines tested in this work are not consistent with the 0.41 gm/mi standard and are about a factor of two higher than the stock values. The higher HC emissions measured on the LBEC-2 engine were probably a result of the additional quench volume created by the slant plug heads which were used to increase the flame speed. Control of HC emissions on the lean burn engine can be achieved by using a catalytic converter near the exhaust manifold. Even at an equivalence ratio of 0.70, the exhaust temperatures are adequate to provide HC reaction in a catalytic converter. Satisfactory use of a catalytic converter to control HC emissions on a lean burn engine has been demonstrated at JPL using hydrogen/gasoline mixtures at an equivalence ratio of 0.53 which produces lower exhaust temperatures than the LBEC-2 engine.

Based on the analysis and experimental work accomplished on this effort, our best technical judgment indicates that the lean burn concept with a catalytic converter has the potential for significantly improving fuel economy over the emission-controlled stock engine while producing emissions consistent with the interim 1977 emissions standard.

8. REFERENCES

1. Schweitzer, P.H., "Control of Exhaust Pollution Through a Mixture-Optimizer," SAE 720254, Jan. 1972.

2. Halstead, M.P., Pye, D.B., and Quinn, C.P., "Laminar Burning Velocities and Weak Flammability Limits Under Engine-Like Conditions," Combustion and Flame 22, 89-87 (1974).

3. Ryan, T.W., et al., "Extension of the Lean Misfire Limit and Reduction of Exhaust Emissions of an SI Engine by Modification of the Ignition and Intake Systems," The Pennsylvania State University, SAE 740105, 1974.

4. Hansel, J.G., "Lean Automotive Engine Operation - Hydrocarbon Exhaust Emissions and Combustion Characteristics," SAE Paper 710164, Esso Res. and Engr. Co., 1971.

5. Bartholomew, E., "Potentialities of Emission Reduction by Design of Induction Systems," SAE PT-2, 192 (1963-66).

6. Eltinge, L., Morsee, F.J., Warren, A.J., "Potentialities of Further Emissions Reduction by Engine Modifications," SAE Paper 680123, 1968.

7. Yu, H.T.C., "Fuel Distribution Studies - New Look at an Old Problem," SAE Trans., Vol. 71 (1963).

8. Liimatta, D.R., et al., "Effects of Mixture Distribution on Exhaust Emissions as Indicated by Engine Data and the Hydraulic Analogy," SAE Meeting at Montreal, Quebec, Canada, June 1971.

9. Takeshi Tanuma, Kenichi Sasaki, Touru Kaneko, and Hajime Kawasaki, "Ignition, Combustion, and Exhaust Emissions of Lean Mixtures in Automotive Spark Engines," Nissan Motor Co., Ltd., SAE Transactions, Vol. 80, 1971 #710159.

10. Evans, A.W., Report on Semi-Stratified Charge Concept (Spark Plug Used as Rich Burning Prechamber), "Retro-Mizer Device, and Dual Ratio Carburetion," Combustion Science and Engineering, Sept. 22, 1969.

11. Kopa, R.D., "Control of Automotive Exhaust Emission by Modifications of the Carburetion System," SAE Paper 660114, 1966.

12. Patterson, D.J., "Cylinder Pressure Variations, A Fundamental Combustion Problem," SAE Paper 660129, 1966.

13. Trayser, D.A., et al., "A Study of the Influence of Fuel Atomization, Vaporization, and Mixing Processes on Pollutant Emissions from Motor Vehicle Power Plants," Battelle Memorial Inst. - Apr. 1969. Phase Report to NAPCA, Contract No. CPA 22-69-9.

14. Lindsay, R., Thomas, A., Woodworth, J. A., and Zeschmann, E. G., "Influence of Homogeneous Charge on the Exhaust Emissions of Hydrocarbons, Carbon Monoxide, and Nitric Oxide from a Multicylinder Engine," SAE Paper 710588, 1971.

15. Little, A. D., Inc., "A Study of Technological Improvements in Automobile Fuel Consumption," U. S. Department of Transportation/U. S. Environmental Protection Agency (Contract DOT-TSC 627), Feb. 1974.

16. Lindsay, R., and Wilson, J., "Heat Pipe Vaporization of Gasoline-Vapipe." Presented at First Symposium on Low Pollution Power and Alternative Automotive Power Systems Coordination Meeting, Oct. 14-19, 1973.

17. Telecon per T. G. Vanderbrug (JPL) with R. Lindsay, (Shell International Petroleum Co. Ltd.), Subject - Availability of Vapipe System for V-8 Engines, Aug. 13, 1974.

18. Telecon per M. W. Dowdy (JPL) with L. Berriman (Dresser Industries) Subject - Status and Availability of Dresserator System, Aug. 27, 1974.

19. Hoehn, F. W., and Dowdy, M. W., "Feasibility Demonstration of a Road Vehicle Fueled with Hydrogen Enriched Gasoline." Paper presented to 9th Intersociety Energy Conversion Engineering Conference, Aug. 26-30, 1974, San Francisco, Calif.

20. Donahue, R. W., and Kent, R. H., Jr., "A Study of Mixture Distribution," presented at the SAE Annual Meeting, Detroit, Jan. 10, 1950.

21. Quader, A. A., "Effects of Spark Location and Combustion Duration on Nitric Oxide and Hydrocarbon Emissions," SAE Paper 730153, 1973.

22. Burgett, R. R., Leptich J. M., and Sangwan, K. V. S., "Measuring the Effect of Spark Plug Gap and Ignition System Design on Engine Performance," SAE Paper 720007, 1972.

23. Harrington, J. A., et al., "A Study of Ignition System Effects on Power, Emissions, Lean Misfire Limit, and EGR Tolerance of a Single-Cylinder Engine-Multiple Spark Versus Conventional Single Spark Ignition," Ford Motor Co., SAE 740188, 1974.

24. Bolt, J. A., and Harrington, D. L., "The Effects of Mixture Motion Upon the Lean Limit and Combustion of Spark-Ignited Mixtures," SAE Paper 670467, 1967.

25. Barton, R. K., et al., "Cycle-by-Cycle Variations of a Spark Ignition Engine - A Statistical Analysis," SAE 700488, May 1970.

26. Winsor, R. E., and Patterson, D. J., "Mixture Turbulence - A Key to Cyclic Combustion Variation," SAE Paper 730086, 1973.

27. Arrigoni, V., Calvi, F., Conetti, G. M., and Pozzi, V., "Turbulent Flame Structure as Determined by Pressure Development and Ionization Intensity," SAE Paper 730088, 1973.

28. Starkman, E. S., Strange, F. M., and Dahm, T. J., "Reaction Front and Pressure Rise Rates Measured Simultaneously in Spark-Ignition Engines," SAE Journal 67, Part 2, July-Dec. 1959.

29. Matsuoka, Shin; Yamaguchi, Takehisa; and Umemura, Yukio, "Factors Influencing the Cyclic Variation of Combustion of Spark Ignition Engine," SAE Paper 710586, 1971.

30. Gabele, P. A., "The Effect of Intake Valve Modification on Cycle-by-Cycle Variations in an SI Engine," M. S. Thesis, The Pennsylvania State University, March 1971.

31. Sakai, Yasuo, Miyazaki, Hiroaki, and Mukai, Losaburo, "The Effect of Combustion Chamber Shape on Nitrogen Oxides," SAE Paper 730154, 1973.

32. Bolt, J. A., and Holkeboer, D. H., "Lean Fuel/Air Mixtures for High-Compression Spark-Ignited Engines," SAE Trans. Vol. 70 (1962) p. 195.

33. Obert, E. F., "Internal Combustion Engines and Air Pollution," 3rd Ed., Intext Educational Publishers, New York and London (1973).

34. Robison, J. A., and Brehob, W. M., "The Influence of Improved Mixture Quality on Engine Exhaust Emissions and Performance," Western States Combustion Institute Meeting, October 25-26, 1965.

35. Haskell, W. W., and Legate, C. W., "Exhaust Hydrocarbon Emissions from Gasoline Engines - Surface Phenomena," SAE 720255, 1972.

36. Wentworth, J. T., "Effect of Combustion Chamber Surface Temperature on Exhaust Hydrocarbon Concentration," SAE 710587, June 7-11, 1971.

37. Lee, R. C., "Effect of Compression Ratio, Mixture Strength, Spark Timing and Coolant Temperature upon Exhaust Emissions and Power," Paper 710832 presented at SAE National Combined Fuels and Lubricants, Powerplant and Truck Meetings, St. Louis, Oct. 1971.

38. Daniel, W. A., "Engine Variable Effects on Exhaust Hydrocarbon Composition (A Single-Cylinder Engine Study with Propane as the Fuel," SAE Paper 670124, General Motors, 1967.

39. Wentworth, J. T., "More on Origins of Exhaust Hydrocarbons - Effects of Zero Oil Consumption, Deposit Location, and Surface Roughness," SAE Paper 720939, 1972.

40. Gottenberg, Olson, and Best, "Flame Quenching During High Pressure High Turbulence Combustion," Combustion and Flame, Quarterly Journal of the Combustion Institute, Volume VII, 1963.

41. Prasse, H. F., McCormick, H. E., and Anderson, R. D., "New Piston Ring Innovations to Help Control Automotive Engine Emissions, " SAE Paper 730006, 1973.

42. Hydrogen-Enrichment-Concept Preliminary Evaluation (Final Report), JPL Report 1200-237, prepared for EPA Office of Alternative Automotive Propulsion Systems, 3 July 1975 (Preliminary).

43. Blumberg, P., and Kummer, J. T., "Prediction of NO Formation in Spark-Ignited Engines - An Analysis of Methods of Control, " Combustion Science and Technology (1971), Vol. 4, pp. 73-95.

44. Houseman, John, Molinari, L. F. and Dowdy, M. W., "Lean Combustion of Hydrogen/Gasoline Mixtures, " presented at the Symposium on Chemistry of Combustion in Engines in Philadelphia, 6-11 April 1975.

NASA — JPL — Coml., L.A., Calif.